AKTET **ISSN 2073-2244**
Journal of Institute Alb-Shkenca **www.alb-shkenca.org**
Revistë Shkencore e Institutit Alb-Shkenca **Copyright © Institute Alb-Shkenca**

VLERËSIMI I NIVELIT TË MBETJES SË SULFONAMIDEVE NË MISHIN GJEDHIT NË SHQIPËRI ME ANËN E KROMATOGRAFISË SË LENGËT

ASSESSMENT OF SULFONAMIDE RESIDUE LEVEL IN BOVINE MEAT IN ALBANIA BY HIGH PERFORMANCE LIQUID CHROMATOGRAPHY

ALMA EMIRI [a], ENTELA TRESKA [b], SUELA MYFTARI [c],
[a]Tirana University, Faculty of Natural Sciences, Chemistry Department, Bulevardi Zogu I, 1001 Tirana, ALBANIA,
[b]University Hospital of Obstetrics and Gynecology "Qeen Geraldine", Bulevardi Zogu I, 1001 Tirana, ALBANIA
[c]Food Safety and Veterinary Institute, 1001Tirana, ALBANIA
e-mail: emirialma@yahoo.com

PËRMBLEDHJE
Në praktikat veterinare moderne përdoren medikamente veterinare te kafshët të destinuara për produkte shtazore. Ekspozimi i njerëzve perkundrejt këtyre produkteve të cilat përmbajnë nivele sinjifikative të mbetjeve të antibiotikëve, mund të shkaktojë çrregullime për shendetin e njeriut. Synimi i këtij studimi ishte implementimi i një metode analitike për përcaktimin e mbetjeve të sulfonamideve në mishin e gjedhit dhe vlerësimi i nivelit të mbetjeve të tyre në Shqipëri gjatë periudhës 2010-2013. Monitorimi i mbetjeve të 26 mostrave të indit të gjedhit çoi në identifikimit e dy rasteve pozitive (7.7%). Shkaku i prezencës të mostrave positive ka qenë administrimi jo siç duhet i sulfonamideve ose mosrespektimi i periudhës së eleminimit të medikamentit. Si përfundim, hapi i parë për parandalimin e mbetjeve është ndërgjegjësimi i individëve dhe i organizatave në lidhje me problemin nëpërmjet edukimit të personelit veterinar, organizatave dhe agjencive qeveritare si dhe duhet të shmanget përdorimi jo racional i antibiotikëve.
Key-words - Sulfonamidet, Mbetje, Medikament veterinar, Mish gjedhi, Kromatografi e lëngët.

SUMMARY
Today, in modern farming practices, veterinary drugs are given to food-producing animals. Human exposure to animal products containing significant levels of antibiotic residues may cause intestinal disorders, and also may lead to the creation of antibiotic resistant bacteria, which is a big concern to public health. The aim of the current study was the implementation of an analytical method for the determination of sulfonamide residues in bovine meat and the evaluation of residual levels of these sulfonamides in Albania, during period 2010-2013. Monitoring of sulfonamide residues in 26 bovine tissue samples led to the identification of 2 positive samples (7.7%) in different areas of Albania. The cause of the positive samples' presence has been linked to improper administration of sulfonamides or improper withdrawal periods. Finally, in order to prevent inadequate residue levels, individuals and organizations have to be made aware of the problem through education by veterinary personnel, organizations, and governmental agencies; irrational use of antibiotics in field veterinary practices should be avoided.
Key-words - Sulfonamides, Residue, Drug, Bovine meat, Liquid chromatography

Introduction

Today, in modern farming practices, veterinary drugs are given to food-producing animals. The presence of pharmacologically active chemicals in a food-producing animals can give rise to the occurrence of residues in food. Human exposure

to animal products containing significant levels of antibiotic residues may cause immunological responses in susceptible individuals and reproductive or intestinal disorders, in addition to the creation of antibiotic resistant bacteria in humans which is a big concern to public health[3].

Aim of the current study was the implementation of an analytical method for the determination of sulfonamide residues in beef meat and the evaluation of residual level of these sulfonamides in Albania, during period 2010-2013. To achieve this, a simple and fast sample preparation method was used to separate the extracted compounds. Sulfonamides were analyzed by high performance liquid chromatography (HPLC), with diode array detection (DAD) used as a detection technique. The analytical methodology developed in tissue matrices was validated in accordance with EU legislation, Commission Decision 2002/657/EC[1]. EU regulatory bodies have set maximum residue levels (MRL) for muscle, fat, liver, kidney and milk at 100 µg/kg, defined as sum of all parent substances present within the sample (Commission Regulation (EU) No 37/2010)[2].

Material and method

Test samples (26 bovine tissue samples) were collected from different farms and local markets in Albania, during 2010-2013. About 100 g of meat sample was packed and stored at -20 °C until the time of analysis.

An extraction method similar in principle to methods described by Di Sabatino M. was adopted for the analysis of meat samples[4].

The meat sample was ground and homogenized, and 15 g of this sample was placed in a 125 mL centrifuge tube. The pH was adjusted to 5.5 by adding 10% acetic acid solution. A 25 mL mixture of acetone/chloroform (1 : 1) was added and the sample was homogenized for 3 min using an Ultraturrax homogenizer. The tube was sonicated for 10 min and was centrifuged at 1500 g for 5 min. The organic layer was filtered through a funnel containing a paper filter with 5 g anhydrous sodium sulfate. The extraction procedure was repeated twice. The filter was washed with 25 mL acetone/chloroform (1 : 1) and the filtrate was added to the extracted solution. Finally, 5 mL glacial acetic acid was added to this solution.

A cationic SPE cartridge was used as follow: cartridge was washed with: 2 mL of a solution of methanol–ammonia (1 + 1); 15 mL bidistilled water; 3 mL 1N HCl; 15 mL bidistilled water, and 3 mL methanol. The cartridge was then dried for 10 min; were eluted 3 mL hexane for 3 times and 2 mL methanol–chloroform solution (1 + 1) containing 5% glacial acetic acid. The prepared mixtures were loaded in a cartridge. The cartridge was washed 3 times with 10 mL portions of methanol–chloroform (1 + 1) containing 5% glacial acetic acid. SAs were eluted by 1.5 mL methanol–ammonia (1 + 1) from the cartridge. The best flow for the sample elution was 5–6 mL/min. The purified solution was first dried with a gentle flow of nitrogen, dissolved with 5 mL methanol, and finally filtered with a 0.45 µm syringe filter into a glass vial. The solution was then injected into the LC system.

The LC system was consisted of a Hewlett-Packard (HP) 1100 series Quaternary Pump, a HP 1100 series DAD detector. Separation was carried out on a Supelcosil LC-18 DB (250 x 4.6 mm, 5 µm) column at room temperature with a Supelguard LC-18 (20 x 4.6 mm, 5 µm) guard column. HPLC eluents were: A) Acetonitrile, B) 2% aqueous acetic acid solution. The gradient was initiated with 90% A, was followed by a linear increase to 60% A over 16 min and 60% A for 4 min. The system was returned to 90% A in 1 min and was re-equilibrated for 4 min before the next injection. The flow rate was 1 mL min-1 and the injection volume was 10 µL. The wavelength was set to 270 nm.

Results and Discussion

In this study, high performance liquid chromatography (HPLC) and the DAD detector were used for analyzing the sulfonamide group. The developed method was fully validated as a quantitative confirmatory method according to the EU Decision 2002/657/EC. Parameters taken into account were: linearity, specificity, recovery, precision, decision limit (CCα) and detection capability (CCβ). SAs instrumental linearity was

evaluated by drawing calibration curves with five concentrations of 25, 50, 100, 150, 200 µg kg^{-1} analytes in matrix, 2 replicates per concentration level. The regression coefficients (R^2 > 0.99) of curves indicated a good fit for all the analytes and confidence limits were satisfactory for every line.

Specificity was tested by analyzing 20 blank tissue samples. The absence of any interfering peaks at the analytes retention times in chromatographic runs demonstrates that the sample cleanup procedure was suitable. Retention times were: sulfanilamide 3.79 min, sulfadiazine 6.73 min, sulfapyridine 7.764 min, sulfamerazine 8.467 min, sulfamethazine 9.897 min, sulfachloropyridazine 12.59 min, sulfaquinoxaline 13.775 min.

Method recovery and precision were evaluated by spiking representative blank tissue samples with SAs, resulting in three analytical series, each series with three concentration levels (50 - 100 - 150 µg kg^{-1}) and seven replicates per concentration level. Trueness was expressed in terms of recovery rate and precision, repeatability (intra-day) and within-laboratory reproducibility (inter-day), as relative standard deviation (CV%). The data shows that the repeatability and the reproducibility for all the analytes were below 10.2 and 9.1 respectively with recoveries above 79%.

Decision limit (CCα) and detection capability (CCβ) were calculated by applying the calibration curve procedure described in EU Decision. Representative blank bovine tissue samples were spiked at 0.5xMRL; 1xMRL; 1.5xMRL.

The method was employed for monitoring of 26 samples collected in bovine muscle sales centers and different farms in different areas of the country for the detection of residues of sulfonamides. The average concentrations of residues of sulfonamides in bovine muscle samples are given in Table 1.

From the 26 samples analyzed for the period from February - Mars and September 2011, January -March 2012, and Mars 2013, nine samples (34.6 %) had detectable concentrations of sulfonamides, where two of the positive samples (7.7%) exceeded the recommended MRL. Figure 1 shows chromatogram of a positive sample.

Table 1. Concentrations of sulfonamides residues in bovine muscle.

Sample No.	Sample identity	Concentration recovered (µg kg^{-1})
1	Durrës	112.1
2	Gosë-Kavajë	163.9

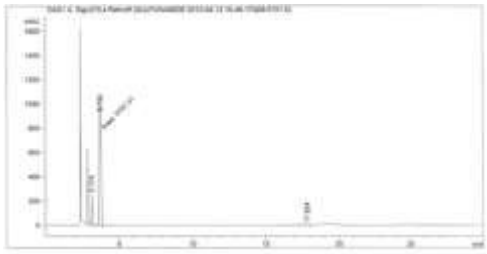

Figure 1. Chromatogram of positive bovine muscle sample. Concentration of sulfanilamide was 163.5 µg kg-1, obtained with DAD detector at 270 nm. Retention time was 3.784 min.

Conclusions

Monitoring of sulfonamides residues in 26 bovine tissue samples by high performance liquid chromatography (HPLC), and DAD detector led to the identification of 2 positive samples (7.7%) in different areas of Albania.

Surveillance of sulfonamide over time in a regular manner is necessary to update the distribution level and to estimate its public health importance. Although few samples were collected, determination of sulfonamide prevalence in this study may provide useful information on the current situation of the sulfonamide in meat available to consumer in the retail markets of Albania and to take measures accordingly. The contamination level (7.7%) of meat samples by sulfonamides in general was lower than previous reports in other states in EU. The cause of the positive samples' presence came mostly from a lack of information of farmers on the risks representing veterinary drug residues in animal products in consumer health. Sulfonamides have been improperly administered or the proper withdrawal period has not been observed.

Finally, the first step in residue prevention is to make individuals and organizations aware of the problem through education by veterinary personnel, organizations, and literatures and governmental agencies. The second step is conducting rapid screening procedures for the analysis of antibiotic residues and prohibition of food containing antibiotics more than the MRL. The third step is avoidance of the irrational use of antibiotics in field veterinary practices.

References

1. Commission Decision 2002/657/EC of 12 August 2002 implementing Council Directive 96/23/EC concerning the performance of analytical methods and the interpretation of results. Off. J. Eur. Comm. 2002 L221: 8-36.

2. Commission Regulation (EU) No 37/2010 of 22 December 2009 on pharmacologically active substances and their classification regarding maximum residue limits in foodstuffs of animal origin. Off. J. Eur. Union 2010 L15: 1-72.

3. Nisha AR (2008), Antibiotic Residues - A Global Health Hazard. Veterinary World, 1(12): 375 - 377.

4. Sabatino MD, Anna PD, Luigi MB and Bruno SD (2007), Determination of 10 Sulfonamide Residues in Meat Samples by Liquid Chromatography with Ultraviolet Detection. Journal of AOAC international. 90: 598-603.

AKTET **ISSN 2073-2244**
Journal of Institute Alb-Shkenca **www.alb-shkenca.org**
Revistë Shkencore e Institutit Alb-Shkenca **Copyright © Institute Alb-Shkenca**

THE NONDESTRUCTIVE METHOD OF ACOUSTIC IMPULSE RESPONSE IN CHARACTERIZING TOMATOES FIRMNESS COEFFICIENT DURING STORAGE

I. ALIU[A], S. RENDEVSKI[B], N. MAHMUDI[A], R. POPESKI-DIMOVSKI[C],
[a] Faculty of Natural Sciences and Mathematics, State University of Tetovo, bul. Ilinden, b.b., 1200 Tetovo, Republic of Macedonia
[b]Faculty of Electrical Engineering, University "Goce Delcev", ul. Krste Misirkov, b.b., 2000 Stip, Republic of Macedonia
[c] Faculty of Natural Sciences and Mathematics, University "Ss. Cyril and Methodius", ul. Gazi Baba, b.b., 1000 Skopje, Republic of Macedonia

SUMMARY
Nowadays, consumers are more cautious about the quality of food. For this reason, numerous destructive and nondestructive methods are used to assess the food quality. Color and firmness factor are the most important parameters for quality evaluation of fruits and vegetables. These food parameters can be determined by nondestructive methods, such as the acoustic impulse response method. The objective of this research was to experimentally evaluate the ability of nondestructive acoustic impulse response method for monitoring the tomato firmness change during storage and to predict the shelf life of the fruit. An experimental setup for implementation of the acoustic impulse response method was developed. The changes of the dominant resonant frequency, firmness factor, elasticity coefficient and integral acoustic intensity were followed over storage time of the tomatoes. The changes of the resonant frequency was found more prominent and hence it can be used for quantifying of tomato firmness.
Key words: Firmness, tomato, acoustic impulse response

INTRODUCTION

Tomatoes firmness is a very important feature since it is connected to their expiry date. Therefore, the determination and the pursuit of firmness are of interest to evaluate the quality of various fruits and vegetables including tomatoes as well. The firmness and stiffness factor of a tomato can be estimated non-destructively from the measurement of its resonant frequency [1],[2]. This research shows that acoustic impulses, with which tomatoes respond after the application of force, correspond to the parameters of the dominant frequency, the coefficient of elasticity and firmness as well as the integration of the signal received from the tomatoes [3]. Lengthening the residence time of stored tomatoes has shown that the integral intensity is in correlation even with the parameters such as the dominant frequency, the coefficient of elasticity and firmness. The acoustic impulse response (AIR) method has been suggested by many researchers to investigate the quality of some fruits and vegetables associated with firmness and elasticity [3]. Acoustic response measurements give a reliable indication of the change in mechanical properties of fruit before, during and after harvest [4] Researchers for the purpose of quality assessment of apples and tomatoes during storage experiment studied commercially available non-destructive firmness sensors, based on acoustic impulse response (AFS) and on low-mass impact (SIQ-FT) [5]. An experimental system for nondestructive evaluation was discovered based on the flexibility of microphone piezoelectric sensors [6]. With this method, tomatoes are hit with a pendulum sphere (or a sphere with the elastic spring) and tomatoes response signals are recorded with a microphone as a sensor. The firmness coefficient

is calculated on the basis of the frequency of tomato response signal and sample mass. The firmness coefficient, which for spherical fruits was first proposed by Abbott 1968 [7] and was modified by Cooke and Rand [8], can be calculated according to equation (3):

$$F_i = f^2 m^{\frac{2}{3}} \quad (1)$$

where F_i is the firmness coefficient with unit $[F_i] = \left[\frac{kg^{\frac{2}{3}}}{s^2}\right]$, f is the dominant frequency $[f] = [Hz] = [s^{-1}]$ and m is mass $[m] = [kg]$. The same method is applied on some products, for example: apples [9], [10], [11], watermelons [12], [13], etc. To reduce errors due to sample differences as well as injuries after the collision, it is preferred to change the position of collision and the average response is obtained after three hits on the equatorial surface of the samples [14].

Cooke and Rand in 1973 [8] proposed a mathematical model to analyze acoustic response of the fruit after the collision and they showed that the module of elasticity (the Young's modulus) can be considered according to equation (2):

$$E_c = f^2 m^{\frac{2}{3}} \rho^{\frac{1}{3}} \quad (2)$$

where E_c is the module of elasticity that has the dimension of pressure (Pa).

ρ – is the density, $[\rho] = \left[\frac{kg}{m^3}\right]$.

The best correlation is established between the integral intensity and dominant frequency of the acoustic signal response of Melody tomatoes, therefore the dominant frequency would be the best firmness index of tomatoes.

The tomato flesh is not strong due to fluid-filled bags. However, the tomatoes firmness is a very important feature, determined conventionally by destructive compression and penetration tests or non-destructive method of acoustic impulse response.

Some detailed information from the AIR method as well as the use of piezoelectric sensor enable tomato quality assessment after storage using tomato acoustic signal response after the collision [15].

MATERIAL AND METHOD

Melody tomatoes (lycopersicum esculentum) were obtained from "Agroprodukt" orangery in Negotino (Polog) near Gostivar, Republic of Macedonia on 19 October 2014. Tomatoes were selected on the basis of color and size (175±20g), shown in Figure 1.

Samples were selected based on the color ratio (red-green); so as to be with 10-15% green surface while the rest of the surface in red (pale red). Tomatoes were chosen from the orangery employee with the researcher supervision during the time when they could be stored. Twenty-seven samples were chosen for the experiment. The storage was done in a semi dark environment research laboratory and average temperature of 15ºC.

The experiment was conducted by pendulum collision method using the acoustic impulse response (AIR).

The mass was determined during the experiment days using the electronic weighing-machine Tehnica exacta. The reduction of size was measured during storage as well. Mass loss was calculated according to the equation: $m_l = \left[\frac{m_i - m_f}{m_i}\right] 100\%$ where m_l is the reduced mass in percentage, m_i the initial mass and m_f the final mass.

It is concluded that the reduced mass was about 5% of the initial mass of all tomatoes. This is due to the removal of water during the 11 days period because tomatoes in their structure have a large amount of water.

Density is defined by the principle of Archimedes. The creation of air bubbles on the surface of tomatoes is minimized during this process.

FIRMNESS

Firmness is defined by the integral intensity of the tomato acoustic impulse response after the collision. Collisions are realized in a small area on the equatorial part in three different positions. The acoustic signal response is realized by defining the dominant frequencies of tomatoes. Recording of these signals is carried through the microphone placed under 120º, in order to avoid indirect frequencies (noise).

Firmness was determined after recording signals to a computer through GoldWave software and after the analysis of frequencies as well as integral intensities through Origin Pro 8.5 software. The values of the acoustic signal response parameters were determined by the average values of the signals.

EQUIPMENT AND THE PROCESS OF EXPERIMENTATION

Figure 1 also shows a small sphere which was used to carry out mechanical collisions (elastic collisions). The microphone is used for recording while the analysis of personal frequency from the acoustic signals is done through the OriginLab computer software, as shown in Fig. 2 scheme.

Figure 1.Tomatoes, collision mode and equipment.

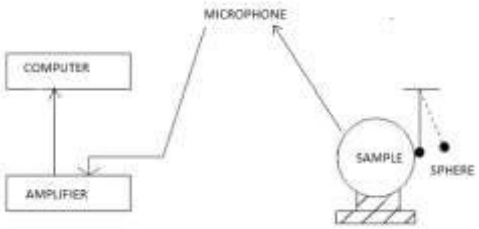

Figure 2.Diagram of the experimental system.

The equipment of mechanical collision is a pendulum with 20 gram aluminum ball placed in an elastic spring. Movements are carefully realized so that the movement angle is not greater than 15º, therefore the striking force is approximately constant. The collision is carried out under 120-130º angle to the direction of the microphone (sensor) used for recording, in order to avoid the direct transmission of collision with the microphone. The collision process is done in various positions in the equatorial plane as well in order to avoid collision in the part softened by the previous hits.

The acoustic signal response was received using the microphone and recorded by the GoldWave software in a personal computer that has served as a database. GoldWave signals were divided and reinforced and then transferred to OriginPro 8.5 for further analysis; the dominant frequency was divided then using FAST FOURIER TRANSFORM (FFT). This was done through the transformation of response signals from time to frequency domain. The highest frequency (f) is obtained from the dominant frequency.

The firmness coefficient (index) is marked with F_i and Young module of elasticity with E_c.

Integral intensity is calculated using the integral divided by the maximum amplitude.

RESULTS AND DISCUSSION

Tomatoes dominant frequency – The change of tomatoes dominant frequency during storage period is shown in the Figure 3. The first raw of table on Figure 1 shows the day of the conducted experiment while the second raw shows the corresponding average value of the dominant frequency.

As seen above, the average dominant frequency falls by increasing the duration of storage. The average values of the dominant frequency are decreased from 108, 75 Hz on

the first day of experimentation to 66, 66 Hz on day 11 of storage.

Days	0	4	7	9	11
Aver.f	108.75	103.36	84.92	68.76	66.66

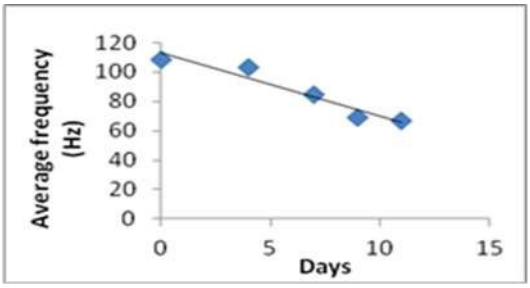

Figure 3.The dependence of the average value of dominant frequency on different days of storage.

Decreasing of the firmness coefficient during storage is shown in the Fig. 4. The average values of the firmness coefficient are decreased from 4017.6($kg^{\frac{2}{3}} \cdot s^{-2}$) on the first day to 1458.6 $kg^{\frac{2}{3}} \cdot s^{-2}$ on the last 11 day.

The integral intensity during the tomato storage gives a dependency as in the diagram shown in Fig. 5. As seen, the integral intensity is decreased between days 7-9 when there is a rapid ripening and then a slight increase. This obviously comes from the end of the ripening process of those green parts.

Days	0	4	7	9	11
Aver.F_i	4017.6	3592.5	2400	1568	1458.6

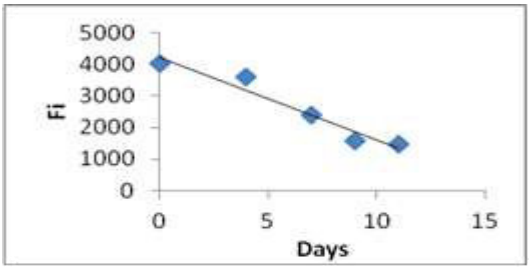

Figure 4. Changing the firmness coefficient values during the days of tomato storage.

Days	0	4	7	9	11
In/A_{max}	239.8	209.8	205.2	138.1	152.72

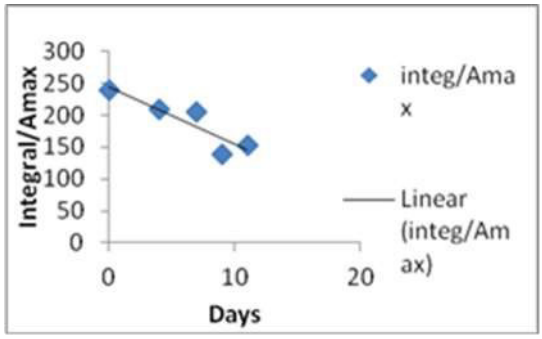

Figure 5.The dependence of integral intensity of storage duration.

CONCLUSION

According to the results obtained by the method of acoustic impulse response applied to Melody tomatoes, after collecting and storing them in semi dark room with temperature 12-15ºC, we can conclude that the method of acoustic impulse response is a reasonably sensitive method for detecting small changes of tomatoes firmness.

This is observed from the accuracy of frequency changes and integral intensity over time. By analyzing value changes of these parameters, as well as the firmness coefficient for this type of tomatoes according to the described storage conditions, it seems that they can be stored or displayed on sale up to a maximum of day 9 from the start of collection, i.e., beginning of storage

REFERENCES

[1] Acoustic impulse-response technique for evaluation and modeling of firmness of tomato fruit**,** *Postharvest Biology and Technology, Volume 17, Issue 2, October, 999, Pages 105-115,* Sarah Schotte, Nele De Belie, Josse De Baerdemaeker.

[2] Influence of Global Shape and Internal Structure of Tomatoes on the Resonant Frequency**,** *Journal of Agricultural Engineering Research, Volume 66, Issue 1, January 1997, Pages*

41-49, Jan J. Langenakens, Xavier Vandewalle, Josse De Baerdemaeker.

[3] GALILI, N., SHMULEVICH,I. and BENICHOU , N.1998. Acoustic testing for fruit ripeness evaluation . Trans . ASAE *41*,399-407.

[4]The Acoustic Impulse Response Method for Measuring the Overall Firmness of Fruit**,** *Journal of Agricultural Engineering Research, Volume 66, Issue 4, April 1997, Pages 251-259,* F. Duprat, M. Grotte, E. Pietri, D. Loonis, C.J. Studman.

[5] Postharvest firmness changes as measured by acoustic and low-mass impact devices: a comparison of techniques**,** *Postharvest Biology and Technology, Volume 41, Issue 3, September 2006, Pages 275-284,* Bart De Ketelaere, M. Scott Howarth, Leo Crezee, Jeroen Lammertyn, Karel Viaene, Inge Bulens, Josse De Baerdemaeker

[6] ABBOT, J. A. 1994,Firmness measurements of fleshy harvested "Delicous" apples by sensory methods, sonic transmission, Magness Taylor, and compression. J .Am. Soc Hortic. Sci. *119*, 510-515.

[7] ABBOT, j, A,BACHAN, G. S, CHILDERS, N, F.,FIZTERALD, J. V. and MATUSIK, F. J. 1968 Sonic techniques for measuring texture of fruit and vegetables. Food Technol. *22*, 635-645

[8] COOKE, J. R. and RAND, R. H. 1973. A mathematical study of resonance in intact fruit and vegetables using a three media elastic sphere model. J. Agric. Eng. Res. *18*, 141-157

.

[9] YAMAMOTO, H., IWAMOTO,M. and HAGINUMA, S. 1980.Acoustic impuls response method for measuring natural frequency of intact fruits and preliminary applications to internal quality evaluations of apples and watermelons. J. Texture Studies *11*,117-136.

[10] ARMSTRONG, P. H., ZAPP, R. and BROWN. G. P. 1990. Impulse excitation of acoustic vibrations in apples for firmness determination. Trans. ASSE *33*, 1353-1359.

[11] LILJEDAHL, L. A. and ABBOT, J. A. 1994. Changes in sonic resonance of "Delicous" and "Golden Delicous"apples undergoing accelerated ripening. Trans. ASAE *37*, 907-912.

[12] CHEN, P,1996. Quality evualutation technology for agricultural products. *Proceedings International Conference Agricultural Machinery Engineering,* Seoul Korea, vol. pp. 171-204

[13] DIEZMA, B. I. RUIZ-ALTISENT. M. and BARREIRO, P. 2004. Detection of internal quality in seedless watermelon by acoustic impulse response. Biosyst. Eng.*88*, 221-230

[14] CHEN, H. and BAERDEMAEKER, J. 1993 Effect of apple shape on acoustic measurements of firmness. J. Agric. Res. *56*, 253-266.

[15] CHEN, H. 1993. Analysis on the acoustic impulse resonance of apples for nondestructive estimation of fruit quality . PhD thesis Dissertation, the Agriculture 236, Katholicke University Leuven, Belgium.

AKTET
Journal of Institute Alb-Shkenca
Revistë Shkencore e Institutit Alb-Shkenca

ISSN 2073-2244
www.alb-shkenca.org
Copyright © Institute Alb-Shkenca

LIQUID AND SUPERCRITICAL CO_2 EXTRACTION OF SOME HEAVY METALS FROM AQUEOUS SOLUTION USING SODIUM DITHIOCARBAMAT AS CHELATING AGENT

JETON HALILI[1], ALTIN MELE[2], ARSIM MALOKU[1], LIRIDON BERISHA[1], TAHIR ARBNESHI[1]
[1]University of Prishtina, Faculty of Mathematical and Natural Sciences, Department of Chemistry, Prishtina, Kosovo.
[2]University of Tirana, Faculty of Natural Science, Department of Chemistry, Tirana, Albania
Corresponding author: jetonhalilich@gmail.com

SUMMARY
The extraction with CO_2 of three heavy metals Cu, Pb, and Cd from aqueous samples was studied in the presence of sodium dithiocarbamate as chelating agent. The extraction was carried out with liquid CO_2 at 72 bar and 30 ^{0}C and with supercritical CO_2 at 200 bar and 60^{0}C in a 20 ml stainless steel extractor. After adding the CO_2 on the aqueous metal solution, the pressure and temperature were set and the two phase system was stirred for 40 min. The pH of the solution was kept 6 using a buffer. After the extraction, the CO_2 was released slowly through a restrictor. The remaining aqueous solution in the extractor was analyzed for its metal content by inductively coupled plasma (ICP-OES), determining the recovery of the metal by CO_2. The highest recoveries obtained were 86.96% for Cu, 81.5% for Cd and 65,0 % for Pb, when using supercritical CO_2.
Key words: Supercritical CO_2, heavy metals, extraction, ICP-OES

1. INTRODUCTION

In industrialized countries, heavy metals are a particular problem for the environment, because many of them are stable in the environment for hundreds or even thousands of years. There are several methods for monitoring and cleaning up environmental samples from heavy metals. Traditional extraction methods, have been used for decades, but these methods are time consuming and environmentally unacceptable. The technology of supercritical fluid extraction (SFE) offers the opportunity to efficiently extract both relatively non-polar analytes as well as ionic materials (such as metal ions) that can be mobilized with the addition of complexing agents. The supercritical fluid extraction (SFE) method is becoming popular alternative technique for the extraction of a wide range organo-metallic and inorganic analytes (**Wang J et al. 1995**). The high diffusivity, low viscosity and variable solvent strength as a function of density (P, T) are some of the attractive features of supercritical fluids **(D.R. Gere et. al 1983)** Carbon dioxide is the most commonly used solvent as SCF, due primarily to its low critical parameters (T_C = 31.1 ^{0}C, P_C =7.38 MPa), being inexpensive, non-toxic, non-flammable, readily available and recycling capability.. Direct extraction of metal ions by supercritical CO_2 is known to be highly inefficient because of the charge neutralization requirement and the weak solute-solvent interactions **(CUI Zhao-jie et. al.2000)**. The solubility of metal ions in the fluids is crucial. However, by converting charged metal

ions into neutral metal chelates using organic chelating agents, this solubility can be enhanced. So, the selection of suitable agents is critical in the chelating-SCE of metal ions. **(C.M. Wai et. al. 1993)**

Data from the literature regarding the study of the solubility of complexes in super-critical fluid is very limited. Recently, **(E. Laintz et al. 1991)** has measured the solubility of different metals (Ni^{+2}, Co^{+3}, Cu^{+2}, Na^{+}, Bi^{+3}, dhe Hg^{+2}) complexed with ligands; *diethyl dithio-carbamate* (DDC) and *bis (trifluoroetil) ditio-karbamatet* (FDDC) in supercritical $C0_2$. Extraction of metal ions from an aqueous phase into CO_2 is complicated by the presence of carbonic acid, which lowers the pH of the aqueous phase to approximately 3. While some metals are extracted efficiently at pH ~ 3, other metal ions, cannot be efficiently extracted at such an acidic pH. Under these conditions, a large excess of ligand is often required to achieve complete extraction of the targeted metal **(Toews, K.L et. al. 1995).**

The main objective of this research is to develop techniques of extraction with CO_2 in liquid and solid samples and depth understanding of the process of extraction with super-critical fluid. Complex metal ions were determined in the presence of Sodium Diethyl-dithio-carbamate. It is done the optimize of the extraction factors to give better results as qualitative and quantitative, without neglecting the use of statistical and instrumental analytical methods to achieve fast quantitative verification

The objective of this research is divided into several segments:

1. The study of the effect of pressure and temperature in the extraction process and the study of the interaction between these two independent variables
2. Study the influence of pH value and role of modifier in the extraction process
3. Study the possibility application of SFE-CO_2 technology on an industrial scale by recycling solvent and ligand in order to reduce operational expenses.

2. MATERIAL AND METHODS

2.1. Reagent

ICP standard solution of Iron, Lead and Cadmium (Fluka) were obtained. Sodium diethyl dithio-carbamate trihydrate (MERCK) were used as chelating agent. Citrate - Phosphate buffer were used to vary the pH of the aqueous phase. Methanol extra pure (Merck) was used as reagent of reaction and collecting agent. The reagents used were all analytical grade and of ultra-pure quality. De-ionized water is used in all experiments.

2.2. Analytical techniques

Were used several analytical techniques to monitor the outcome of experiments conducted during this study

2.3. ICP-OES

The measurements were performed using the PerkinElmer®Optima™ 7300 DV ICP-OES instrument with sequence parameters as follows: frequency, 27.12 MHz; Power, 1.1 kW; argon were used as inert gas in three cases Ar/Ar/Ar/: cooling gas Ar, 14.0 L min^{-1}; conductor gas Ar, 0.5 L min^{-1} and nubelizer Ar, 1.0 L min^{-1}; pressure 2.4 bar flow rate 1.0 mL min^{-1}; wavelength of monocromator from 165–460 nm. Wavelength of heavy metals: Cd: 228.80 nm (3 s), Cu: 324.75 nm (3 s, Pb: 220.35 nm (5 s),

2.4. Apparature

All experiments were carried out in a supercritical fluid extraction apparatus at the Technical University of Graz, Institute of Chemistry. To carry out the objectives of this study, the supercritical extraction system shown in Fig. 1 was used. All extractions were performed

using a special stainless steel cylindrical extractor vessel (20ml) with two glass windows (MAXOS 30x15mm) to observe phases. A cold trap with a mixture of water and methanol was used to collect the samples. For the analysis of the metal ions extracted, an Inductively Coupled Plasma/Optical Emission Spectrometry was used.

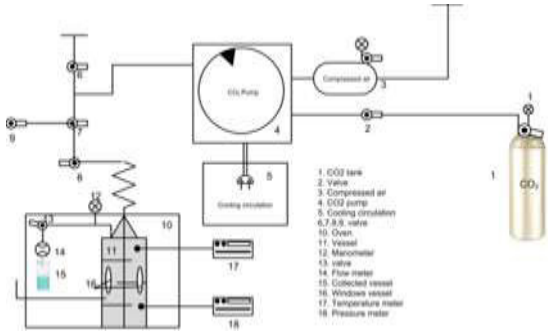

Figure 1. *Aparature for extraction with supercritical CO_2*

2.5. Procedure

10 ml of 2 mg/L concentration metal solution was prepared from the stock standard solution of Cu, Pb and Cd. The solution was buffered to pH 6.0 with Citrate -Phosphate buffer. The sample was placed in extraction cell and equivalent amount of chelating agent (sodium dithiocarbamat trihidrat) was added. Carbon dioxide was supplied from a supply tank, maintained at a pressure of approximately 53 bar. The extraction was carried under near critical condition with liquid CO_2, temperature (30^0C), pressure (72 bar) and supercritical condition temperature (60^0C), pressure (200 bar). The solute was extracted at a constant temperature and pressure of CO_2 for 60 min, called static extraction followed by a 40 min dynamic extraction. Then the solute was removed from the extraction vessel, and the vessel was flushed with the fresh CO_2 for 20 min to collect any solute that had precipitated within the system during depressurization. When the extraction was completed, solution was removed from the extraction vessel and was digested for 20 min in a microwave with HNO cycle (65%) at a temperature of 180 °C. The subsequent solutions were analyzed with ICP-OES (Inductively Coupled Plasma / Optical Emission Spectrometry). The extraction efficiencies were calculated based on the amount of the metal ion in the aqua sample before and after the extraction

3. Results and discussion

From standard solutions were prepared 2mg/L solution of Cu, Pb and Cd. The solution was buffered using a phosphate - citrate buffer in pH=6

Then 10 ml of each solution was placed in extraction vessel and added corresponding amount of ligand (NaDDTC)

The extraction is performed in:

- Temperature 30 degrees Celsius and 72 bar pressure for 30min
- Temperature of 60 degrees Celsius and 200 bar pressure for 30 min

The results are presented in following tables and diagrams.

Table 1. *Percentage extraction of Cu, Pb and Cd in temperature and pressure (30^0C, 72 bar) and (60^0C, 200 bar)*

Metali/Presioni	Cu	Pb	Cd
72 bar	68.86%	45.82%	80.5%
200 bar	86.96%	65.2%	81.5%

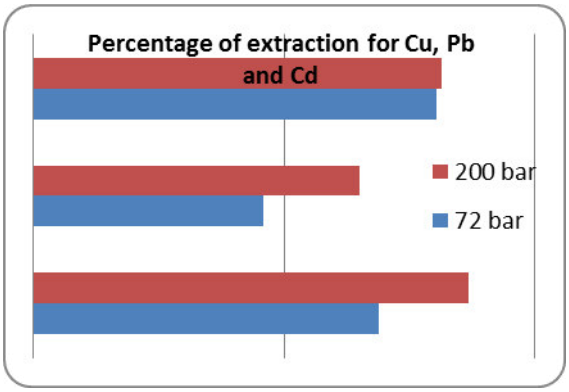

Figure 2. Graphical representation of extraction of Cu, Pb and Cd in the presence of modifiers in temperature and pressure (30^0C, 72 bar) and (60^0C, 200 bar)

The use of supercritical fluid for extraction of various substances found wide applications recently. This method is now used to determine the total contents of (organometalic) complex compounds. Recently SFE technique was used by **(Y.Liu et. al. 1994**). In preliminary experiments, organometallic mercury compounds were extracted with super-critical fluid using CO_2 as solvent and 5% to 10% methanol as modifier and the extraction rate was 64-89%. **(C.M. Wai et al 1993)** during their research, they concluded that metal ions can be extracted with SFE using CO_2 in the presence of suitable ligands. They have reported the application of SFE for the extraction of Cu^{2+}, Cd^{2+}, Zn^{2+} and Hg^{2+} in the presence of ligand lithium bis (trifluoroethyl) dithiocarbamate (LiFDDC). Negatively charged ligand ($FDDC^-$) reacts with metal ions to form neutral chelat complexes which are soluble in CO_2. The extraction of heavy metals (Cd^{2+}, Zn^{2+} and Pb^{2+}) using different dithiocarbamates was also researched by (**Wang and Marshall 1994**). They found that increasing the solubility of the compound depends on the length of the alkyl chain of dithiocarbamates. Water samples of these metals were extracted in dynamic form, and extracted complexes were collected in chloroform, then treated with nitric acid and their concentration was measured by ICP-MS. Research undertaken by **(Moonsung Koh et. al 2005)** during extraction of metals with two different ligand, NaDDC and Cyanex-272, show that the NaDDC is more effective in the extraction of metals that Cyanex-272. The authors, all the experiments have performed in pressure 200 bar and temperature 60 ^{0}C and for Cu extraction efficiency is higher than 70%, whereas for other metals (Pb, Zn, Cd, Co) ranges from 20-50%. The results of our research regarding the extraction of Cu, Pb and Cd from water samples in the presence of ligand NaDDC are related to the results of Koh Moonsung. The values of pressure and temperature of super-critical fluid used are the same (p = 200 bar and T = 60 ^{0}C), whereas the percentage of extraction of these metals were; 86.96% Cu, 81.5% Cd and Pb 65.2%. NaDDC ligand has limited solubility in CO_2 and could easily decompose in pH value <4, for this reason, during our research we added excess ligand and we used phosphate-citrate buffer to stabilize the pH value. Metals such as Cu, Pb and Cd form a stable complexes with ligand NaDDC in pH value from 5-7, then as a compromise we chose pH value = 6 using phosphate-citrate buffer. NaDDC ligand decompose in acidic solution in Dietilamin and carbon disulfide according to the following reaction.

$$(C_2H_5)_2NCS_2^- Na^+ + HA \rightarrow (C_2H_5)_2NH + CS_2 + Na^+ + A^-$$

REFERENCES

1.C.M. Wai, Y. Lin, R.D. Braner, S. Wang and W.F. Beckert, *Talanta, 40* (1993) 1325.

2.CUI Zhao-jie, LIU J un-cheng, GAO Lian-cun , WEI Ying-qin "Extraction of copper ions by snpercritical carbon dioxide". *Journal of Environmental Sciences* VoL 12,No. 4 ,pp. 444-447 ,2000

3.D.R. Gere, R. Board and D. McManigill, Anal. Chem., 54 (1983) 740-745.
4.E. Laintz, C.M. Wai, C.R. Yonker and R.D. Smith, J. Supercrit. Fluid, 4 (1991).
5.Moonsung Koh, Kwangheon Park,* Doohyun Yang, Hakwon Kim, and Hongdoo Kim*. "*The Synergistic Effect of Organophosphorus and Dithiocarbamate Ligandson Metal Extraction in Supercritical CO2*", Bull. Korean Chem. Soc. 2005, Vol. 26, No. 3.
6.Toews, K.L., Shroll, R.M., Wai, C.M., Smart, N.G. *Anal. Chem.* 1995. 67*,* 4040.
7. Wang J and Marshall W D, *Analyst,*. 1995, 120, 623.
8.Wang and W.D. Marshall, *Anal. Chem., 66* (1994) 1658
9.Y. Liu, V. Lopez-Avila, C. Charan, M. Alcaraz and W.F. Beckert, presented at the *Fifth International Symposium on Supercritical Fluid Chromatography and Extraction, Baltimore, MD, USA, January II-14,* 1994, poster F-18..

AKTET **ISSN 2073-2244**
Journal of Institute Alb-Shkenca **www.alb-shkenca.org**
Revistë Shkencore e Institutit Alb-Shkenca **Copyright © Institute Alb-Shkenca**

FACTORS AFFECTING PROFITABILITY OF INSURANCE COMPANIES IN KOSOVO
FAKTORËT QË NDIKOJNË NË FITIMIN E KOMPANIVE TË SIGURIMIT NË KOSOVË

ALBULENA SHALA, YLLKA AHMETI, VLORA BERISHA, SKENDER AHMETI

a) Universiteti i Prishtinës "Hasan Prishtina" Fakulteti Ekonomik, Prishtinë, Republika e Kosovës
E-mail: albulena.shala@hotmail.com; skender.ahmeti@yahoo.com
b) Banka Qendrore e Kosovës, Prishtinë, Republika e Kosovës,e-mail: ahmeti.yllka@gmail.com
c) Universiteti "Haxhi Zeka", Pejë, Republika e Kosovës, e-mail: vlorab_402@hotmail.com

PËRMBLEDHJE

Performanca e kompanisë luan rol kryesor në drejtim të rritjes së industrisë e cila në fund të fundit çon në suksesin e përgjithshëm të ekonomisë. Në këtë hulumtim përpjekja është të shqyrtojmë faktorët që ndikojnë në fitimin e kompanive të sigurimit në Kosovë për periudhën 2009-2012 për 11 kompani të sigurimit. Për këtë qëllim, ROA është marrë si variabël e varur, ndërsa madhësia, rritja, jetëgjatësia-mosha, raporti i aktiveve fikse, raporti i likuiditetit, leverazhi dhe vëllimi i kapitalit janë përzgjedhur si ndryshore të pavarura. Të dhënat dytësore janë te marra nga raportet vjetore të kompanive të sigurimit, të publikuara në web faqe të BQK-së. Rezultati tregon se raporti i likuiditetit dhe vëllimi i kapitalit janë në mënyrë të konsiderueshme dhe pozitivisht te lidhur me fitimin. Në kontrast me këtë, madhësia e kompanisë dhe raporti i aseteve fikse treguan shenje negative por të rëndësishme me fitimin e kompanive.

Fjalët çelës: fitimi, faktorët, kompanitë e sigurimit, likuiditeti;

SUMMARY

The company's performance plays a leading role towards the growth of the industry which ultimately leads to the overall success of the economy. This research effort examines the factors affecting the profit of insurance companies in Kosovo for the period 2009-2012 to 11 insurance companies. The study was quantitative in nature. It adopted the longitudinal time dimension, specifically, the panel method and ordinary least square regression.For this study, ROA is taken as the dependent variable, while size, growth, life expectancy, age, fixed assets ratio, liquidity ratio, leverage and capital volume were selected as independent variables. Secondary data are taken from annual reports of insurance companies, published on the CBK web site. The results show that the ratio of the volume of liquidity and capital are significantly and positively related to acquisition. In contrast, the size of the company and the ratio of fixed assets showed a significant, but negative relationship with corporate profitability.

Key words : profit, factors, insurance companies, liquidity

INTRODUCTION

The insurance sector in any country can have a great impact on economic growth and development (Brainard, 2008; Ward & Zurbruegg, 2000). Previous studies on the determinants of profits were concentrated mainly in the banking sector (Bourke, 1989; Short, 1979; Molyneux and Thornton (1992), Demirguc-Kunt and Huizinga (2000), Goddard et al. (2004) as cited in Athanasoglou et al.). Only a small number of previous studies are based on the determinants of profit in the insurance sector.

These factors can be classified as internal factors of industry and of the macroeconomics (Ayele, 2012).

Al-Shami (2008) has conducted a study on the determinants of profit in a panel data of 25 insurance companies during the period from 2006 to 2007 that were listed on the stock

market in the United Arab Emirates. He concluded that firm size had a direct and a significant impact on the profit, while the volume of capital has had a direct impact, but irrelevant to the profit, the firm's life-time did not have an impact, while the leverage and risk ratios had an inverse connection and significant with the profit. Malik (2011) investigated the relationship between capital volume and ROA as a measure of profit for the insurance industry in Pakistan and found positive and statistically significant relation between capital and profit.

Ikonic, et.al (2011) analyzed the performance of insurance companies in Serbia applying the CARMEL method, and found that the level of capital is a determinant of profit. The research objectives of this study are:

1. To identify the internal factors that affect the profits of insurance companies in Kosovo.
2. To determine the relationship between profits and internal factors of the insurance companies.

In order to meet the objectives of this study, we have developed a model where we use return on assets against a group of explanatory variables that we deem may explain the levels of profit of the insurance companies in Kosovo.

The model is shown below:

$$ROA_{it} = \beta_o + \beta_1 GROW_{i,t} + \beta_2 SIZE_{it} + \beta_3 TANG_{it} + \beta_4 LIQ_{it} + \beta_5 AGE_{it} + \beta_6 VOC_{it} + \beta_7 \mathrm{LEV}_{it} + \varepsilon_{it}$$

RESULTS AND DISCUSSION

The Descriptive Statistics - The higher the return on assets, the effect on profit will be higher in the insurance firms. From descriptive statistics, the average return of the assets of insurance firms in Kosovo is 5:07% with a dispersion of 41.22%. This shows that the return variations on assets will not rise above 41, 22%.

From descriptive statistics, the leverage-total debt in relation to total assets ranges from minimum of 4.34% to 93%. This shows that the debt variance to assets in Kosovo's insurance companies do not exceed 88.66%. However, as shown in the descriptive statistics, some insurance companies may have up to 36.28% debt to their total assets. This shows that insurance firms use less debt, and this will make the latter more attractive to many more clients, thus increasing their premiums. And, this eventually lead to higher level of return on profit.(Eric Kofi Boadi et al., 2013).

Table 1: Definitions of the dependent and the explanatory variables of the empirical model

β_o	is konstant
ROA_{it}	Return on Assets (ROA)= Net Income before Taxes / Total Assets
GROW it	Change in Total Assets
$SIZE_{it}$	Size=total assets in log value
$TANG_{it}$	Tangibility = (Fixed assets / total assets)
LIQ_{it}	Liquidity = (Current Assets / Current Liabilities).
AGE_{it}	Age = (The difference between the current year and the year of establishment of the company).
LEV_{it}	Leverage = (total debt / total assets).
VOC_{it}	The volume of capital =Log of Equity Capital
ε_{it}	The error term.
Note: Formulas are collected from the previous studies.	

Table2. Descriptive Statistics

Variables	N	Min	Max	Mean	SD
ROA	1	-1,21	1,18	0,05	0,41
LEV	1	0,04	0,93	0,58	0,21
LIQ	1	0,13	3,72	1,15	0,97
SIZE	1	9,09	16,89	13,64	3,27
AGE	1	1,00	12,00	7,13	2,96
GROW	1	-0,48	0,90	0,14	0,23
TANG	1	0,00	0,99	0,17	0,24
VOC	1	7,28	15,68	12,19	3,57
Valid N	11	Note: Note: Results computed by using Gretl 1.9.8.			

Regarding fixed assets from the above descriptive statistics is indicated that participation is by 0, 09 % and 99.86 % mostly. However, the variability of insurance firms about their fixed assets to total assets is 99.77%. Distribution of fixed assets to total assets is 16.95%. From descriptive statistics

fixed assets of insurance companies are 99.95 of their total assets. This means that insurance firms have assets that can be used for more than one fiscal year to generate revenue (Eric Kofi Boadi et al., 2013). Regarding liquidity according to descriptive statistics, insurance firms pay their current liabilities 0.13 times and not more than 3.72 times. However variability of insurance firms about their liquidity will not increase above 3.84 times. The average rate of current assets to current liabilities is 1.14 times. Insurance firms are able to use their current assets to generate profit.

Table 3: Model Summary
Number of periods: 4
Dependant variable: ROA
Std. error stable (HAC method)

Mean dependent var	0,051	S.D. dependent var	0,412
Sum squared resid	3,480	S.E. of regression	0,311
R - Square	0,524	Adjusted R Square	0,431
F-Statistics (7, 36)	5,656	Prob(F-Statistics)	0,0001
Log likelihood	-6,619	Akaike info criterion	29,237
Schwarz criterion	43,511	Hannan-Quinn criter.	34,531
Rho	0,132	Durbin-Watson stat.	1,348

R-square at the Table 3 shows that 52% of the variation in the dependent variable (ROA) is explained by changes in seven independent variables. Adjusted R-square is slightly below the R-squared value of 43%. F-statistic shows the validity of the model with 5,656 of its value that is significantly higher than Prob. F (critical P for F), which has a value of 0.000.

Testing Hypothesis: The regression result in Table 4 clearly shows that there is a positive relationship between return on assets and liquidity. Beta coefficient for this variable is positive and significant at the 5% level with a critical p-value of 0.027. The t-test value is 2.294, which is greater than the critical value and the null hypothesis of no relationship between the two variables is rejected. Therefore, there is a significant positive relationship between return on assets and liquidity.

Table 4 Regression Summary

Variable	β	Std. Error	t-test	p-value		VIF
const	0,015	0,259	0,058	0,954		
LEV	0,010	0,292	0,035	0,972		4,590
LIQ	0,117	0,051	2,295	0,027	**	1,851
SIZE	0,106	0,014	7,656	<0,000	***	3,576
TANG	-0,616	0,301	-1,99	0,054	*	1,599
VOC	0,099	0,014	7,097	<0,000	***	3,887
GROW	0,229	0,089	2,563	0,015	**	1,157
AGE	0,028	0,031	0,894	0,377		3,194

Notes: Significance level: * is 1%, ** is 5% and *** is 10%.
VIF- Variance inflator factor.

It is clear from Table 4 that there is a negative relationship between return on assets and the size of the company. Beta coefficient for size is pozitive and significant at the 1% level with a critical P at 0.000. The t-test value is -7.656 which is greater than the critical p-value. Therefore, the null hypothesis of no relationship is rejected. Thus, there is a significant pozitive relationship between size and return on assets.

There is also a negative relationship between return on assets and tangible assets. Beta coefficient for tangible assets is negative and significant at the 1% level with a critical P at 0054. The t-test value is -1.99, which is greater than the P-critical value. Therefore, the null hypothesis is rejected. Thus, there is an important relationship of fixed assets and return on assets. An inverse relation between them is consistent with the findings of Eric Kofi Boadi (2013). Consequently, while this ratio increases, it can affect the decline on profit and other factors that could affect profit. With this significant inverse relationship, a percentage change in fixed

assets will have a significant effect on the profit of insurance firms. Any change in fixed assets will affect the total assets, and thus this may reduce the profit level.

Beta coefficient for the capital volume is positive and significant at 1% with a P-value of 0.000. Its t-test value is 7.097, which is greater than the critical value and thus the null hypothesis is rejected. Therefore, there is a significant positive relationship between return on assets and equity volume.

Positive and significant relationship between the capital volume and profits of insurance companies means that insurance companies with high capital reduce their cost of funding, or have lower needs for external funding resulting in higher profit. The regression result in Table 4 clearly shows that there is a positive correlation between return on assets and the company's growth. Beta coefficient for this variable is positive and significant at the 5% level with a P-critical 0,014. T-test value is 2.563, which is greater than the critical value and thus null hypothesis is not accepted. Therefore, there is a significant positive relationship between return on assets and the size of the company. Positive linkage and statistically significant between growth rate and profits of insurance companies means that insurance companies with the highest growth rate in terms of their total assets are also in a better position to be profitable.

Beta coefficient for leverage and longevity is positive but not significant. The t-test value is less than the critical value. Therefore, there is no significant relation between return on assets and company's life expectancy, and the leverage.

CONCLUSION

The objective of the study is to examine the determinants of profit insurance companies represented by ROA for the period 2009-2012 for 11 insurance companies in Kosovo. Variables tested in this study are: life expectancy of the company, size, and the volume of capital leverage, growth of the company, tangible assets and liquidity.

By the verification of the hypotheses, we have found that ROA is positively affected by the volume of capital, liquidity ratio and the company's growth and negatively affected by size and fixed assets. . Also at at Table 4, for the model, the results show that VIF (variance inflation factor) for all variables is less than 5%, this indicates that the model is free from multicollinearity. Based on the research findings the following reachable recommendations were presented for this study:

It is positive to have high consideration of increasing the company assets. Because the size of the company is an important factor as it influences its competitive power. Small companies have less power than large ones; hence they may find it difficult to compete with the large firms particularly in highly competitive markets.

Great attention should be paid to volume of capital. Result also shows that volume of capital was significantly and positively related to profitability. Macro economic variables such as interest rate change, number of insurers, inflation could not be included.Future research studies may consider more variables, both company specific and macro economic variables.

References:

- Adams M., Hardwick P. and Zou H., (2008),Reinsurance and Corporate Taxation in the United Kingdom Life Insurance Industry, Journal of Banking and Finance, Vol. 32.

-Ahmed N., Zulfqar A., Ahmad U., (2011), Determinants of Performance: A Case of life Insurance Sector of Pakistan, International Research Journal of Finance and Economics ISSN 1450-2887 Issue 61 (2011).

- Ammar, A., Hanna, A. S., Nordheim, E. V., and Russell, J. S. (2003), Indicator variables model of firm's size-profitability relationship of electrical contractors using financial and economic data. Journal of Construction Engineering and Management, 129(2): 192–197.

-Boadi,.E.K., Antwi, S., Lartey, V.C.,(2013); Determinants of profitability of insurance firms in Ghana" International Journal of Business and

Social Research (IJBSR), Volume -3, No.-3, March 2013;

-Desheng Wu Z., Sandra V. &Lianga (2007), Simultaneous Analysis of Production and Investment Performance of Canadian Life and Health Insurance Companies, Computers and Operations Research, Vol. 34, Issue. 1.

-Dragana Ikonic, Nina Arsic and Snežana Miloševic, (2011), Growth Potential and Profitability Analysis of Insurance Companies in the Republic of Serbia, Chinese Business Review, 10 (11), 998-1008.

- Hafiz Malik, (2011) Determinants of Insurance Companies Profitability: An Analysis of Insurance Sector Of Pakistan, Academic Research International, Volume 1, Issue 3

- Treacy, M. (1980). Profitability patterns and firm size. Working Paper No. 1109-80. Cambridge, MA: Massachusetts Institute of Technology, Alfred P. Sloan School of Management.

- Wright K. M. (1992), The Life Insurance Industry in the United States an Analysis of Economic and Regulatory Issues. Country Economics Department the world Bank Policy Research Working Paper (wps 857);

AKTET **ISSN 2073-2244**
Journal of Institute Alb-Shkenca **www.alb-shkenca.org**
Revistë Shkencore e Institutit Alb-Shkenca **Copyright © Institute Alb-Shkenca**

ANALIZË HAPËSINORE E SHTRESËS SË QYMYRIT NË VENDBURIMIN SIBOVC JUGPERENDIM
SPATIAL ANALYSIS OF COAL SEAM IN SIBOVC SOUTH WEST COAL DEPOSIT

NASER PECI[1], BEHXHET SHALA[1], FLURIJE SHEREMETI – KABASHI[1]
[1] Departament of Gjeology – Faculty of Geosciences, University of Mitrovica "Isa Boletini". Industrial Park, 40000 Mitrovicë, KOSOVA
naser.peci@uni-pr.edu

PERMBLEDHJE
Kosova është e pasur me rezerva të linjitit që vlerësohen në rreth 10 miliardë tonë, të përqendruara në basenin qymyror të Kosovës. Vendburimi Sibovc jugperendim gjendet në pjesën qendrore të basenit të Kosovës. Gjithësejt 231 shpime kërkimore kanë qenë në dispozicion për zonën e Sibovcit JP. Analiza hapësinore apo statistika hapësinore përfshinë një seri të teknikave për analizimin e të dhënave hapësinore. Rezultati i këtyre metodave varet nga vendndodhja e provave që janë objekt i analizës. Softverët për aplikimin e këtyre analizave hapësinore kërkojnë çasje në të dy karakteristikat: në vendndodhje dhe atributet e tyre. Në këtë punim është kryer analiza hapësinore e të dhënave dhe janë prodhuar harta duke përdorur softverin Surfer. Për variablat si: tavani, dyshemeja, trashësia e shtresës së qymyrit, raporti steril/qymyr, vlera kalorike dhe sulfur janë krijuar njën sërë hartash (kombinim i hartave të provëmarrjes, hartave të izolinjave dhe 3D harta të sipërfaqes).
Fjalët çelës: shtresë qymyri, analiza hapësinore, korrelacioni hapësinor, hartat

SUMMARY
Kosovo has lignite reserves assessed at some 10 billion tons, concentrated in the Kosovo Coal Basin. The deposit Sibovc SW is in the central part of the Kosova Basin. A total of 231 boreholes are available for the Sibovc SW area. Spatial analysis or spatial statistics includes a series of techniques for analyzing spatial data. The initial procedure of analysis includes the set of generic methods of exploratory analysis and the visualization of data, in general through maps. Software for application of this spatial analysis requires access to characteristics: their location and their attributes. In this paper are performed the spatial data visualization and production of maps using Surfer software. For variables such as top, bottom, thickness of coal seam, ratio coal/overburden, calorific value, and sulfur content was created a set of maps (combination of post map, contour map and 3D surface map).
Key words: coal seam, spatial analysis, spatial relationship, mapping

INTRODUCTION

Spatial statistics concerns the quantitative analysis of spatial data, including their dependencies and uncertainties. Understanding the spatial distribution of data from phenomena that occur in space constitute today e great challenge to the elucidation of central questions in many areas of knowledge. Such studies are becoming more and more common, due to the availability of low cost software with user-friendly interfaces . These systems allow the spatial visualization of variables. Besides the visual perception of the spatial distribution of the data, it is very useful to translate the existing patterns into objective and measurable considerations [2][7][8].

The spatial analysis is composed by a set of chained procedures whose aim is to choose an inferential model that explicitly considers the spatial relationship present in the phenomenon. The initial procedures of analysis include the set of generic methods of exploratory analysis and

the visualization of data, in general through maps. These techniques permit the description of the distribution of the variables of study, the identification of observations that are outliers not only in relation to the type of distribution but also in relation to its neighbors and to look for the existence of patterns in spatial distribution [3] [6].

The main goal of spatial analysis for this coal deposit is to clarify several key parameters that characterize the coal seam and its quality. This study attempts to achieve the numerical characterization main parameters of coal seam, and its differentiation from the background. In this work, raw data after pre-processing have been mapped as image and set of maps (contour and 3D surface maps) [7][8].

MATERIAL AND METHODS

Formation of coal deposit is one of the products of geotectonic evolution of theKosovo basin. In the central part of coalbearing of the Kosova Basin, the most important deposits of lignite are Bardh, Mirash, Sibovc (fig.1) [1].

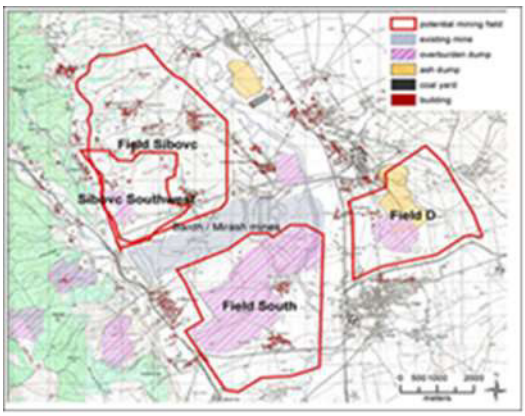

Figure 1. Map shown position of Sibovc southwest deposit in Kosovo coal basin (Steag 2006

The basement of the Kosovo Basin and the exposed surrounding areas are built up by Palaeozoic to Mesozoic crystalline rocks. The basin fill consists of Upper Cretaceous strata which are uncomfortably overlain by Tertiary clays of Pliocene age in which lignite is interbedded. Simplified the coal bearing sediments can be subdivided from the base to the top as follows: green clay, lignite formation, grey and yellow clay [1].

A total of 231 exploration drilling results are analyzed in the area Sibovc south west.

Statistical methods have been widely applied to interpret coal seam parameters and coal quality:

Univariate statistical methods - univariate statistical methods (i.e. involving observations with only one variable) can be used to organise and extract information from a data set of values for a single element [4][5].

The statistical parameters of the distributions of the coal seam parameters in Sibovc SW coal deposit are summarized in Table 1.

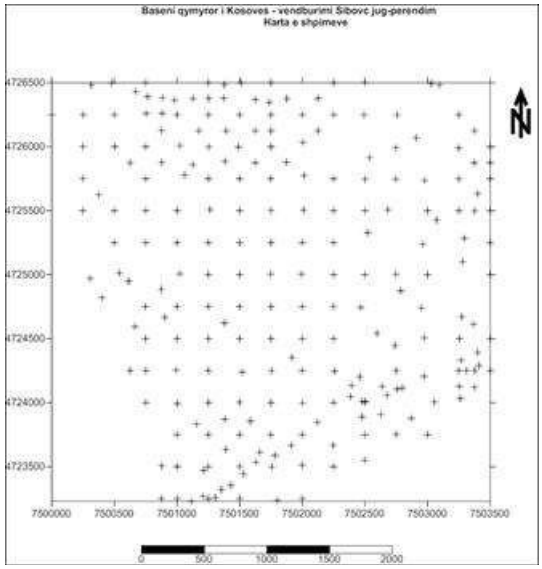

Multivariate statistical analysis - a range of multivariate statistical methods can be used to assess the relationships within multi-element data sets. These methods commonly include: correlation matrices (using linear regression to test the correlation between pairs of elements) [4] [5].

Potential correlations between the various analyses have been addressed by calculation of the Pearson product-moment correlation coefficients (table 2).

Spatial analysis - spatial analysis or spatial statistics includes a series of techniques for analyzing spatial data. Consequently, grid file used to draw the different maps (Post, Contour map and 3D surface map) for each parameter separately. At last, the illustrated maps were interpreted for analyzing of coal seam parameters.

For this porpose it is used of SURFER 9 software, by making a method, geostatistically. SURFER is a contouring and 3D surface mapping program, which quickly and easily transforms random surveying data, using interpolation, into continuous curved face contours. [6][7][8][9]. The draw maps are given in Figure 3.

Table 1: Statistical parameters of the coal seam parameters

Statistical Parameter / variables	*Top of coal seam [msl]*	*Bottom of coal seam [msl]*	*Thickness of coal seam [m]*	*Ratio overburden/coal thickness [m3/t]*	*Calorific value [kJ/kg]*	*Ash [%]*	*Sulfur total [%]*
Mean	546.35	486.89	59.57	1.09	8387.41	15.01	1.15
Standard Error	1.26	1.99	1.22	0.06	47.84	0.14	0.04
Median	543.14	480.90	62.90	0.93	8512.66	14.67	1.13
Mode	559.40	480.00	59.50	#N/A	#N/A	15.58	#N/A
Standard Deviation	19.17	28.30	17.34	0.85	623.72	1.81	0.28
Sample Variance	367.44	801.07	300.67	0.72	389030.94	3.27	0.08
Kurtosis	1.47	2.32	0.66	11.27	0.67	1.72	-0.24
Skewness	0.47	1.09	-0.89	2.77	-0.69	1.02	0.42
Range	130.90	184.22	92.30	5.82	3623.63	10.73	1.16
Minimum	494.62	430.60	2.30	0.10	6059.77	11.29	0.65
Maximum	625.52	614.82	94.60	5.92	9683.40	22.02	1.81
Sum	126206.45	98351.63	12093.37	210.12	1425860.27	2567.29	57.64
Count	231	202	203	193	170	171	50

Table 2 Correlation matrix of the coal seam parameters

	The depth of top coal seam [m]	**The depth of bottom coal seam [m]**	***Thickness of coal seam [m]***	***Top of coal seam [msl]***	***Bottom of coal seam [msl]***	***Ratio overburden/coal thickness [m3/t]***	***Calorific value [kJ/kg]***	***Ash [%]***
The depth of top coal seam [m]	**1**							
The depth of bottom coal seam [m]	**0.87**	**1**						
Thickness of coal seam [m]	-0.19	0.31	**1**					
Top of coal seam [msl]	-0.53	-0.56	-0.10	**1**				
Bottom of coal seam [msl]	-0.26	-0.60	**-0.70**	**0.80**	**1**			
Ratio overburden/coal thickness [m3/t]	0.68	0.34	-0.63	-0.43	0.07	**1**		
Calorific value [kJ/kg]	0.11	0.23	0.26	-0.25	-0.35	-0.08	**1**	
Ash [%]	-0.15	-0.24	-0.19	0.30	0.34	0.02	**-0.90**	**1**

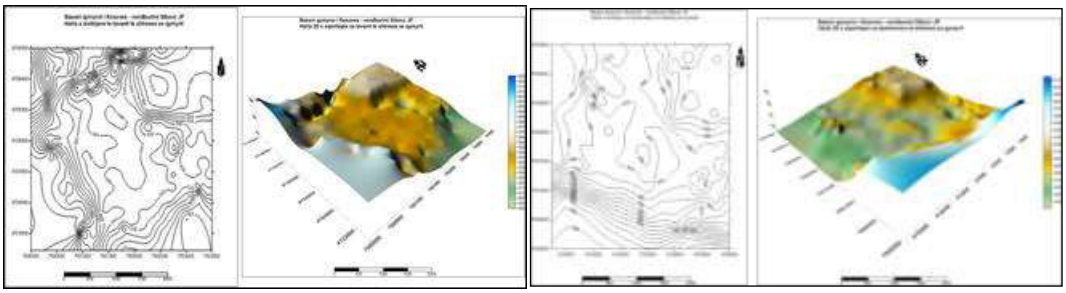

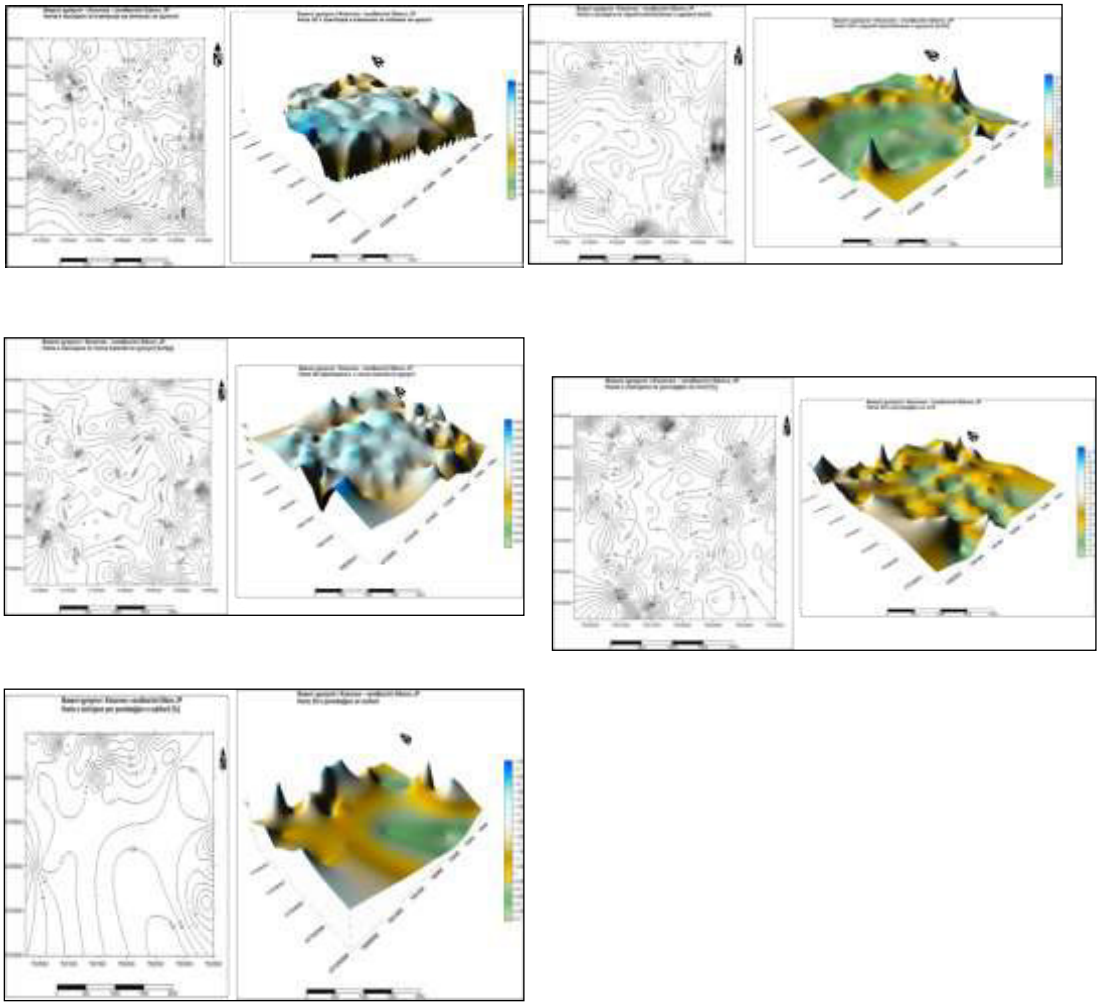

Figure 3 Contour and 3D Surface map for a) top of coal seam, b) bottom of coal seam, c) thickness of coal seam, d) ratio overburden/coal thickness, e) calorific value, f) ash content and g) sulfur content

RESULTS AND DISCUSSION

Creating grid files for each variable taken in consideration by which then are built contour maps and 3D surface maps is used kriging algorithm with linear variogram with these specifications:

The top of the coal seam appears with higher value of altitude in the northeastern and northwestern of deposit. The central part of the deposit is more consistent with the value of altitude 535-545 m. The bottom of the coal shows higher altitude in the southern part of the deposit (570 - 610m). The lowest value of bottom occurs in the eastern part of the deposit (430-450) m.

The thickness of the coal seam has spatially continuous throughout whole deposit. In the central part of the deposit thickness varies 65.0 - 75.0 m which exceeds the average for the entire deposit 59.6 m. This is confirmed by the symmetry of the left to statistical analysis. Ratio overburden/coal seam (thickness) in most part of the deposit have variation 0.6 - 1.2 m3/t with average 1.01 m3/t for all deposit.

Calorific value of the coal appears less variable in the central part of the deposit to the value of 8600 - 9100 kJ / kg. This value varies from 6059.8 - 9683.4 kJ / kg averaged 8387.4 kJ / kg (calculated at 45% moisture content). In most part of deposit ash content is 13.50 – 14.50 % which is below average (15.01 %). In most part (central and southern) sulphur is presented with the values of 0.8 - 1.1%. Higher values are in the northern part of the deposit (about 1.2%).

Very high negative correlation (r = -90) between calorific value and ash content proves spatial analysis. Correlation coefficients show that very strong positive correlations exist and among depth of top – depth of bottom coal seam (0.87), strong correlation between top – bottom (0.80), and median respectively a weak relationship between other variables [4][5].

CONCLUSIONS

This paper is a consolidation of information regarding main parameters that characterize the coal seam and its quality of southwest Sibovc coal deposit.

The thickness of the coal seam is larger in central part and decrease gonig from the east. Ratio overburden/coal seam indicate good conditions of mining the deposit.

REFERENCES

1. STEAG Consortium (2006) “Complementary Mining Plan for Sibovc SW – in Final report for KEK”, Prishtina, Kosovo.

2. Reimann C, Filzmoser P, Garret R, Dutter R (2008): Statistical Data AnalyzisExploined – Applied Environmental Statistics with R, Wiley, England.

3. Davids C J (2002) : Statistics and data analysis in Geology. Third edition. The University of Kansas. USA.

4. Peci N, Zenun Z, Krasniqi R, Sinani B, Berisha S (2014): Trace metals in stream sediment of Kosova based on statistical analysis of lead, zinc, copper, nickel, chromium and cobalt. 14th International Multidisciplinary Scientific GeoConference SGEM 2014; Volume 1, 383-390/

5. Peci N, Shala B, Maliqi G (2014): Distribution of heavy metals in stream sediments in Mitrovica region, Kosovo. International Journal of Ecosystems and Ecology Sciences (IJEES). Volume 4, issue 4/527-532.

6. Peci N, Elezaj Z, Hajra H, Mulaj S (2012): Spatial analysis of stream sediment sampling geochemical data for selected elements, volcanic complex Mitrovicë – Samadrexhë. AKTET – Journal of Institute Alb-Shkenca; Vol. V,No.2/163 – 166.

7. Peci N, Shala B, Hajra H , Baruti B (2012): Spatial analysis of the Drenica coal basin – field Skenderaj, Kosovo12th International Multidisciplinary Scientific GeoConference SGEM;/Volume III/401 – 408.

8. Surfer: Contouring and 3D surface mapping for Scientifics and Engineers. www.goldensoftware.com

9. Peci N, Hoxha I, Hajra H, Baruti B ,Mulaj S (2011): Decision making using geostatistical analysis: case studyof a Ni-silicat deposit “Çikatovë e Vjetër” – Kosovo. 11th International Multidisciplinary Scientific GeoConference, Albena, Bulgaria, 2011, Volume I, 51-58..

AKTET **ISSN 2073-2244**
Journal of Institute Alb-Shkenca **www.alb-shkenca.org**
Revistë Shkencore e Institutit Alb-Shkenca **Copyright © Institute Alb-Shkenca**

LUVISOL IN KOSOVO – AGE AND CLIMATIC CONDITIONS OF ITS FORMATION
LUVISOLE NË KOSOVË – MOSHA DHE KUSHTET KLIMATIKE TË FORMIMIT

BEHXHET SHALA[a]*, NASER PECI[a], FLURIJE SHEREMETI-KABASHI[a], GANI MALIQI[a]
a. Geology Departament, University of Mitrovica "Isa Boletini", PIM, 40000 Mitrovicë, Republic of Kosovo.
*behxhet.shala@umib.net

PËRMBLEDHJE
Në Kosovë ka shume pak hulumtime dhe informacione rreth proceseve gjeologjike të periudhës së Kuaternarit në përgjithësi, dhe kushteve klimatike të kësaj periudhe në veçanti. Një ndër treguesit e zhvillimeve të këtyre proceseve janë dëshmuar të jenë llojet e tokave dhe niveli i zhvillimit të tyre. Toka e cila është trajtuar në këtë punim është e llojit Luvisol dhe gjendet mbi depozitimet deluviale. Qëllimi i këtij punimi është dëshmimi i tokës Luvisol në Kosovë, përmes një profili mbi depozitimet deluviale afër Mitrovicës, si dhe tendenca për përcaktimin e moshës dhe kushteve klimatike të formimit. Përmes rilevimit gjeo-morfologjik të vendndodhjes së këtij profili, si dhe përshkrimit litologjik dhe analizave fiziko-kimike të secilit prej horizonteve të tij, janë nxjerr konkluzione se toka në fjalë ka filluar së formuari me përfundimin e glacialit të fundit, së paku 11,5 ka përpara kohës së sotme nën kushte klimatike mesatare të nxehta dhe me lagështi të mjaftueshme.
Fjalët çelës: Toka, Luvisole, klima, mosha, Holocen, deluvial

SUMMARY
In Kosovo there is limited research and information about the geological processes of the Quaternary period in general, and specifically about the climatic conditions of that period. One of the indicators of the development of these processes has proven to be also the soil type and level of their development. Soil type which is addressed in this paper is the Luvisol, formed on deluviale depositions. The purpose of this paper is the evidence of this type of soil in Kosovo, via a profile on deluviale deposits near Mitrovica, and attempt to determine the age and climatic conditions of its formation. Through geo-morphological survey of location, lithological descriptions of soil profile and physic-chemical analysis of each of its horizons, conclusions are that the soil in question has started its formation by the end of last glacial, at least 11 500 years BP, under temperate humid-climate conditions.
Key words: Soils, luvisols, climate, age, holocene, deluvial

Introduction

In Shupkovc of Mitrovica, near the main road Mitrovica - Pristina, by mining for construction purposes, is exposed a ca. 100 m wide and over 5 m deep sedimentation package. In the upper sediment part is noticed a soil with a good differentiated horizons. From the perspective of Quaternary geology research, soil development is of particular importance. They represent not only stratigraphic horizons, but also location indicators that characterize certain climatic conditions. This has been encouraged for the research of this soil, trying through its developmental characteristics to show the climatic conditions and the age of its formation. So far it was not found any evidence of research of soil in this context in Kosovo. In the absence of paleo-climatic data from Kosovo, as reference were taken paleo-climatic conditions in the region (mainly from the latest international research in the sediments of Ohrid and Prespa lakes), although even those are scarce. In terms of the relationship between the level of development of a land and its age, although very

carefully (taking into account the influence of local factors in the development of soil), were obtained references from Germany, lower Rheine river. This research should be understood as a first attempt of clarification of these relationships: type of soil/climatic conditions age.
According to the existing geological map (DGM 1: 100.000, Mitrovica, 2006), sediments in which the soil is developed, are quaternary fluviatile deposits (old river terrace), while the soil (according to the map of the soil of Kosovo, 1: 200.000, 2006) is a brownised Smonica in the process of brownisation. This research shows that the sediments are of deluvial type, while developed soil in them is a Luviso

Materials and Methods

Investigation of a soil in the context of the age and climatic conditions of its formation, besides lithological and physic-chemical investigation of soil, of particular importance are geological and geomorphological characteristics of the location of the soil. For this reason it was done geological and geomorphological survey of the location, lithological description of the profile, and for each of the soil horizons are analyzed some of the key indicators that show the development of the soil, as granulometry (ISO 11277:2009), pH (ISO 10390:2005), CaCO3 (ISO 10693:1995), humus and nitrogen (ISO 14235:1998).

Location morphology and geological settings

Exposed profile at elevation of 530 m a.s.l. is located in the contact area between the mountains in northeast and the alluvial plain of Sitnica river (ca. 500 m a.s.l.) in the southwest. In the first 50-70 meters is presented a slight increase of the terrain in the northeastern direction, following a significant rise of elevation. Mountains are built mainly from volcanic-sedimentary rocks complex of Tertiary and Mesozoic, while the flat part of the Holocene fluviatile deposits.
The upper part of the profile, of a thickness of ca 2,6 m, consists of layers of fine alluvial sediments. With the exception of single fragments of rocks (rarely any piece with diameter over 1 cm) consist mainly of fine sandy silt.
The bottom sediment package consist of mixed building materials, from clay to rock fragments of sizes from a few cm. Thickness of these exposed layers are reaching over 2m. Rock fragments are mostly angular or slightly rounded. In some places are dominated from rock fragments packages with poor matrix, piled and oriented in certain directions, which indicates the direction of movement of surface water and transported material. The composition of the rocks are corresponding to that found above the deposition area were from are transported.
Starting from the profile surface up to a depth of several centimeters in the lower sediment package, are presented some soil horizons which vary in color, lithology and structure.

Profile construction

First horizon from the surface (Ah) has a thickness of about 20 cm and is made up of clayey fine sand with small single rock fragments. It is permeated from grass roots and has a brown to black color, as a result of humus content (up to 4.6%, Figure 4.1). The material shows a plate structure as a result of anthropogenic activities. Downwards lies Bv_1-Horizon, brown, composed from sandy silt with a low content of clay and only single rock fragments. It has a thickness of about 50 cm and is presented with a coherent structure. The next Btv-Horizon is a light dark brown with a thickness of about 30 cm. Besides some individual rock fragments, it consists of a clayey silt layer with a coherent structure and some weak polyhedrons. Under the Btv-Horizon we have again a brown Bv_2-Horizon, which consists of silt with fine sand and coherent structure. Unlike the horizons above, below horizon Bv_2 is presented a 90 cm thick Bt-Horizon, where the clay content now reaches up to 10%. It is dark brown and has a polyhedrons structure. This horizon passes gradually downwards in the next brown Bv_3-Horizon of 60 cm thickness. The upper brown part brown, consisted from clayey fine sand with rock fragments (d>1cm), passes to the gray brown

bottom part, composed of just slightly rounded rocky fragments (with a diameter of several mm to several cm) in a clayey sandy matrix.

Besides the differentiation of Bt-Horizon in relation to the accumulation of clay and polyhedral structure, another specific characteristic is the profile decalcification. While from the top to the depth of 2.90 m calcium carbonate content is low (ca. 2%, Fig. 4.1), it increase significantly downwards (up to 8,8%), and 2,90 m can be considered as the decalcification depth. Under this horizon continues horizon C, composed from sequence layers of ca. 50 cm thickness, composed of layers of sand and rock fragments of various sizes and layers composed mainly of skeletal rocks and with poor matrix. Since the upper parts of the horizon are grey brown, in the bottom part, downwards, is dominant grey white color. Rock fragments are mostly angular and composed from quartzite, white quartz, phyllite, sericite schist, and the volcanic rocks (Quartz latite) largely weathered and loamy.

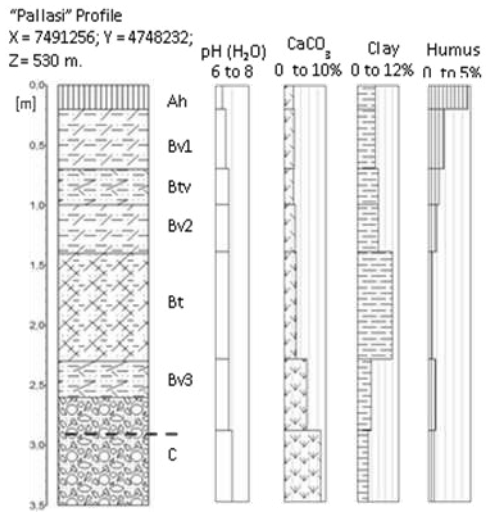

Fig. 4.1: Schematic presentation and physic-chemical analysis of the profile

Results and Discussion

Geological construction and morphology of the location shows deluviale deposits, formed under certain climatic conditions that favor strong erosion and transport. These climatic conditions are known from the cold periods, which compared to present are characterized by lower mean annual temperature and precipitation and lack of vegetation, primarily forest. During the cold climate of the last glacial (Weichselian) vegetation was primarily an open steppe assemblage dominated by grasses, Artemisia and goosefoot [5]. Under these conditions the rocks undergo physical weathering. Afterwards in the warmer phases, followed by higher precipitation and snow melting, it can come to the transport stream in the form of rocky masses flows mixed with water. These mixed rock masses are deposited at the bottom of the slopes, where the transport energy is reduced. Such climate conditions are known during the glacial periods in the Balkans. Therefore, these deposits can be described to such climatic conditions and probably during the last glacial maximum. The lowest moraine deposits of the last glacial in the region, at the elevation of 1600 m to 2200 m, are formed during the old Dryas [3]. Deposits older than this age will likely be subject to erosion of the last glacial, while during the postglacial it is difficult to say there have been such climatic conditions suitable for the erosion and transport of such magnitude. Also difference in elevation of ca. 27 m between these sediments and Sitnica alluvial plain indicates an age that is older than Holocene. During the Neogene are known fracture tectonic activities, which are characterized by vertical movement, elevation and dipping of separated blocks in the region. Kosovo basins have undergone continuous subsidence, while the surrounding mountains lifting-up with about 0.4 mm/year [10].

So considering the geological settings of these sediments and the location morphology, it can be assumed that these sediments are deposited not later than at the time of the last glacial maximum.

From lithological construction and physical-chemical analysis can be seen that these sediments have undergone chemical alteration and soil-forming processes. Decalcification has gone up to ca. 2.90 m depth. Although in the

upper horizons is present a low content of carbonates, based on the morphology of the terrain, it can be supposed that this came from re-calcification. Decalcification was followed by the processes of displacement of clay from the upper horizons and its accumulation in the Bt horizon. An issue to be discussed is the differentiation of Btv-Horizon, which shows signs of development, but analytically not clearly differentiated. If Btv would be confirmed with additional analyses (eg. mikromorphological) this would represent a double soil. In other words, after the formation of Bt has been a time of such climatic conditions that have caused erosion of the former horizons on Bt. Then in re-deposition sediments have occurred soil developing processes and are developed existing horizons (Ah, Bv_1, Btv, Bv_2). From the existing analytical data is difficult to obtain a conclusion whether the former horizons on top of Bt are eroded and then are re-deposited the present one. However, Bt horizon indicates a good development, not only for the texture, structure and color, but also the thickness. All those presented above show a mature soil.

It is known that for developing of a Luvisol are needed climatic conditions characterized by moderate temperature and sufficient moisture. Such conditions are known in the region since the early Holocene, ca. 11500 BP [4], [6]. In the absence of paleo-climatic data from Kosovo, as reference data are taken from the region, respectively from research done on Lake Ohrid and Prespa. Although carefully, based on more or less similar characteristics related to today's climate, morphology and position in relation to climate factors (the proximity to the Adriatic Sea, altitude, rain shadow of the surrounding mountain ranges) between area of lakes Ohrid & Prespa and Kosovo (squares in Fig. 5.1), paleo-climatic conditions of these two regions could be considered as comparable in the regional context. Many investigations of soils [7], [2], [8], proved the relationship between age and level of their development and therefore they play an important stratigraphic role. Soil formation processes, starting from chemical weathering of the parent material, decalcification, the formation of humus and clay to washing up and accumulation of clay, humus and sesquioxsides, are slow processes. It is known that the processes leading to the formation of Luvisole are processes of thousands of years. Soils with a developed Bt-Horizon (Luvisole) are generally considered as soils with an age not less than 5000 to 6000 years. Based on studies on the river terraces in "Niderrhein", Germany, the youngest fluviatil sediments on which soils with a Bt are formed (even less developed) are older than 5000 years [9].

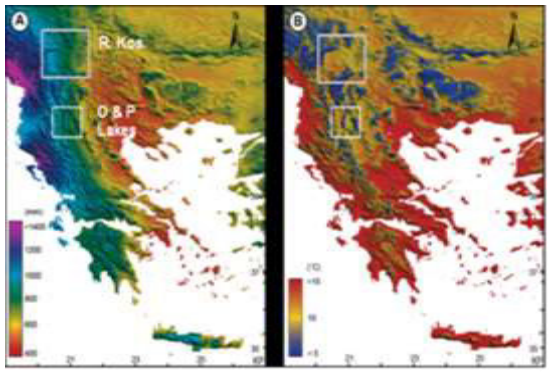

Fig. 5.1: Mean annual precipitation and temperature (modified after WorldClim; Hijmans et al., 2005 in Panagiotopoulos, 2013

Conclusion

Given the scale of soil development, geological building, geomorphological position and climatic conditions favorable to its development, it can be said that this soil has begun its formation at the latest by the beginning of the Holocene (ca. 11500 years BP). This is the time when it started the rising of temperature and precipitation by creating favorable conditions for the formation of such a soil. To conclude, if we have to do with a double soil, more detailed research is required

Literature

1.Beak Consultants GmbH (2005): Kosovo Geoscientific Maps – Geological Map – Pilot map, Report.

2.Brunnacker K (1978b), Der Niederrhein im Holozän. Fortschr. Geol. Rheinl. u. Westf., 28, 399-440, Krefeld.
3.Kuhleman J, Milojevic M, Krumrei I, & Kubik WP (2009), Last glaciation of the Šara Range (Balkan peninsula): Increasing dryness from the LGM to the Holocene. Austrian Journal of Earth Sciences Volume 102, 146-158, Vienna.
4.Leng JM, Baneschi I, Zanchetta J, Wagner B, und Vogel H (2010), Late Quaternary palaeoenvironmental reconstruction from Lakes Ohrid and Prespa (Macedonia/Albania border) using stable isotopes. Biogeosciences Discuss. 7, 3815–3853.
5.Morley M, (2007), Mediterranean quaternary rockshelter sediment records: a multi-proxy approach to environmental reconstruction, Dissertation. Department of geography, University of Manchester.
.
6.Panagiotopoulos K (2013), Late Quaternary ecosystem and climate interactions in SW Balkans inferred from Lake Prespa sediments, Dissertation. Köln.
7.Schirmer W (1983), Die Talentwicklung an Main und Regnitz seit dem Hochwürm. Geol. Jb., A 71, 11-43. Hannover.
8.Schroeder D (1983), Beziehungen zwischen Stratigraphie und Bodengenese bei Hochflutlehmen des Niederrheins. Geol. Jb. A 71, 73-107. Hannover.
9.Shala B (2001), Jungquartäre Talgeschichte des Rheins zwischen Krefeld und Dinslaken, Dissertation. Duesseldorf.
10.Stanic N, Markovic M, Pavlovic R, Komarnicki (1997), Neotectonic investigations in the Kosmet area, Proceedings of the Field Meetings in Yugoslavia. Spec. Publ. Geoinstitute, No. 21, p. 71-77. Belgrade

AKTET **ISSN 2073-2244**
Journal of Institute Alb-Shkenca **www.alb-shkenca.org**
Revistë Shkencore e Institutit Alb-Shkenca **Copyright © Institute Alb-Shkenca**

DETERMINATION OF WEIGHT CHANGE IN MARBLE WITH ULTRASONIC MEASUREMENTS DURING FREEZE – THAW CYCLES

PËRCAKTIMI I NDRYSHIMIT TË MASËS NË MERMER PËRMES MATJEVE ME ULTRATINGUJ GJATË CIKLEVE NGRIRJE - SHKRIRJE

FLURIJE SHEREMETI-KABASHI[a]*, BEHXHET SHALA[a]
a. Geology Departament, University of Mitrovica "Isa Boletini", PIM, 40000 Mitrovicë, Kosovo.
flurije@lycos.com

PËRMBLEDHJE

Kërkimi ka pasur qëllim përcaktimin e ndryshimit të masës së mermerit gjatë 100 cikleve ndërruese ngrirje – shkrirje. Matjet janë zbatuar në bërthama të mermerit Carrara me gjatësi 7cm dhe diametër 4,5cm, nga projekti internacional EUROMARBLE. Gjatë këtyre matjeve është regjistruar humbja e masës në bërthama të mermerit pas çdo cikli të dhjetë në fazën e shkrirjes. Po ashtu, në çdo bërthamë është regjistruar edhe ndryshimi i strukturës përmes matjeve me ultratinguj. Provat e hulumtuara tregojnë dukshëm ndikimin e cikleve ndërruese ngrirje – shkrirje në ndryshimin e strukturës së mermerit. Provat humbin në peshë në mes 0,12% dhe 0,17%, derisa shpejtësia e ultratingujve në mes provave në gjendje të thatë dhe të ngopura me ujë ndryshon në mes 1,14 dhe ,1,8 Km/s. Me rritjen e cikleve në prova e mermerit rriten mikroçarjet dhe poroziteti. Rritja e shpërndarjes së poreve dëshmohet edhe me vrojtimet me mikroskopinë elektronike me skanim.
Fjalët çelës: mermer, ndryshimi i masës, matjet me ultratinguj.

SUMMARY

The aim of the research was to assess the determination of the weight change of marble during the 100 freeze – thaw cycles. Measurements were carried out on Carrara marble core 7 cm length and 4.5 cm diameter, from EUROMARBLE international project. During these measurements are registered weight losses in the cores of marbles after each ten cycles in the thaw phase. Also, in each core is registered the change of structure with ultrasonic measurements. The studied samples show clearly the influence of the freeze - thaw alternate cycles in change of structural in marble. The samples lose weight between 0.12% and 0.17%, while the ultrasonic velocity varies in the dry state and saturated with water between 1,14 and 1,8 km/s. With increasing the cycles grow in marble core samples microcracks and the porosity. Increased distribution of pores is also evidenced by observations with the scanning electron microscope.
Key words: marble, weight change, ultrasonic measurements.

1. INTRODUCTION

As in Europe and beyond it, a major part of the cultural heritage of every nation is formed from marble. Currently are more than 200 marbles species in all five continents in the trade, that use for different kinds of monuments, buildings, sculpture, and especially for facades (Siegesmund et al. 2008). However, since the last century, the rate of decay of marble is increasing. Marbles in the open air are greatly affected by climatic conditions and air pollutants. Environmental pollution, which influences rock surfaces over the last decades, increases weathering processes. On the other hand, changes in temperature and freeze thaw successions can cause stone to lose their strength and finally the breakdown of a whole structure. The bending of marble plates is not only observed on historic tombstones but

also on modern buildings like Finlandia Hall in Helsinki (Ritter 1992). The weathering phenomena of marble are still under discussion. According to several authors (Neumann 1964, Quervan 1967, Widhalm, 1996, Siegesmund 2002), the insolation, thermal expansion, freeze cracking are responsible for the deterioration of crystalline marbles. Rock fabric controls the mechanical and physical properties such as porosity and permeability. Although marble is a dense material, due to the pore size distribution, which often exhibits a maximum at 10 µm (Poschlod 1990), the water can penetrate deep into the pore spaces (Snethlage et al. 1999). When water freezes in porous stones occurs frost cracking due to a 9% volume expansion. The aim of this study is to determine experimentally the influence of the 100 freeze – thaw cycles on marble deterioration. Ultrasonic velocity as non-destructive method allows to determine the degree of deterioration because ultrasonic velocity decreases with increasing loosening of crystal contact planes (Sheremeti-Kabashi at al 2000). So it is very important to find out whether ultrasonic velocity can be used to determine the weight change in marble.

2. MATERIALS AND METHODS

2.1. Sample material

For the investigations were carried out Carrara marble cubes of 20 x 20 x 20 cm, core 7 cm length and 4.5 cm diameter, from EUROMARBLE exposure program. In the text and figures are designated with the following abbreviations:
P6: fresh, unweathered cube
6A1, 6B1, 6C1, 6D1, 6E1: drill cores, taken from fresh cube P6

2.2. Ultrasonic measurements

For the petrophysical investigations and the determination of the change of the structure with ultrasonic measurements on each core, arbitrary measurement directions were plotted. All measurements were carried out with an Ultrasonic USME-C from Krompholz/Pirna using an emitter with 46 KHz frequency, in Labor Dr. Ettel & Dr. Schuh, in Munich. For explanation, the methodology of measurement on the drill cores is depicted in figure 1.

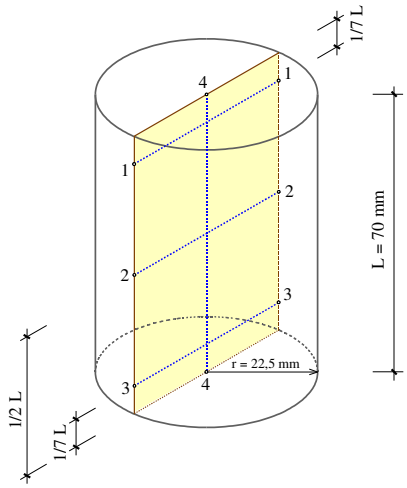

Figure 1: Position of the ultrasonic measurement directions in the drill core

2.3. Freeze – thaw cycles

The long-term freeze-thaw cycles has been carried out according to DIN 52104.
Sample preparation: drying to constant weight at 105 ° C; cooling down at room temperature; total saturated with water under atmospheric pressure
Experimental Procedure: freeze - thaw cycles; storage of samples under water in plastic cans; long-term cycles 100, 12 hours freeze of -30 ° C and 12 hours thaw + 30 ° C;
Experimental evaluation: determination the loss of weight by weighting after each ten cycles in thaw phase and determination the change of weight by using non-destructive measurements of the ultrasonic wave

2.4. Scanning electron microscopy

For the observe the loss of cohesion along grain boundaries of calcite crystal after freeze- thaw cycles were made preparates and analyzed by scanning electron microscopy (SEM), DSM 960 A, in LMU, in Munich.

3. RESSULTS AND DISCUSSION

3.1. Freeze – Thaw process

As shown in figure 2, each marble drill core, during the freeze - thaw cycles is affected with the loss of weight and the change of ultrasonic velocity. After each cycle can be concluded that a significant mass loss corresponds a decrease in ultrasonic velocity. Köhler (1988) introduced ultrasonic velocity for assessing the degree of weathering of marble. He established the following scale:

quarry fresh marble	$v_p > 5$ km/s
good state	$v_p = 4 – 5$ km/s
acceptable state	$v_p = 3 – 4$ km/s
beginning destruction	$v_p = 2 – 3$ km/s
endangered state	$v_p = 1 – 2$ km/s
total structural disintegration	$v_p < 1{,}5$ km/s

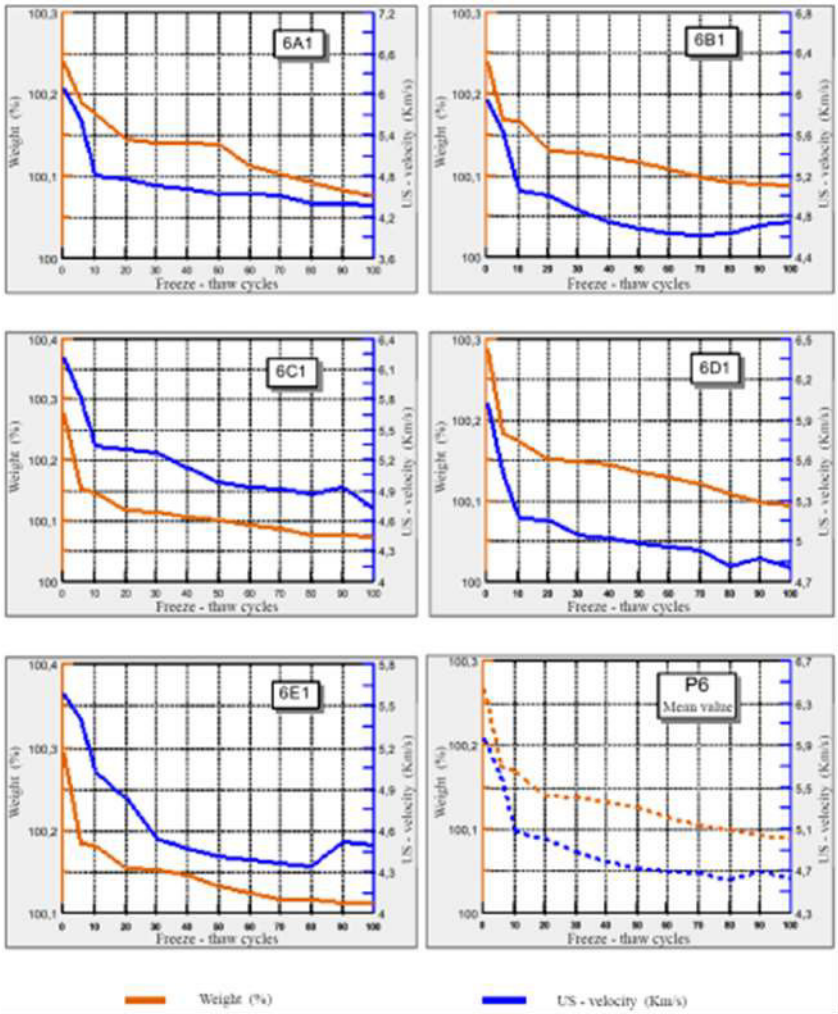

Fig. 2: Change of weight and ultrasonic velocity in marble sample P6

The deterioration of marble drill core during freezing depends on the pore size distribution and the water saturation. The boundary between the macro and micro pores is about 0.1µm. Whether a stone contains more small pores or less large pores, is a fundamental difference

(Fitzner 1988). In the case of marbles the pore size in the unweathered samples has a maximum between 0,08 and 0,8 µm with total pore volume 8,33 % , but after the 100 freeze - thaw cycles the pore size increases to 0,2µm with total pore volume 14%. (Sheremeti-Kabashi at al 2012). Also presence of capillary pores with pore size > 0,5µm and well connected to each other enables penetration of water deep into the stone (Thomachot 2002). When water freezes and the ice expands in the pore spaces weakens the stone fabric, respectively crystal contact planes. The calcite crystal shows an extreme anisotropic thermal expansion, with value $\alpha = 26 \times 10^{-6\ K-1}$ parallel and $\alpha = -6 \times 10^{-6}\ K^{-1}$ perpendicular to the c-axis (Kleber 1959). The irregular expansion and contraction of calcite crystals during the heating and cooling under dry and water saturated causes a detachment of the grains and disintegration of the structure. On the other hand, in the calcite crystal ultrasonic velocity shows maximum of v_p = 7,73 km/s parallel to the a-axis and a minimum of v_p = 5,71 km/s parallel to c-axis. As measurements show, the progressive loss in weight in all drill core, 6A1. 6B1, 6C1 and 6E1 are caused by progressive microporosity, respectively the loss of shape and cohesion along calcite crystals boundaries due to the crystallization pressure of the ice growth (Ondrasina 2002). To weight loss corresponds very well the decrease of ultrasonic velocity. The highest and rapid decrease of ultrasonic velocities and weight loss can be observed between 1 and 10 freeze - thaw cycle, because the pore size distribution increases and freezing in this period is most effective (Sheremeti – K. at al 2012) A small difference in change of weight and ultrasonic velocity values is observable between 30 and 80 cycle .From cycle 80 can be seen an increase of ultrasonic velocity by decrease of loss weight of marble samples, depending on pore size distribution. After 100 freeze - thaw cycles, all the drill cores showed weight and ultrasonic velocity change. The average value of the loss weight of marble sample P6 is 0,15%. In the case of ultrasonic velocity, in saturated samples, the average value increased from 4,64 km/s (dry state) to 5,97 km/s (wet state), so 28,7%. After 100 freeze-thaw cycles the average us-velocity has dropped by 4,39 km/s (wet state) and 2,98 km/s (dry state), respectively 26,5% and 32,1%. The average us-velocity of samples P6 plot in the range of 2,0 – 3,0 km/s, beginning destruction (according to Köhler scala).

3.2. Scanning electron microscopic analysis

The observations with electron microscopy (figure 3) show big change in marble fabric after 100 freezes - thaw cycles. Petrographic sections of the rock samples demonstrated microfracturing and the loss of cohesion along calcite crystals boundaries due freeze-thaw process. As can be seen from figure the crack propagation occurs more along grain boundaries (intergranular) and microcracks are interconnected, which helped water absorption of the sample. But it can also be clearly seen the cracks in grain (intragranular). Marble with predominant intergranular cracks or often with mixed intergranular and intragranular cracks, in the case of well oriented marble is a dangerous type of stone with low strength, so in many cases it is necessary conservation (Sheremeti-K. at al 2011)

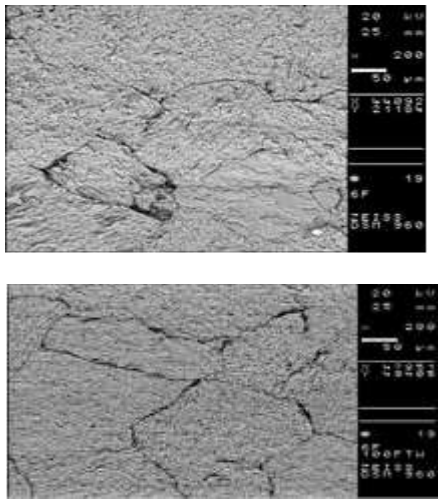

Fig. 3: Observations with the scanning electron microscope in marble P6 sample before and after 100 freeze- thaw cycles

4. CONCLUSION

The development of non-destructive test methods for time is an important research goal. The investigations demonstrate that the non-destructive character of ultrasonic velocity is appropriate to assess the weathering of marble. The method, however, requires measurements in lot of directions of a marble samples. By this method it is possible to calculate the breakdown of marble by the growth of ice within cracks, because ultrasonic velocity decreases with increasing total porosity. The results obtained from ultrasonic velocity correspond very well with measurements of the weight change of marble during freeze - thaw cycles. Weight change due to freeze-thaw process of 0,15% attenuates ultrasonic velocity in marble sample about 1,5 km/s. This method it is more influenced by the loosening of crystal contacts and can therefore be interpreted as a measure for decay evolution that confirms Köhler scala.

5. Ackonowledgement

F. Sh. K. thanks the DAAD, Prof. dr. Rolf Snethlage and Labor Dr. Ettl & Dr. Schuh for generously support.

6. REFERENCES

1. DIN 52104 Frost-Tau-Wechsel-Versuch.

2. Fitzner B. (1988) Untersuchung der Zusamm. zwischen dem Hohlraumgefüge von Natursteinen und physikalischen Verwitterungsvorgängen.Mitt. Ing. U. Hyd. 29, Aachen.

3. Kleber W. (1959)Einführung in die Kristallographie, VEB Verlag Technik, Berlin.

4. Köhler W. (1988) Preservation Problems of Carrara Marble Sculptures in Postdam, proceeding VI Intern. Congress on Deterioration and Conservation of Stone, Torun.

5. Neuman R. (1964) Geologie für Bauingenieure, Berlin.

6. Ondrasina J., Kirchner D., Siegesmund S. (2002) Freeze-thaw cycles and their influence on marbledeterioration, a long term experiment, Geo. Soc. Spec. Publ, 205, 8-17.

7. Poschlod K. (1990) Das Wasser im Porenraum kristalliner Naturwerksteine und sein Einfluss auf die Verwitterung, Diss. LMU, München.

8. Quervain F. (1967) Technische Gesteinskunde, Basel.

9. Ritter H. (1992), Marmorplatten sind falsch dimensioniert, Stein, 1, 18-19.

10. Siegesmund. S. (2008) Das Marmor-Problem, Naturstein 9, 96-101.

11. Siegemund S., Weiss T., Vollbrecht A. (2002) Natural Stone, Weathering Phenomena, Conservation Strategies and Case Studies, Introduction, Geo. Soc. Spec. Publ. 205, 1-7.

12. Sheremeti-K. F., Snethlage R.., Shala B. (2012) Përcaktimi i shpërndarjes së madhësisë së poreve në mermerin e alteruar dhe të freskët, Aktet V, 2 179-185.

13. Sheremeti-K. F., Snethlage R. (2000) Determination of srtuctural anisotropy of Carrara marule with ultrasonic measurements, 9th Intrnational Congress on Deterioration of Stone, Venice, 247-253.

14. Sheremeti-Kabash F,. Snethlage R. (2000) Determination of srtuctural anisotropy of Carrara marule with ultrasonic measurements, 9th Intrnational Congress on Deterioration of Stone, Venice, 247-253.

15. Snethlage R., Ettl H., Sattler L. (1999) Ultraschallmessungen an PMMA-getränkten Marmor Skulpturen, Z. dt. geol. Ges., 150/2, 387-396.

16. Thomachot C., Jeannete D. (2002) Evolution of the petrophysical properties of two types of Alsation sandstone subjected to simulated freeze-thaw conditions, Geo. Soc. Spe. Publ> 205, 19-32.

17. Widhalm C., Tshegg E., Eppensteiner W. (1996) Anisotropic thermal expansion causes deformation of marble cladding, ASCE, 10, 5-10..

AKTET
Journal of Institute Alb-Shkenca
Revistë Shkencore e Institutit Alb-Shkenca

ISSN 2073-2244
www.alb-shkenca.org
Copyright © Institute Alb-Shkenca

MECHANICAL WAVE ERTHQUAKE-GENERATED IN ADRIATIC SEA

ADISA DABERDINI[1], RRAPO ORMËNI[2]
Institute of GeoSciences, Energy, Water and Enviroment, UPT, Tirana, Albania
E-mail: adisadaberdini@hotmail.com, rrapo55@yahoo.com

SUMMARY
This study shows a general model of earthquake-generated mechanical wave in Adriatic Sea, and a adaption of the studied earthquake scenario in this sea. We selected six extended areas with potencial source. For each area it was set a reliable maximal earthquake. After the event accuring, we saw the simulated wave in these areas. Simulations were based in the non linear equations solved. For each event we calculated the wave, maximal height of water and the time of movement toward te coast in the secelted object near a in the Adriatic Sea. To perform this study, we calculated the expected impact, and maximal wave which is generated during an earthquake in the areas with a hight impact. Our approach is based in regional techtonical data of Adriatic coast, and their expexted impact. This study showed that some baromethrical features are decisive in the determination of mechanical move energy of tsunami.
Key words: mechanical wave, earthquake, earthquake in the Adriatic Sea, tsunam.

INTRODUCTION

The Adriatic Sea is an elongated basin stretching NW-SE in the central Mediterranean Sea. It has been struck several times by tsunamis. The northwestern portion of the Adriatic basin is also the most vulnerable because of its large low-topography coastal area extending for over 150 km. From the regional tectonics standpoint, the Adriatic Sea falls in the middle of the Adria plate that is being pushed by Africa northward against stable Europe. (ALIAJ, S., The Albanian orogen: Convergence zone between Eurasia and the Adria microplate.) Overall, the Adria is affected by active compression and overridden by thrust belts on all sides. The purpose of this work was to assess systematically the potential threat posed by earthquake–generated tsunamis on the Albanian coastline of the Adriatic Sea, following the approach proposed by LORITO et al. (2008). To this end, we first compiled a database of potentially-tsunamigenic earthquake faults, then used them as input in the preparation of scenarios of maximum water height (above mean sea level) based on numerical simulations of tsunami propagation. Potential tsunami sources were selected from the seismogenic sources listed in version 3.0.4 of the Database of Individual Seismogenic Sources (DISS WORKING GROUP, 2007; BASILI et al., 2008), adapted to the modeling needs and integrated with additional data, particularly for the eastern side of the basin. Our scenarios supply at-glance information of the expected tsunami impact onto the target coastline and can be progressively updated as knowledge of earthquake source advances. As such, our approach can be easily converted into an application program for disaster prevention from which results can be handed out to a variety of stakeholders, such as civil protection agencies or land-use planners. The results of our work include the determination of the maximum water height along of the Adriatic Albanian coastline calculated for six source zones located inside or very close to the Adriatic Sea. All profiles of maximum water heights are given in aggregated form together with averages and standard deviations. Maxima were also classified in a three level code of expected tsunami threat. Finally, we

explored the role of specific bathymetric features in controlling the focalization-defocalization of tsunami energy.

Fig.1. Tectonic sketch map of the Adriatic basin. The double-headed arrow indicates the floating path of the Typical Faults. a) Coastal and Offshore Croatia; b) Montenegro; c) Albania – Northern Greece; d) Northern Apennines; e) Apulia; f) Kefallonia-Lefkada.

1. METHOD

To assess the potential threat posed by earthquake-generated tsunamis in the Adriatic Sea we adopted the method developed by LORITO et al. (2008). We systematically carried out a number of simulations for all source zones that can possibly affect the target coastlines. A Source Zone (SZ) includes an active tectonic structure at regional scale that is made up of a number of individual fault segments, each one capable of releasing a significant earthquake. For each SZ we identified a Maximum Credible Earthquake (MCE) and an associated Typical Fault (TF). We let the TF float along the entire SZ and computed a tsunami scenario at regular intervals. To assess the MCE for each SZ we selected the largest earthquake that has ever occurred in that zone and for which there exists, or is possible to obtain, a reliable magnitude estimation. The TF is defined by parameters that must comply with both the seismological properties of the MCE and the tectonic properties of its parent SZ. Strike, dip and rake were slightly adjusted as needed to account for the internal geometric variations of the SZ at each position of the TF. The amount of slip was derived from the seismic moment of the MCE, using the formulations by KANAMORI and BRODSKY (2004). Steps were taken at one or half fault length to guarantee a sufficient spatial sampling of the tsunamigenic structure. At each new position the TF was made to release its MCE by uniform slip over the entire fault plane. The initial seawater elevation associated with the earthquakes generated by the floating TF was assumed equal to the coseismic vertical displacement of the sea bottom computed according to OKADA's (1985, 1992) formula. Rupture was assumed to be instantaneous, and the initial velocity field was assumed to be identically zero. For the numerical modeling of the tsunami propagation we used the nonlinear shallow water equations that were solved numerically by means of a finite - difference method on a staggered grid (MADER, 2001). We set the boundary conditions as pure wave reflection at the solid boundary, by setting to zero the velocity component perpendicular to the coastline. Full wave transmission was set at the open boundary (open sea). The sea-floor topography was taken from the ETOPO2 bathymetric data set (SMITH and SANDWELL, 1997), that we oversampled at 0.5 arcmin to achieve a sufficient sampling of the wave features. We fixed a minimum depth of 10 meters, then modified all shallower bathymetry accordingly. We performed a distinct numerical experiment for each fault position in each SZ. From each simulation we extracted the maximum water height above sea - level (HMAX) profiles along the Adriatic coasts. The HMAX was calculated at the points adjacent to the coastline, that is at a fixed water depth of 10 meters. The HMAX values along the target coastline were then grouped according to the causative source zone. For each group we then calculated the absolute maximum, the average, and the standard deviation of the HMAX values. Finally,

we set three HMAX thresholds at 0.05, 0.5, and 1.0 m and coded the different levels of threat as marine, land and severe land threat, respectively. Nevertheless the HMAX represents an average coastal level that is certainly appropriate for comparing risk levels and for tsunami preparedness, provided that a caveat is included specifying that the wave height can be locally higher (CAPUTO, M., and FAITA, G. 1984).

1.2 TSUNAMIGENIC SOURCE ZONES IN THE ADRIATIC SEA

The Adriatic Sea is mostly surrounded by active fold-and-thrust belts and strike-slip faults. Frequent earthquakes occur along these well-known fault zones, most of which run close to the coastlines or in the open sea and are thus potential sources for tsunamis. The largest earthquakes (M > 7) occurred near the eastern margin of the central Adriatic Sea, along the Montenegro portion of the Dinaride-Albanide chain, and at the southern end of the basin near the Ionian Islands along the Kefallonia-Lefkada rightlateral shear zone. Most of the remaining structures exhibit a potential for earthquakes of magnitude 6 B M B 7, thereby holding a significant tsunamigenic potential. This section describes the local tectonic setting of the six selected Source Zones grouped into four major tectonic domains. The reasoning followed to define the Typical Fault (TF) of each zone will also be illustrated.

1.3 DINARIDES, ALBANIDES AND HELLENIDES

A contractional belt longer than 1,000 km runs along the eastern margin of the Adriatic Sea from the southern Alps, to the north, to the Kefallonia-Lefkada Fault, to the south. This fold-and-thrust belt is usually split into three different domains named Dinarides, Albanides and Hellenides, respectively from north to south, that started forming as a consequence of the subduction of Adria under the European plate. Adria acts as an indenter pushing northward into stable Europe. Stronger earthquakes mostly concentrate in the Albanides and Hellenides. The outer portion of these chains is partly located offshore and characterized by numerous thrust fronts that all seem to be currently active. Available focal mechanisms indicate predominant SW-NE shortening; reverse faulting earthquakes dominate

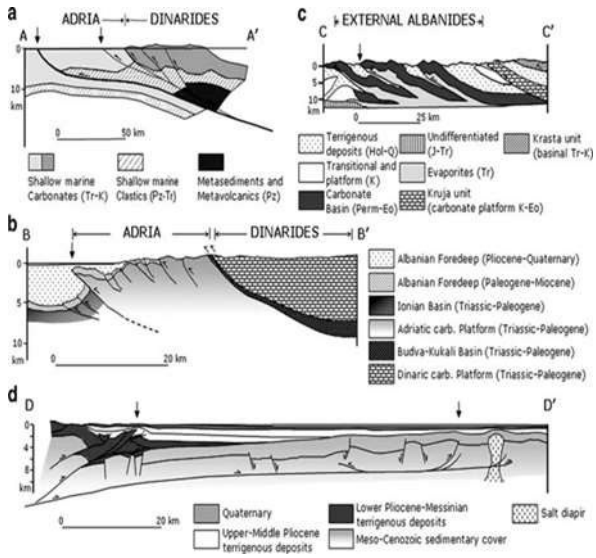

Fig. 2. Cross sections of the main thrust structures. Vertical arrows indicate the position of the active fronts selected for the modeling. a) Dinarides and; b) Montenegro; c) Northern Albania offshore; d) Northern Apennines.

Albania — Northern Greece. In the southern Adriatic Sea, the submerged edge of the Apulia platform acts as an indenter in the European plate. Here continental collision creates a series of NW-SE thrusts fronts involving the Apulian platform itself (Fig. 1), occasionally interrupted by NE-SW strike-slip faults. Seismic profiles image the solethrust at about 10 km depth. The Albania offshore is characterized by shallow instrumental seismicity with many 4 < M < 5 earthquakes (DUNI et al., 2003), although numerous larger events (up to MW 6.8) are reported by historical catalogues (e.g., PAPAZACHOS and PAPAZACHOU, 1997). The offshore area of northern Greece is also characterized by shallow seismicity, nonetheless events in the magnitude range of 6 to 7 are frequent. Most earthquakes exhibit reverse focal mechanisms over NW-SE planes both in Albania and northern Greece. We

identified the Albania - Northern Greece SZ (Table 1) as made of three segments that cover the set of thrust fronts with the highest potential for tsunami generation.

Source Zone	L (km)	W (km)	D (km)	Slip (m)	Strike (deg)	Dip (deg)	Rake (deg)	MCE (Mw)
Coastal Croatia	16	7	1	0.6	312	40	110	6.1
Offshore Croatia	11	6.6	2	0.6	305	45	80	6
Montenegro	50	20	1	2.5	312	35	82	7.2
Albania-N Greece	36.2	16	1	2	337	35	96	7
Northen Apennines	12	8	2.5	0.6	140	30	90	6.1
Apulia	34	15	1	0.9	275	80	173	6.7
Kefallonia-Lefkada	110	18	3	2	27	60	162	7.3

Table 1. Summary of parameters of the Typical Faults shown in Fig 1. L: fault length; W: fault down-dip width; D: depth of top edge of fault below sea level. MCE: Maximum Credible Earthquake for the given fault

2.MODELING RESULTS

We analyzed the tsunami impact expected on the Adriatic coasts of Italy as a result of earthquakes generated in each of six independent SZs. All tsunamis generated by a single SZ were grouped together. The corresponding HMAXs expected along the Adriatic coastline of Albania are shown as profiles of their maximum, average and average plus one standard deviation, respectively. Abscissa values are distances along the coastline and increase from south to north from an arbitrarily chosen starting point since the true length of coastlines depends on the yardstick used, these are not intended to be accurate distances but rather a practical way to map the HMAXs values along the coastline. We also emphasized the threat level by color coding the background of each diagram. We decided to adopt a three-color code: yellow for marine threat, corresponding to 0.05 m < HMAX < 0.5 m; orange for land threat, corresponding to 0.5 m < HMAX < 1 m; red for severe land threat, corresponding to HMAX > 1 m. This choice is coherent with the approach followed by ALLEN and GREENSLADE (2007), who proposed a three-level stratified warning method and set a threshold of 0.5 m between marine and land threat based on WHITMORE (2003).

3. DISCUSSION

We investigated the potential effects on the Albanian coasts of the Adriatic Sea for all the earthquake source zones that are known to be capable of generating tsunamis. To this end we used an approach that combines a detailed knowledge of the tectonic setting of the source zones with the evaluation of the tsunami impact onto the target coastline. This was done by introducing the concept of a typical fault that is sized after the maximum credible earthquake of the area and is let floating along its parent source zone. By displaying the aggregated HMAX values throughout target coastlines our method allows an easy comparison between the effects of different source zones and shows the relative level of tsunami threat for different stretches of the coast. The results of our modeling could also serve as input data for detailed studies of local effects, provided that finer bathymetry data are available. The purpose of our work is to provide an estimation of HMAX for an earthquake occurring at any position along a known source zone rather 2132 M.M. Tiberti et al. Pure appl.

geophys., than just for a specific past earthquake. Historical tsunamis of the Adriatic Sea were recently reviewed by PAULATTO et al. (2007), who also carried out simulations for a set of earthquakes in six potential source zones. Their approach, however, substantially differs from ours as the earthquake sets are defined considering three magnitude values and three depth values at two locations, inland and offshore, for each source zone; the results are then shown in terms of maximum water height and arrival time at selected localities (MARAMAI, A., GRAZIANI, L., and TINTI, S. (2007)).

4.CONCLUSIONS

Following the approach proposed by LORITO et al. (2008) we defined a maximum credible earthquake and an associated typical fault for each of six source zones potentially threatening the Adriatic coasts of Italy with sizable tsunamis. For each of the zones we let a pre-defined typical fault float along the entire source zone and computed a tsunami scenario at regular intervals. We then aggregated the maximum water heights above the mean sea level of each source zone and performed calculations of their maxima, averages and standard deviations along the target Adriatic Sea coasts of Albania. We finally coded the resulting tsunami threat for three different levels defined as: marine, land and severe land, shown in yellow, orange and red, respectively. We also found that some bathymetric features are crucial in determining the focalization defocalization of tsunami energy. We also compared the threat posed by the investigated sources to that associated with earthquake sources in the Hellenic Arc. We found that the latter is potentially more destructive than the former, although the effects of small local sources can outpace those of the Hellenic Arc sources at specific locations. This is partly due to bathymetric effects, which can either reduce or enhance the threat posed by sources falling at specific locations. We believe our results can be a valuable guidance for designing early warning systems, assessing risk and planning land-use for the coasts of Albania.

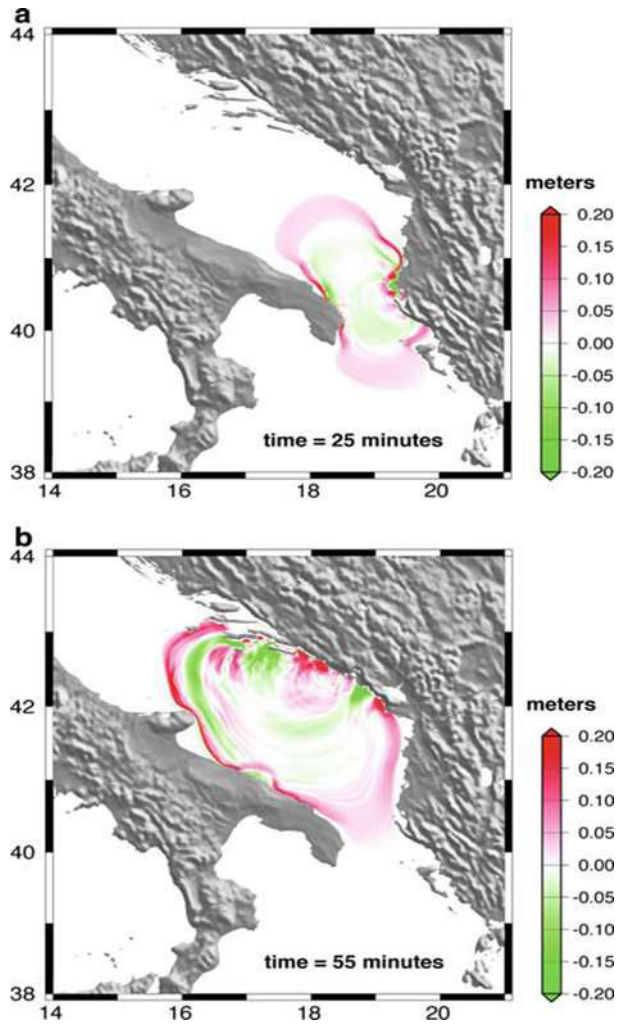

Fig. 3. Snapshots of the tsunami wave height for two selected faults: a) in the Albania–Northern Greece SZ; b) in the Montenegro SZ.

REFERENCES

ALIAJ, S., The Albanian orogen: Convergence zone between Eurasia and the Adria microplate. In The Adria Microplate: GPS Geodesy, Tectonics and Hazards (eds. Pinter N. et al.) (Springer, Netherlands 2006) pp. 133–149.

ALJINOVIC´ , B., PRELOGOVIC´ , E., and SKOKO, D. Tectonic processes on the contact of the Adriatic Platform and theDinarides in the area of the Northern Dalmatia, Conf. on Mechanics of

Jointed and Faulted Rock, Inst. Of Mech/Tech. Univ. of Vienna, Proc. (A. A. Balkema, Rotterdam/Brookfield, 1990) pp 179–182.

BASILI, R., and BARBA, S. (2007), Migration and shortening rates in the northern Apennines, Italy: Implications for seismic hazard, Terra Nova 19, 462–468, doi: 10.1111/j.1365-3121.2007.00772.x.

CAPUTO, M., and FAITA, G. (1984), Primo catalogo dei maremoti delle coste italiane, Atti Accademia Nazionale dei Lincei, Memorie Classe Scienze Fisiche, Matematiche, Naturali s. VIII 17, 213–356.

DEL BEN, A. (2002), Interpretation of the CROP M-16 seismic section in the Central Adriatic Sea, Mem. Soc. Geol. It. 57, 327–333.

DE MARTINI, P. M., BURRATO, P., PANTOSTI, D., MARAMAI, A., GRAZIANI, L., and ABRAMSON, H. (2003), Identification of tsunami deposits and liquefaction features in the Gargano area (Italy): Paleoseismological implication, Ann. Geophys.-Italy 46, 883–902.

DRAGAS˘EVIC´ , T. (1983), Oil geologic exploration in the Montenegro offshore in Yugoslavia, Nafta 7–8, 397–404.

.

FINETTI, I.R., and DEL BEN, A., Crustal tectono-stratigraphic setting of the Adriatic Sea from new CROP seismic data. In CROP, Deep Seismic Exploration of the Mediterranean Region (ed. Finetti I R.) (Elsevier, 2005) pp. 519–547.

HERAK, M.J. (1991), Dinarides. Mobilistic view of the genesis and structure, Acta Geologica 21, 35–117.

KUK, V., PRELOGOVIC´ , E., and DRAGIC˘ EVIC´ , I. (2000), Seismotectonically Active Zones in the Dinarides, Geologica Croatica 53, 295–303.

MARAMAI, A., GRAZIANI, L., and TINTI, S. (2007), Investigation on tsunami effects in the central Adriatic Sea during the last century – A contribution, Nat. Hazards Earth Syst. Sci. 7, 15–19.

MARKUS˘IC´ , S., HERAK, D., IVANC˘ IC´ , I., and SOVIC´ , I. (1998), Seismicity of Croatia in the period 1993–1996 and the Ston-Slano earthquake of 1996, Geofizika 15, 83–101.

“Modeli i Shpejtesive te valeve Sizmike”-Institute of Geoscience, Ormeni 2008.

AKTET **ISSN 2073-2244**
Journal of Institute Alb-Shkenca **www.alb-shkenca.org**
Revistë Shkencore e Institutit Alb-Shkenca **Copyright © Institute Alb-Shkenca**

THE EFFECT OF SHAPE FACTOR AND MATERIAL PROPERTIES TO THE STIFFNESS OF SEISMIC ELASTOMERIC ISOLATORS
NDIKIMI I FAKTORIT TË FORMËS DHE PARAMETRAVE TË MATERIALEVE NË NGURTËSINË E IZOLATORËVE SIZMIK ME GOMË TË ARMUAR

AGIM SERANAJ
Departamenti i Mekanikës së Strukturave, Fakulteti i Inxhinierisë së Ndërtimit,
Universiteti Politeknik i Tiranës, Shqipëri
agimseranaj@yahoo.com

Përmbledhje - Si rezultat i përpjekjeve të shumta të inxhinierëve drejt aplikimit të izolimit sizmik në bazë, ekzistojnë shumë lloje izolatorësh. Parametrat kryesorë të izolatorëve janë ngurtësia e tyre vertikale dhe horizontale. Kryesisht ata karakterizohen nga ngurtësi e madhe vertikale, por me ngurtësi të vogël horizontale. Në mënyrë që të projektohen izolatorë me kosto efektive nevojiten materialet e duhur dhe përdorimi optimal i tyre. Në këte punim analizohet efekti i materialit të matricës, të fibrave dhe trashësisë të tyre në ngurtësinë e izolatorëve me faktor të ndryshëm forme. Analizat kryhen në fazën lineare duke përdorur programin SAP2000. Prej studimit të rezultateve arrihet në konkluzionin se për të rritur efektivitetin e izolatorit duhet përdorur gomë me modul elasticiteti dhe koeficient Puasoni të madh, fibrat e çelikut mund të zëvendësohen me fibra karboni apo E-glass. Faktori i formës ka ndikimin më të madh në ngurtësinë vertikale.
Fjalët çelës: Izolator, ngurtësi vertikale-horizontale, faktor forme

Summary - As a result of many engineering efforts toward application of seismic base isolation, there exist many types of isolators. The main parameters of isolators are their vertical and horizontal stiffness. Mostly they are characterized by high vertical stiffness, but with low horizontal stiffness. In order to design the cost effective isolator it is needed to find the proper materials and to use the optimal quantities of them. Here is analyzed the effect of matrix and fiber materials and their thickness to the stiffness of isolators with different shape factor. The analyses are performed by linear modeling using the software SAP2000. Studying the results we come to conclusions that the isolators are effective if we use rubber with higher value of module of elasticity and Poisson ratio, and the steel can be replaced with carbon fiber or E-glass. The highest influence to the vertical stiffness is taken from the shape factor.
Key words: Isolator, vertical-horizontal stiffness, shape factor

1. Introduction

Due to engineer effort for the application of seismic isolation, there are many types of isolators and isolated structures in the world. To extend this valuable earthquake-resistant strategy to housing and other public buildings, it is necessary to reduce the cost and weight of the isolators. The reinforced elastomeric isolators are composed by matrix and fiber. The main parameters of isolators are their vertical and horizontal stiffness. Mostly they are characterized by high vertical stiffness, but with low horizontal stiffness. In order to design the cost effective isolator it is needed to find the proper matrix and fiber materials and to use the optimal quantities of them. In this paper we will analyze the effect of matrix material to the stiffness of isolators with different shape factor. In addition we will analyze the effect of fiber material and their thickness to the stiffness of isolators with different shape factor. The analyses are performed by linear three dimension finite element modeling using the existing software SAP2000. From research results and graphic

presentation of vertical and horizontal stiffness of isolators for various parameters of the matrix and fibers, we reach several conclusions regarding the design of effective isolators.

The main purpose of seismic isolation is the reduction of two basic parameters; the acceleration and the deformation of the structure (inter story drifts). To achieve this goal the isolators should have certain parameters. In order to reduce the seismic force we need to increase the flexibility of the system (structure - isolator), so the isolators should have low horizontal stiffness. On the other hand, isolators must have high vertical stiffness to withstand big vertical loads of the structure. The isolator is considered a composite matrix-fiber device. In the current practice, the matrix usually is rubber, while the fibers are made of steel or carbon placed in horizontal layers. The rubber matrix provides the required horizontal flexibility of the isolators, while the fiber layers increase vertical stiffness by reducing the bulging effect of the rubber. Studies of the behavior of the isolators have shown the influence of some properties to the horizontal and vertical stiffness of isolators. Mostly they are classified in three main groups: shape factor, rubber compressibility and fiber flexibility.

2. Modeling, Materials and their properties

Using SAP2000 software the isolators are modeled with Finite Element in linear phase. SOLID element is used for the matrix and SHELL element for the fiber. The lower joints have stationary hinges while the upper joints are free. On the top of the isolator are applied external vertical (P_v) and horizontal (P_h) forces. The applied loads are uniformly distributed on the surface of the isolator.

The geometric parameters of the isolator are shown in Figure 1. The dimensions a, b, h, and the thickness of matrix and fiber layers are, t_m and t_f, respectively.

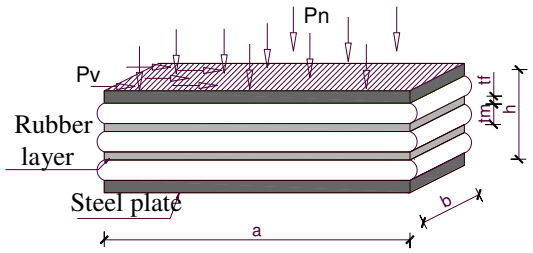

Figure 1. Geometric parameters of the isolator

In this study are used the materials with their properties as shown in Table 1.

Table 1. Materials properties used in analysis

No.	E_m kN/m^2	u_m	E_f kN/m^2	t_f mm
1	600	0.499	4E+8	0.2
2	3000			0. 2
3	6000			0. 2
4	6000	0.450	4E+8	0. 2
5		0.495		0. 2
6		0.499		0. 2
7	6000	0.499	4E+7	0. 2
8			2E+8	0. 2
9			4E+8	0. 2
10	6000	0.499	4E+8	0. 2
11				0.4
12				2

As shown in Table 1 are considered: 3 types of rubber, low stiffness, medium stiffness and high stiffness rubber; 3 different Poison's coefficient and 3 types of fiber materials, E-glass with E_f=4·10^7, kN/m^2, steel with E_f=2·10^8 kN/m^2 and carbon fiber with E_f =4·10^8 kN/m^2.

The deformation form of one layer of the isolator due to applied forces, is shown schematically in Figure 2.

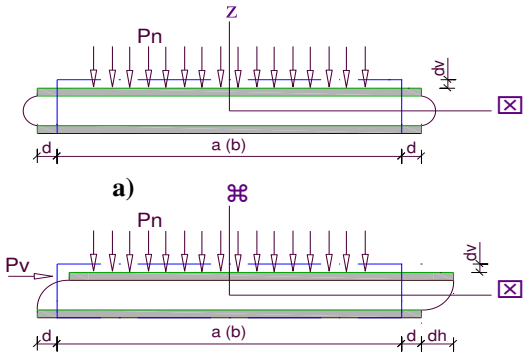

Figure 2. The deformation form of one layer of the isolator; a) under vertical load, b) under vertical and horizontal load

By definition, the shape factor *S*, is the ratio between the loaded area A = a x b and the free area of one rubber layer (a x b) x $2t_m$. Thus:

$$s = \frac{a\ x\ b}{(a\ x\ b)\ x\ 2t_m}$$

The horizontal and vertical stiffness are defined by the expressions:

$$K_h = \frac{P_h}{d_h} \quad \text{and} \quad K_v = \frac{P_v}{d_v}$$

In this paper we will determine the horizontal and vertical stiffness of the isolator for each case of study.

3. Case of Analysis

With the purpose of studying the influence of the main parameters of the matrix material (rubber) E_m, υ_m and fiber E_f, t_f, three types of isolators are considered: Type 1: axbxh=25x25x24 cm, Type 2 25x50x24 cm, Type 3 50x50x24 cm, and for each type of isolators four different number of layers are modeled: 4, 8, 16 and 32 layers in order to analyze the effect of the shape factor, S.

4. Analysis results

From the performed analysis we provide the horizontal and vertical values of the displacement of isolators. Using the expressions given before we determine the horizontal stiffness, K_h and the vertical stiffness, K_v. These results are shown in the following tables. Table 2 shows the values of the shape factor. Table3 shows the results of the horizontal stiffness. Table 4 shows the results of vertical stiffness

Table 2. The shape factors for the analyses

	Type 1 (25 x 25 x 24)				**Type 2** (25 x 50 x 24)				**Type 3** (50 x 50 x 24)			
	4	8	16	32	4	8	16	32	4	8	16	32
1 - 9	1.05	2.10	4.23	8.57	1.39	2.80	5.64	11.4	2.09	4.20	8.45	17.1
10	1.05	2.10	4.23	8.57	1.39	2.80	5.64	11.4	2.09	4.20	8.45	17.1
11	1.05	2.12	4.29	8.82	1.40	2.82	5.72	11.8	2.10	4.23	8.58	17.6
12	1.09	2.25	4.85	11.5	1.45	3.00	6.47	15.3	2.17	4.50	9.71	23.0

Table 3. Horizontal stiffness of isolators (kN/m)

No.	**Type 1**				**Type 2**				**Type 3**			
	4	**8**	**16**	**32**	**4**	**8**	**16**	**32**	**4**	**8**	**16**	**32**
1	78	83	85	86	161	167	170	171	337	342	345	346
2	235	247	254	255	480	498	509	511	996	1017	1029	1034
3	465	490	506	509	950	990	1014	1019	1942	2008	2045	2060
4	410	425	442	450	827	855	885	901	1881	1936	1976	1998
5	437	463	485	491	890	933	973	983	1912	1978	2022	2043
6	465	490	506	509	950	990	1014	1019	1942	2008	2045	2060
7	385	434	470	490	791	880	944	982	1329	1580	1770	1901
8	455	484	502	507	932	978	1007	1016	1860	1961	2018	2045
9	465	490	506	509	950	990	1014	1019	1942	2008	2045	2060
10	465	490	506	509	950	990	1014	1019	1942	2008	2045	2060
11	471	494	508	510	961	995	1018	1021	1990	2035	2060	2068
12	483	503	510	515	980	1010	1031	1032	2035	2058	2073	2075

Table 4. Vertical stiffness of isolators (kN/m)

No.	Type 1			Type 2			Type 3		
	8	16	32	8	16	32	8	16	32
1	5279	16706	24582	12912	38052	55279	40790	97087	129702
2	15533	48450	71839	37793	109769	161031	117440	277008	375940
3	30211	92421	138122	72993	207900	308642	221484	516796	714286
4	4503	5337	5681	9590	10963	11476	20788	22683	23356
5	14970	31486	40750	37244	69735	86133	104548	159744	185701
6	30211	92421	138122	72993	207900	308642	221484	516796	714286
7	20458	50659	83333	45893	107759	177963	114351	238949	388350
8	28818	85324	129870	68823	190114	287356	202020	461894	660066
9	30211	92421	138122	72993	207900	308642	221484	516796	714286
10	30211	92421	138122	72993	207900	308642	221484	516796	714286
11	31075	96899	143678	75586	219780	321543	234742	554017	751880
12	31847	101010	148368	77519	232558	333333	246914	588235	784314

In Figures 3 and 4 are shown the relation between the horizontal or vertical stiffness and characteristics of the matrix or the fiber for different shape factors of the isolator

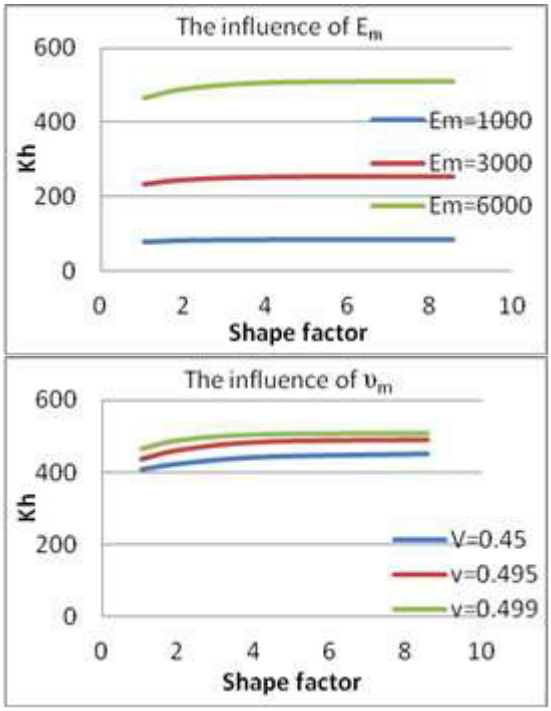

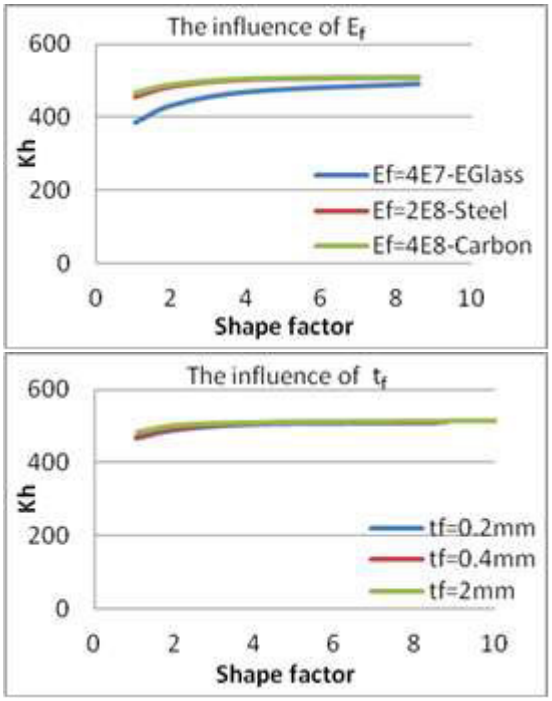

Figure 3. The influence of isolator materials in its horizontal stiffness - Isolator Type 1

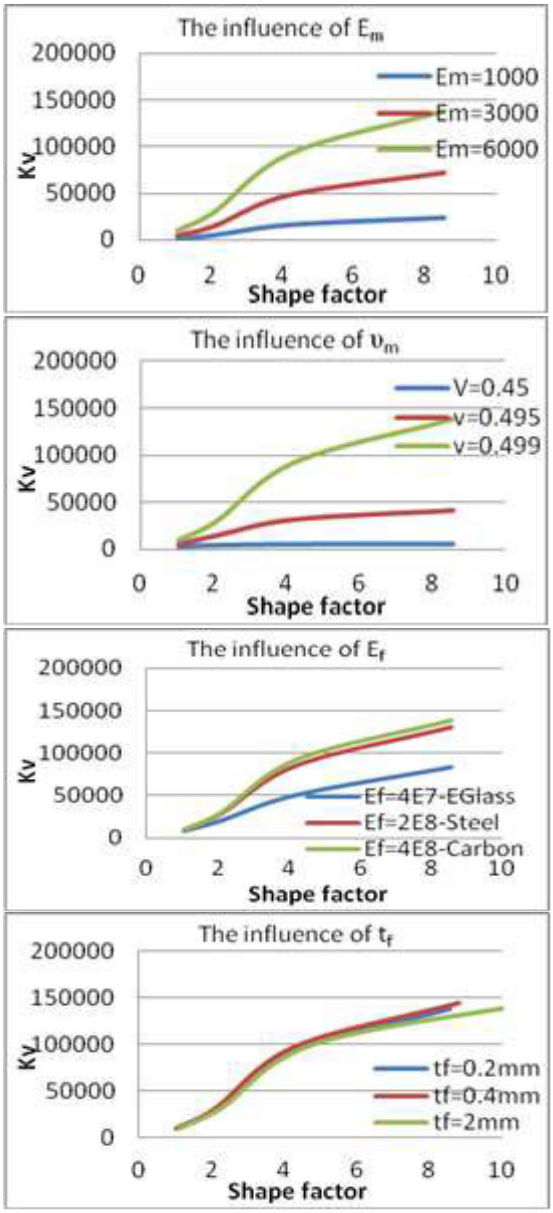

Figure 4. The influence of isolator materials in its vertical stiffness - Isolator Type 1

5. Conclusions

The rubber's modulus of elasticity (E_m) has a big influence on horizontal and vertical stiffness of the isolator, which becomes bigger with the increase of the shape factor. It is recommended the use of rubber with high modulus of elasticity.

The rubber's Poison's coefficient (υ_m) doesn't influence the horizontal stiffness, but it has a big influence in the vertical stiffness. For small values of this coefficient, the increase of the shape factor value does not lead to increased vertical stiffness. Using the rubber with high Poison's coefficient is more effective on isolator design.

The fiber's modulus of elasticity (E_f) has almost no influence on horizontal stiffness but a small influence on the vertical stiffness. For a 10 time increase of the modulus of the fiber, the vertical stiffness becomes approximately 2 times bigger. The replacement of the steel fiber with cheaper material is acceptable. The fiber thickness (t_f) has no influence on the horizontal and vertical stiffness, despite the increase of the shape factor. To produce low cost isolators we should use slender fibers and more reinforcement layers.

With the increase of the shape factor (S), the vertical stiffness increases significantly while the horizontal stiffness doesn't change for all values of materials properties. To produce low cost isolators, the shape factor value should be high.

6. References

1. Alan N. G. (2001), "Engineering with Rubber", Cal Hansec Verlag, Munich;

2. Kelly, J. M. (1980), "Testing of a Natural Rubber Base Isolation System by an Explosively Simulated Earthquake", UCB/EERC–80/25;

3. Kelly, J. M. (2002) "Analytical and Experimental study of Fiber-Reinforced Strip Isolators", PEER 2002/11, Berkeley;

4. Kelly, J. M., Chalhoub M. S. (1987), "Earthquake Simulator Testing of a Combined Sliding Bearing and Rubber Bearing Isolation System", UCB/EERC–87/04;

5. Kelly, J. M., Quiroz E. (1992), "Mechanical Characteristics of Neoprene Isolation Bearings", UCB/EERC–92/11;

6. Taniwangsa W., Clark P. W., Kelly J. M. (1995), "Natural Rubber Isolation Systems for Earthquake Protection of Low-Cost Buildings", UCB / EERC – 95 / 12.

AKTET **ISSN 2073-2244**
Journal of Institute Alb-Shkenca **www.alb-shkenca.org**
Revistë Shkencore e Institutit Alb-Shkenca **Copyright © Institute Alb-Shkenca**

SELECTION OF AN OPTIMAL TRANSPORT CHAIN TAKING INTO CONSIDERATION COSTS
ZGJEDHJA E ZINXHIRIT OPTIMAL TRANSPORTUES DUKE MARRË NË SHQYRTIM KOSTOT

RAMADAN DURAKU[a], SHABAN BUZA[a]
[a] Departamenti i Komunikacionit-FIM, Universiteti i Prishtinës "Hasan Prishtina"
Bregu i Diellit p.n, 10000 Prishtinë, KOSOVË.
e-mail: ramadan.duraku@uni-pr.edu

PËRMBLEDHJE
Për përfshirjen e llojeve të ndryshme të transportit është i nevojshëm aplikimi i zinxhirit të transportit. Qëllimi i punimit është zgjedhja e variantit optimal sipas analizës krahasuese të kostove të transportit rrugor-unimodal në raport me zinxhirin e transportit intermodal. Për të analizuar kostot e gjithmbarshme të zinxhirit të transportit, kërkon të njihet madhësia e zinxhirit, intensiteti i operacioneve, shfrytëzimi i teknologjisë, kostot interne dhe eksterne të cilat krijohen në çdo hallkë të tij. Të gjitha kostot e krijuara për zgjedhjen e variantit optimal ndahen në "interne" dhe "eksterne". Subjekt i trajtimit në këtë punim janë kostot interne. Kostot e llogaritura për çdo aktivitet të zinxhirit të transportit sipas varianteve janë dhënë si rezultate përfundimtare në mënyrë tabelore dhe grafike për një shembull konkret të marr si studim rasti. Në përfundim janë dhënë arsyetimet e zgjedhjes së variantit optimal, përparësitë dhe të metat si dhe rekomandimet për aplikimin e tij.
Fjalët kyçe: zinxhir transporti, kosto, transport intermodal, variantat, studim rasti.

SUMMARY
For including of different types of transport is necessary to apply the transport chain. The purpose of paper is the selection of an optimal variant by comparative analyses of costs-single modal road transport in relation to intermodal transport chain. To analyze the overall costs of transport chain is required to understand the size of the chain, the intensity of operations, use of technology, intern and extern costs which are generated in each its process. All costs generated for choosing the optimal variant are divided into "internal" and "external". Internal costs are subject of analyses in this paper. Calculated costs for the each activity of transport chain by variants are given as the final results in a tabular and graphical form for one concrete example which is taken as a case study. In conclusion, are given the justifications of choosing the optimal variant, advantages and disadvantages and recommendations for its applications.
Key Words: transport chains, costs, intermodal transport, variants, case study.

INTRODUCTION

Freight transport is growing, where road transport has the greatest increase. As an integral part of logistic system, transport is the activity of transfer and relocation of goods and passengers by transport means (road vehicles, airplanes, ships, trains, etc.). From the perspective of business logistics, transportation is an activity that at the same time is part of logistic system through which is possible to make the transport of goods through the logistics and distribution system. Therefore for the application of different forms of transport is necessary application of transport chains [1].

TRANSPORT CHAIN

From the production of a product to its destination for consumption or use must be

carried out a series of processes. This path that describes the product in all required processes and services is known as "transport chain" [2]. Transport chain is a cluster, respectively a series of mutual interest and related links (partners and active participants), which enables the fast, safe and rational conduct of transport processes for produced products [1]. Each link in the chain of transport represents an active participant e. g. sender-carrier-depositor-terminal-charger-discharger until the product reaches to the end user. Transport chain can be designed as conventional transport, combined and multimodal. Intermodal transport chain starts where load unit charge and discharge ends in the country named as the destination of ordering. A decisive influence on the transport chain has equipment for loading and unloading and spatial position, which influences the choice of transport technology [2].

Characteristics of intermodal transport

Intermodal transport refers to the circulation of goods of the same unit load or vehicle using several successive modes of transport while no delivery of the goods were made while changing the mode of transport [4]. Intermodal transport has found or will find its proper place in the market between water transport, rail long distance and road transport shorter distances. Criteria for selecting optimal transport chain are numerous but the main and most important are considered the transportation costs [3]. Reducing overall costs of intermodal transport chain implementation in relation to road transport chain-unimodal represents a key priority in the selection of optimal variant.

TRANSPORT COSTS

The purpose of this paper is to analyze the cost of intermodal transport chain in comparison with unimodal transport chain. These objectives will be realized by applying appropriate methodology for calculating costs and the analysis of the possibility of reducing certain categories of costs and their impact on overall costs. In general transport costs for selecting the optimal variant of transportation are divided into direct costs (internal) and indirect costs (external) [5]. Internal costs include operating costs of transportation of goods between the sender and ordering. Internal costs are subject to analysis in this paper, such are: transportation costs, time cost and cost of goods' treatment. Greater impact on internal costs has the transportation costs and therefore further analysis is singled out for treatment excluding other two types of costs. External costs are the costs of transport chain which indirectly influence the society and are not the subject of analysis in this paper. They generally depend on the nature of the transport chain, the characteristics of location, distance and distance of nodes (terminals), the intensity of activities in the network, service efficiency and value of input parameters. The cost estimate is the process that is carried out in two hierarchical levels (see Table 1) and (Table 2) [5].

Transport / Type of Costs	Aggregation, Main transport, Distribution
Cost of transportation	T_{tdt}
Cost of time	T_{vdt}
Cost of handling goods	T_{rdt}
External cost	T_{edt}
Totally	T_{udt}

Table 1. Costs classification and allocation of unimodal transport chain

Transport / Type of costs	Agg-regation	Transfer in the initial terminal	Main transport	Transfer to a final terminal	Distri-bution
Cost of transportation	T_{ts}	T_{tf}	T_{tg}	T_{tp}	T_{td}
Cost of time	T_{vs}	-	T_{vg}	-	T_{vd}
Cost of handling goods	T_{rs}	T_{rpt}	-	T_{rkt}	T_{rd}
External cost	T_{es}	T_{ept}	T_{eg}	T_{ekt}	T_{ed}
Totally	T_{s}	T_{pt}	T_{g}	T_{kt}	T_{d}

Table 2. Costs classification and allocation of intermodal transport chain

Therefore, the overall costs of unimodal transport chain are calculated by expression:

$$T_{udt} = T_{tdt} + T_{vdt} + T_{rdt} + T_{edt} \quad (1)$$

While, the overall cost of intermodal transport chain are expressed as:

$$T_{uit} = T_s + T_{vdt} + T_{pt} + T_g + T_{kt} + T_d \quad (2)$$

CASE STUDY

In order to demonstrate the selection of optimal transport chain based on the principle of cost, in this paper has been considered a case study for the transport of energy drink "Mirage Energy-drink" from France to Kosovo. Kosovo representation Company "Mirage" which is located in Pristina is responsible for distribution of this product in Kosovo. Pack of 500 mL which is transported to Kosovo is considered for analysis. This package is then placed in a special box designed to accommodate them. Proceedings of product placement and alignment of the box, the palette is given by (Figure 1) and (figure 2). The annual amount of import is 103 (tons) with the frequency of every two months (six shipments/ year).

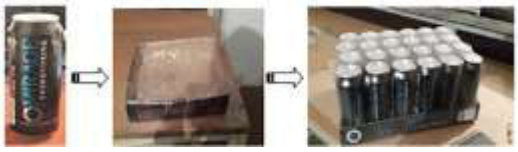

Figure 1. The way of order of 500 mL packaging in box

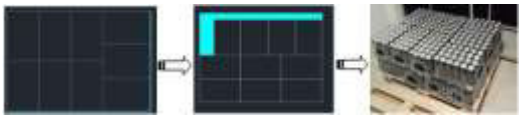

Figure 2. The way the order of the boxes on pallets

This case study addresses two variants of realizing transport chain:

a. ***Variant 1: Direct road transport chain - unimodal and technology with palette, and***

b. ***Variant 2: Intermodal transport chain and technology with container.***

Variant 1 - Direct road transport chain - unimodal and technology with palette

This means that the transport from the sender's warehouse to receiver's warehouse is performed only by means of road transport and application technology without loading and unloading pallets of goods along the transport route. It should be noted that this variant is also currently applicable in the mentioned company. This variant as well as the route of the road transport vehicle circulation is given as in (Figure 3). Road transport chain under Variant 1 is realized by means of road transport of type SCANIA with these dimensions BSAL = 8800 (mm) in length, BSAH = 2327 (mm) in width, and permitted weight of 26 (tons).

Figure 3. Schematic representation and itinerary movement for Variant 1

Further calculations were made for logistical processes and activities according to the Variant 1 transportation chain with expressions according to the literature [9,10] which are presented in tabular form (Table 3) and graphical (Chart 1).

No.	Costs	Logistic costs per unit (€/pallet)	Logistic overall costs(€/year)	Participation (%)
1	Cost of palletization	3.86	417'994	3.23
2	Cost of preparing goods for shipment	0.99	107'599	0.37
3	Cost of loading on the road transportation vehicle	0.84	134.42	0.33
4	Cost of road transport	160.40	17'324.92	91.7
5	Cost of unloading from the road transportation vehicle	0.89	96'04	0.33
6	Cost of warehousing	1.46	157.68	0.33
7	Cost of digesting	4.73	511.21	2.73
8	Cost for holding stocks	1.42	153.36	0.81

Table 3. Presentation of logistic costs for transport logistics chain for Variant 1

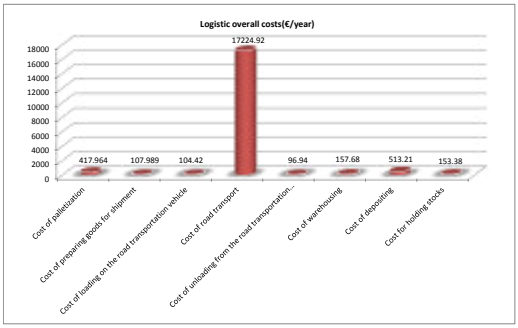

Chart 1. Presentation of total logistics costs for Variant 1

So using the modified expression (1), since in this case the time costs, freight handling costs and external costs are not taken into account, it appears that the overall costs of the transport chain for Variant 1 are:

$T_{udt} = T_{tdt} + T_{vdt} + T_{rdt} + T_{edt} =$ **(**104.42+17224.92+96.94)= 17426.28 (€/year).

Variant 2 - Intermodal transport chain and technology with container

At this variant, the transport from the sender's warehouse to the seaport 1-Venice (Italy) is performed with road transport and container technology. It should be noted that this variant is only a proposal that is not the function (Figure 4). Presented itinerary through (Figure 5) clearly shows that the transport chain is composed of three transport routes that use different methods of transport vehicles (road-sea-road) during which have various cost. These costs are calculated separately for each transport route, which shall be included in the overall cost of transportation costs under this variant.

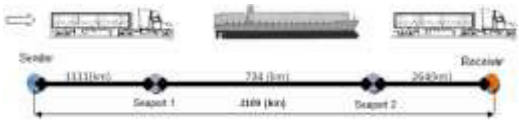

Figure 4. Schematic representation of Variant 2

Figure 5. The route of the movement at Variant 2

Optimal form of placing pallets in containers is carried in place of the sender. It has been decided to be used the road transport vehicle with pulling head with semi-trailer. The data for semi-trailer are: length 12.43 (m), width 2.44 (m), the height from the ground 1.22 (m), 2948 personal weight (kg), number of axes is 2 (PCS), carrying 2 containers of 20 feet and one container of 40 feet. The optimal number of boxes, pallets, containers and transport vehicles as well as other indicators for the overall quantity of goods of 103 (tons) annually by combinations of pallets and containers are provided in Table 4.

Combinations		Combination 1	Combination 2	Combination 3	Combination 4
Types of palettes and containers	unit	Palette 1200×800 mm Container 20ft	Palette 1200×1000 mm Container 20ft	Palette 1200×800 mm Container 40ft	Palette 1200×1000 mm Container 40ft
Number of palettes in a container	pc	11	10	25	22
Number of containers	piece	10	10	5	5
No. of boxes for the whole shipment	piece	7920	8000	9000	8800
No. of palettes for the whole shipment	piece	110	100	125	110
No. of vehicle for the whole shipment	piece	5	5	5	5
Empty weight of the container	ton	2.2	2.2	3.8	3.8
Weight of goods in container	ton	10.8	10.8	24.5	24
Weight of goods in the vehicle	ton	26	26	28.3	27.8

Table 4. Indicators of optimal placement of containers in the transport vehicle

Further calculations were made for logistical processes and activities according to the Variant 2 transportation chain with expressions according to the literature [9,10] which are presented in tabular form (Table 5) and graphical (Chart 2).

No.	Costs	Logistic costs per unit (€/palette)	Logistic overall costs (€/year)	Participation (%)
1	Cost of palettization	3.86	482.5	4.03
2	Cost of preparing goods for shipment	0.99	123.75	1.03
3	Cost of contenerization	1.03125	128.9	1.07
4	Cost of loading the container in road transportation vehicle	0.1992	24.9	0.2
5	Cost of road transport with container	54.66	6832.5	57.11
6	Cost of transfer of container from road transport vehicle on the ship	2.8	350	2.92
7	Cost of sea transport with container	4.63	965	8.07
8	Cost of transfer of container from ship to the road transportation vehicle	2.8	350	2.92
9	Cost of road transport with container	12.98	1622.5	13.57
10	Cost of unloading the container from the road transportation vehicle	0.96	120.45	1
11	Cost of warehousing	1.46	182.5	1.52
12	Cost of depositing	4.75	593.75	4.96
13	Cost of stocks	1.42	177.5	1.48
	Totally	92.54045	11954.2	100

Table 5. Presentation of logistics costs for transport logistics chain for Variant 2

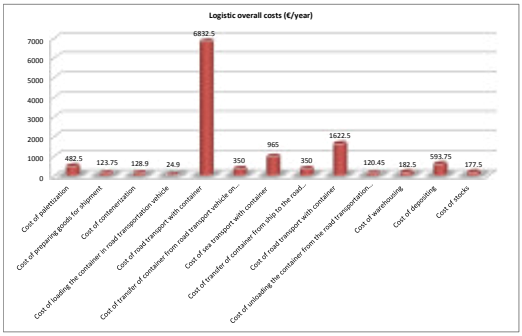

Chart 2. Presentation of total logistics costs for Variant 2

So using the modified expression (2), the overall transport costs are:

$T_{uit}= T_{ts} + T_{tf} + T_{pt}+ T_{tg} + T_{tp} + T_{td}=$
$=24.9+6832.5+350+965+350+1622.5+120.45=10$
265.35 (€/year).

Comparison of overall transport costs under the two alternatives is given graphically by the Chart 3.

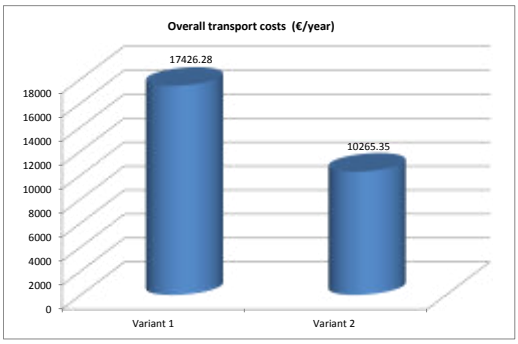

Chart 3. Comparison of overall costs for the two variants

The Chart 3 shows that transport costs as well as follow-up activities for Variant 2 are lower in comparison to the Variant 1 for an amount of 7160.93 (€/year). This results makes easier decision to the transport services manager (shipping companies) to choose among the two variants.

CONCLUSION

In the paper has been analyzed the selection of optimal variant according to the comparative analysis of the costs of unimodal transport chain (Variant 1) in relation to the intermodal transport chain (Variant 2). In the study are taken into consideration and analyzed only internal costs, respectively only transport costs and loading and unloading follow-up activities in terminals and ports. From the results obtained for the two variants can be clearly seen that as the most optimal variant in terms of transport costs for bringing goods annually from "Mirage" from Paris to Pristina is Variant 2, the intermodal transport chain and container technology. Of great importance here is the fact of the introduction of sea transport in the transport chain, where it is known that shipping costs for "ton-kilometer" are much lower compared to road transport or other types of transport which has enabled transport costs decrease at considerable level. However it should be mentioned that the application of other alternatives including intermodal transport must be followed with certain recommendations and measures.

Recommendations and measures for the development of intermodal transport and logistics [7]:

- Development of a network of logistics centers, intermodal terminals,
- Develop competition prices / costs for modes of transport and transport technologies,
- Research and monitoring of flows of goods,
- Development of technical and technological solutions,
- Development of cooperation and coordination in logistics and transportation,
- Adoption and application of legislation which will enable fair competition between different types of transport,
- Establishment of associations and bodies at the national level,
- Provide financial support measures, etc.

REFERENCES

1. Buntak.K, Grgurević,D, Drožđek,I, Međusobni odnos logističkih i transportnih sustava, ISSN 1864-6168, UDK 62, Tehnical journal 6, 2(2012), 228-232.

2. Shkëlqim Gjevori, Sistemet e Transportit, Tiranë, 2010.

3. Vidakovic,M. Tomic,I. Maslaric.M. Izbor Optimalnog transportnog lanca: studija slucaja, I Medunarodna naucna-strucna konferencija Logistika 2010, 18-19 Novembar 2010 godine, Doboj.Prof. Marchal Jean.

4. Multimodal Transport Strategy (2012-2021) and Action Plan (2102-2016) for Kosovo, Egis International, February 2012.

5. Vladeta Gajic, Mr.Marinko Maslaric,Predmetni Zadatak 2, Tema rada:Proracun i analiza troskova intermodalnog i drumskog transportnog lanca, Novi Sad, Maj 2010.

6. T. Peric, J. Pap, I. Suic: Costs of Transport Services and their Significance, Promet-Traffic-Traffico, Vol. 12, 2000, No. 1, 43-52.

7. Leon Jerom, Dr. Zhang Zhaomin, Res. Eng. Kisheva Diana, Feasibility Study on Development of Intermodal Freight Transport Between Belgium and Bulgaria.

8. Snežana T,.Slobodan Z. Development of Intermodal Transport and logistic in Serbia, InternationalJournal for Traffic and Transport Engineering, 2012, 2(4): 380 – 390, DOI: h.p://dx.doi.org/10.7708/ij.e.2012.2(4).08.

9. Udhëzim Nr.581/1, Mbi përcaktimin e tarifave të shërbimit në autoritetin portual Durrës, Tiranë,2013.

10. Hyseni.P. Punim Seminarik-Master nga lenda Logjistika në Transport, UP ”Hasan Prishtina”-FIM, Departamenti I Komunikacionit, Prishtinë, 2014.

11. Duraku R. Logjistika në Transport,Ushtrime të autorizuara-Studimet Master,UP”Hasan Prishtina”-FIM,Departamenti i Komunikacionit, Prishtinë, 2014.

.

AKTET **ISSN 2073-2244**
Journal of Institute Alb-Shkenca **www.alb-shkenca.org**
Revistë Shkencore e Institutit Alb-Shkenca **Copyright © Institute Alb-Shkenca**

MODELING OF KOSOVO'S ROAD NETWORK WITH TRANS CAD COMPUTER PROGRAM

RAMADAN MAZREKAJ, NOL DEDAJ, BETIM REQICA
Mati 1 square, no.78 Prishtina, Republic of Kosovo
rmazrekaj@hotmail.com

Summary: In this thesis we are dealing with Kosovo's road network, the connection of Kosovo's road network with the regional network and European Pan. Modeling of the road network and the traffic of vehicles that pass through this netwrok through the computer program Trans CAD by converting it in a graph with junctions and arcs, and assigning their mathematical relations between parameters and variables that define the flux of goods and passengers passing through the arcs and junctions of this graph. Modeling creates great opportunities to analyze, highlight, stimulate and optimize the system in the function of the demands being addressed to the researchers. In the conclusion of the thesis there are addressed transport capacities of Kosovo's road network, the Albanian road and railway network , Albanian ports. The construction effect of the 6^{th} and 7^{th} road in increasing the importance of Albanian's Ports.
Keywords: Modeling with Trans Cad, road network, Kosovo

1. INTRODUCTION

The current performance of Kosovo's road network is not equivalent with EU's roads and motorway network standards. Failure to change this condition would cause negative effects in Kosovo's general economic development by the unnecessarily and harmful increase of transport costs and problems of road safety as well.

The solution of this circumstance seeks to analyze the road network and the existing traffic of goods, vehicles and passengers, identifying the problems and the method of their solution and also regulating the vehicle circulation scheme, inside Kosovo's road system and in the linking junctions of this network with the Balkans and European ones. Analyzing, recording of interventions in the network and the optimization of Kosovo's road traffic will be executed by modeling of traffic flux for redistribution of goods and passengers based on the simulated scenarios for network integrations.

2. KOSOVO'S ROAD NETWORK

Kosovo's road network is divided into: International (Motowars), Highways (National) and Regional roads, which are administered by the Ministry of Infrastructure (IM), and of local roads, including urban and rural roads administered by the municipalities. The network consists of:

-Motorway – 78 km
-National road – 630.4 km
-Regional – 1294.7 km

The central network consists of (see figure 1):

-The M2 road, which goes from the north border with Serbia, through Prishtina in the southern border with Republic of Macedonia
-The road M25, which comes from Nish (Serbia) towards the west-eastern border with Serbia through Prishtina and Prizren, in the southern border with Albania.
-The M9 road, from the eastern border with Serbia, through Prishtina to Peja and in the western border with Montenegro.
-Main additional roads are M9.1, M22.3, M25.2 and M25.3 which represent branches of those main networks.
-The central network is well organized, with Prishtina in the centre there are well linked all of the country regions with the centre.

The regional network contains two kinds of connections:

-Regional roads that complement the network map, and contain connections with the main axis and regions or connect significant dwelling on a regional basis.
-The other part of regional roads have limited national and even regional significance, and connects small dwellings with the central network.

Figure 1. Kosovo's Road Network Map

2.1. ROAD CORRIDORS AND ALBANIAN PORTS

Main roads in Abania's territory are:

- **The Nation's Road (Road 7**): Durres – Kukes – Morina – Prishtina – Nish
- **The VIII corridor:** Bari, Brindisi – Durres, Vlora – Tirana – Sofje – Burgas, Varna
- **North- Center:** Hoti i Hotit – Shkodra – Gjirokastra – Kakavija

Albanian Maritime Ports are:

- Durresi Port
- Vlora Port
- Shengjin Port
- Saranda Port

2.2. INTEGRATION OF KOSOVO'S ROAD NETWORK IN THE PAN EUROPEAN NETWORK

To integrate Kosovo's road network with Pan – European networks means, first of all, to create a system and a road infrastructure in accordance with demands and standards of the Pan – European road networks and, secondly, to use / promote the geographic position of the main road network of Kosovo, making it capable of fulfilling demands of Pan European road networks towards:

- Having a significant role in the long distance traffic, by shortening those distances;
- Avoiding of the main urban centres of traffic that cross through itineraries of goods and passengers' travel, decreasing the travel time,
- Ensuring the connection with other modes of transport, accomplishing multi modal transports that cause decrease in transport costs and/or decrease of travel time,

-Connecting of confined and peripheral regions with the central regions of European Union, thus prompting further development of those areas and through decrease of transport cost.

Figure 2. Roads and corridor networks in the Balkans

The practical realization an international transit of goods and passengers of Pan –Europian road networks through Kosovo's territory is very much dependent on the political and geo – political factors, but we will focus on the fulfillment of technical manner demands.

Beside the fulfillment of constructive / technical /geometrical demands to road infrastructure, the transport road network should guarantee users a, uniform and continuous, high level of service, comfort, and road safety. Here there are also included the infrastructure for managing of the traffic, user data, which has to do with road accidents, emergencies and electronic collecting of fees.

3. MODELING USING THE TRANS CAD SOFTWARE PROGRAM

One of the most known modeling programs in the field of transport systems is TransCAD. TransCad is world's leading software for Transport Planning and GIS Transport. TransCAD is the first and the only Geographic Information System (GIS) projected particularly for the usage of transport professionals to maintain, indicate, manage and analyze data of the transport.
TransCAD combines GIS and the ability of modeling the transport in a single and integrated platform, thus maintaining priceless capabilities in the process of modeling. TransCAD can be used for all kinds of transport, in every geographic scale or detailed level.

3.1. MODELING OF KOSOVO'S ROAD NETWORK

The classical model that is used in TransCad for the analyzing, optimizing and anticipation of traffic in a road network is the Model with 4 levels that develops according to the protocol and following phases:

- **Trip generation:** defines the frequency of origins and destinations of journeys in each area according to the journey aim.
- **Trip distribution:** adapt origins with destinations, using the function of the Gravitational Model.
- **Modal choice:** determines the journey part between every origin and destination.
- **Defining of the itineraries:** arrange journeys that are done in special ways of transport between origins and destination, according to certain itineraries.

The 4 phase Model that is developed according to the protocol and the following phases:

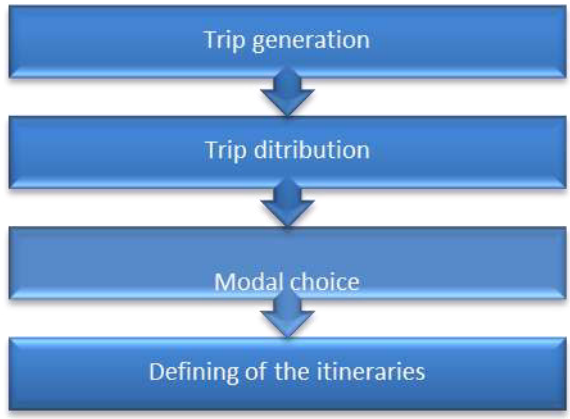

Figure 3. Four levels model for network traffic forecast

Table 1. Travel illustration in O-D

Origin\ Destination	1	2	3	Z
1	T_{11}	T_{12}	T_{13}	T_{1Z}
2	T_{21}			
3	T_{31}			
Z	T_{Z1}			T_{ZZ}

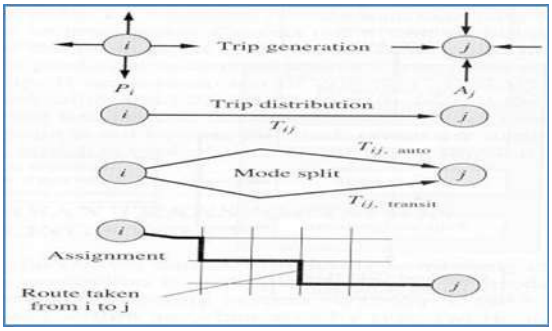

Figure 4. Trip generation and distribution

Tij=k*(Gi^a*Aj^a)/Cij^b .....(1)

Where:
i&j - Origins and Destination Area
T_{ij} . The traffic and passengers flow (road transport)
between **i** and **j** areas
G_i - Number of trips generated by the **i** area
A_j - Number of trips withdrawn by **j** area
C_{ij} - The barrier or resistance towards the trip between **i** and **j** areas (a function of time of the trip between **i** and **j**).
Factors **a, b** and **k** are constant.

Defining of the level of service and density: Density of vehicles is counted using the following equation:

D = vp / S ..... (2)

D - Density (car/km/lane),
Vp - Flow (car/hour/lane), and
S - Average speed of the car (km/hour)

3.2. THE LEVEL OF SERVICE, CAPACITY CALCULATION OF KOSOVO'S ROAD NETWORK

Level of Service (LOS)

- Defines the optimum level of service for a road
- There are six levels of service decided for roads, for which there are designated the letters **A, B, C, D, E** and **F**
- LOS – A presents the best level of service, and LOS – F presents the worst level. The European Standard designates minimal Level of Service C for a road projecting.

When the ratio of road Volume/Capacity reaches 0.8 value, according to European and American standards there is increased the capacity of the road between extending, adding of number of lanes or by passing in a highway after the level of service is evidently worsened.

The maximal value of the ratio Volume/Capacity of road is 1, and this shows that the road has the lowest level of service: F, which signals its blockage.

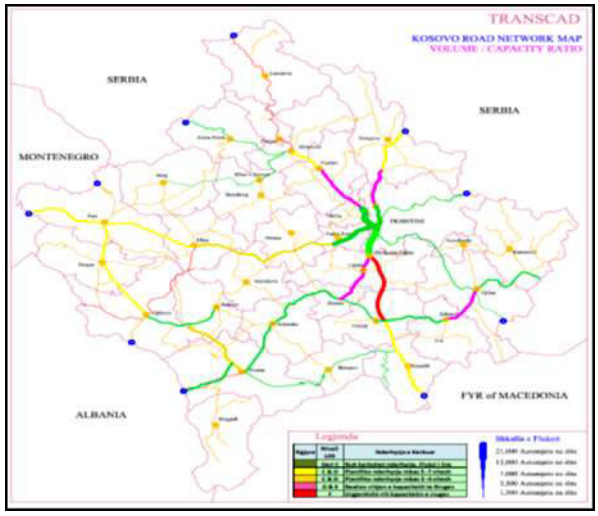

Figure 5. The ratio volume/capacity of Kosovo's road network for 2012 - 2018 - 2021, calculated by Trans CAD

Table 2. The required interventions in road segments according to color code with Trans CAD

Color code	The LOS Level of Service	The required intervention
	To C	No need for increas of road capacity. Free afflux
	C & D	Plan an increase of road capacity after 5-7 years

	C & D	Plan an increase of road capacity after 3-4 years
	D & E	Realize the increase of Road capacity
	F	Urgently increase the road capacity

4. CONCLUSION

Based on the matematical calculations by the software program Trans CAD there was realized the entire modeling of the network, which determines:

- The graph of Kosovo's road network (Fig. 5)
- The necessary database of the geometric parameters of the Traffic for all junctions and this network segments
- Parameters of the level of service for the Kosovo's main road network by
- ADYT (Average Daily Yearly Traffic) and Volume/Capacity,
- The leve of service for a period of time 2012, 2018, 2021

These data (Figure 5, table 2) dictate the necessity of intervention for development and requalification of Kosovo's road network, by determining:

-Existing transport capacity of Kosovo's road network, for goods and passengers.

-Problems and narrow points of this road network and interventions needed to meet standards of European primary road networks.

-The possible transportation capacities of Kosovo's road network which is integrated in the European networks as a direct consequence of accomplishing the standards

- The redistributed and regulated traffic in the European and Kosovo's networks, by recording the volume of goods and passenger traffic that can pass in Kosovo's road network as a consequence of itineraries and minimal costs of the transport that this network can offer.

REFERENCES

1. Mazrekaj R: PhD thesis, study of Integration of Kosovo's road network in Pan European network aimed at sustainable development of transport in the Balkan region
2. SEETO-s "Comprehensive network Development Plan 2012 – Multiannual Plan 2012-2016"
3. Willumsen L.G (1998) Modelling Transport Studies. 1998 California
4. Transport Infrastrukture Regional Study (TIRS) in the Balkans. LOUIS BERGER SA. 2001
5. Technical Assistance: Support in the implementation of the transportation community agreement, Prishtinë 2012.
6. Feasibility Study and Environmental Assessment for Two Main Road Axes in Kosovo (Road VI and VII), 2007
7. The Detail Project Design for motorway on the route from the junction Lipjan up to Hani i Elezit (border with Macedonia), Economic analysis report, 2009.
8. Road traffic flow of vehicles in the streets of Kosovo, the Kosovo Ministry of Infrastructure
9. HCM- 2000

Internet:

www.ebrd.org/

www.oecd.org/cem/

www.iru.org/

www.tinavienna.at/

www.unece.org/trans/

www.worldbank.org.ba/.

AKTET **ISSN 2073-2244**
Journal of Institute Alb-Shkenca **www.alb-shkenca.org**
Revistë Shkencore e Institutit Alb-Shkenca **Copyright © Institute Alb-Shkenca**

NDIHMESA E PROGRAMEVE KOMPJUTERIKE NË SINTEZËN DHE SIMULIMIN E MEKANIZMAVE ME GUNGË

THE HELP OF SOFTWARE IN THE SYNTHESIS AND SIMULATION OF CAM MECHANISMS

MIRANDA KULLOLLI; ARDIT GJETA
Universiteti Politeknik i Tiranës
Adresa Bul. ''Dëshmorët e kombit'' Sheshi Nënë Tereza, Nr4, SHQIPËRI
Email-i: kullolli_m@yahoo.com; agjeta@fim.edu.al

PËRMBLEDHJE
Në ketë punim paraqiten programe kompjuterike edukative, që realizojnë projektimin dhe simulimin e mekanizmave me gungë. Punimi synon të tregojë rëndësinë e programeve (X-Camme, Working Model®) në projektimin e mekanizmave me gungë, që ndihmojnë studentët të kuptojnë më mirë dhe më shpejt sintezën e mekanizmave me gungë. Projektimi i mekanizmave me gungë konsiston në përcaktimin e profilit të gungës, sipas një ligji të caktuar të lëvizjes, rezultatet paraqiten në mënyrë grafike. Analiza kinematike konsiston në përcaktimin e parametrave si zhvendosjen, shpejtësinë, nxitimin dhe pulsin duke njohur më parë profilin e gungës. Më tej është paraqitur simulimi kinematik, ku tregohet dhe qëllimi i këtij punimi. Programet kompjuterike na japin një asistencë në përgatitjen e studentëve, një ndihmesë si nga ana e paraqitjes vizuale dhe ajo praktike, e cila ndihmon në formimin dhe në përgatitjen cilësore të tyre. Në fund, është paraqitur një shembull konkret i projektimit të profilit të gungës.
Fjalët çelës: Analiza, sinteza, program edukativ, mekanizmat me gungë.

ABSTRACT
In this paper are presented educational computer software, which realize the design and simulation of cam mechanisms. The paper aims to show the importance of software like (X-Camme, Working Model ®) in the design of cam mechanisms, as a very important tool for graphic, which help students to understand better and faster cam synthesis mechanisms. Design of cam mechanisms consists in determining the cam profile, according to a certain law of motion. Cinematic analysis consists in setting parameters as displacement, velocity, acceleration and pulse, but first we know the cam profile, the results are shown graphically. Further, kinematic simulation is done with cam mechanisms, which indicate more clearly the scope of the paper. Computer software gives us assistance in preparing students, in the visual appearance and practical, which helps in the formation and the quality of their preparation. Finally, a complete design example done with the software presented is shown.
Key-words: Analysis, synthesis, educational software, cam mechanism.

I-INTRODUCTION

Cam is a mechanical element that uses another element, the follower, for the transmission of a certain movement through direct contact. [1] The movements of the follower can be of different types and are not difficult to design.
Cinematic characteristics of cam mechanism are:
-Displacement
-Velocity
-Acceleration
-Jerk

Design of cam mechanisms consists in determining the cam profile, according to a certain law of motion, velocity, acceleration and pulse allowed. [2]

Cam mechanisms are widely used in technical, to the fact that they are very simple and can be designed to provide precise movements required. However, having as high pairs working elements kinematics have quick consumption, which disrupts their precision of movement. The cams are applied in internal combustion engines, weaving, sewing machines, etc.

The basic data for the synthesis of cam mechanisms

Synthesis of cam mechanisms is done based on some initial data, which can be selected for each specific case based on the data or characteristics of the technological process for which is determined the mechanism based on other constructive character reasoning, the kinematics of dynamic etc. [3]

These data are:

a)Cinematic scheme of the mechanism or the type of cam mechanisms.

b)Law of movement of the follower and the duration of each stage.

c) Law of movement of the follower depending on the time or the angle of rotation of the follower, S=S(t), S=S(ϕ).

d)Some of the main dimensions of the mechanism or other data.

Selection of the program and the law of movement constitute an important phase in the design of the mechanism.

This selection is also made in accordance with technological conditions of the work of the mechanism. The selection of the main dimensions of linkage mechanism is also included in the database for its design.

Synthesis duties are posed for programming of movement when the cam mechanism is the main movement mechanism in a working machine. In such cases, full control of the movement of the follower is conditioned both by the demands of the labor process and by the requirements of dynamic and constructive character. So are controlled the acceleration as well as its derivative. The derivative of acceleration or jerk represents the speed of change of acceleration.

If the acceleration characterizes the forces of inertia, jerk characterizes the speed of change inertia forces. When the jerk has small relative values, the oscillations are easily absorbed by the mechanism. For large acceleration mechanisms is important that the maximum value of the jerk value is finite and small as to be possible. [4]

In general, when we consider the selection of the dependence of acceleration of the working follower, it is desirable that the chart of all time acceleration for full cycle has no interruption and no immediate crossing from a positive value and negative one, be a continuous line and fluid, so that the forces of inertia to change smoothly and do not shock or disconnect the couple kinematic linkage.

II-The synthesis of cam mechanism

The design of cam profiles using the graphical method

Problem: we know the law movement; we have to design the cam in order to force to the driver this law movement.

In general, after we define the displacement based on angle rotation, S=S(θ) it is necessary to design the cam profile.

The design of cam profile

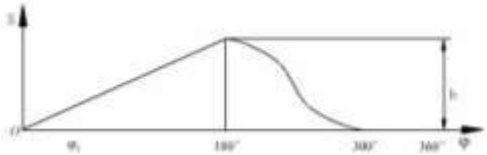

Figure 1. Is shown the displacement based on angle rotation, S=S(θ.

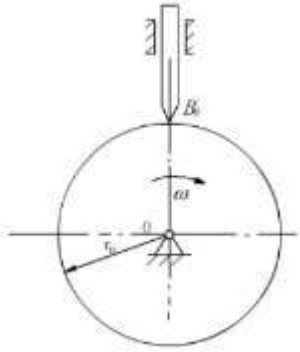

Figure 2. Cam with contact point

Step 1: The divide the graph of displacement, under the oaks, into a certain number of segments.
Step 2: divide the primary circle in the same number of segments.
Step3: Transfer distances from the diagram of displacement directly into cam profile positions.

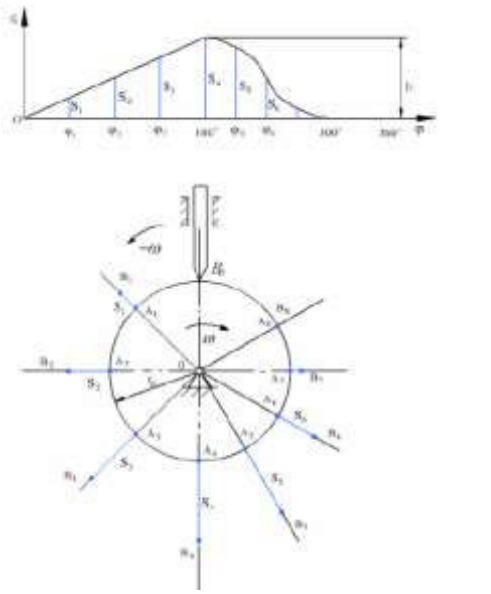

Figure 3. The divide the graph of displacement and circle

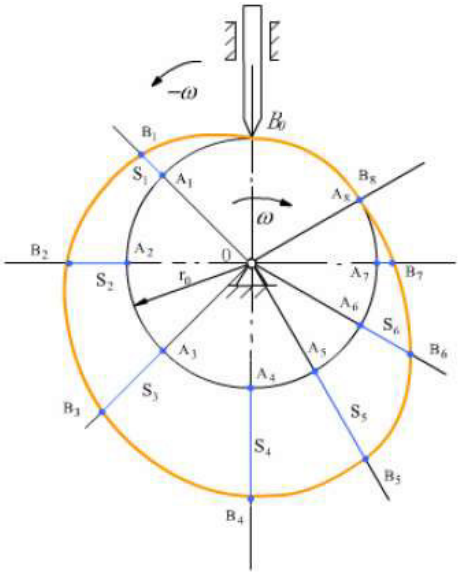

Figure 4. Cam profile required

Step 4: Draw a curve at these points. The obtained curve is a cam profile required.
III-Software application

X-Camme

X-Camme is a Microsoft Excel for analysis of cam mechanisms, including modeling profiles 2D and 3D, cutting and grinding on machine tools. X-Camme is the ideal tool for designers wishing to set the cams with analytical methods and have immediately available CAD models corresponding without having to spend time and resources to solve the problems of modeling. [5]
The analytical part is calculated on a simple Excel interface, allowing you to manage a case study very wide of kinematics problems, also very different from each other.
X-Camme is integrated with popular CAD 2D, 3D and CAM, ME10 e AutoCAD, - Solid Edge, Solid Works, Inventor, Pro/Engineer, etc.
X-Camme generates charts and tables with: Displacement, speed, acceleration, jerk, pressure angle, radius of curvature, dynamic analysis: Fourier Transform (FFT), Hertzian pressure.
The available laws of motion in the X-Camme: Simple polynomial curve (constant speed, Archimedes spiral, parabola, Trigonometric curve (harmonic, cycloid, elliptical, trapezoidal).
IV-Simulation of X-Camme
First open Microsoft Excel because X-Camme is integrated into Microsoft Excel.

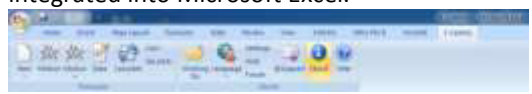

Figure 5. X-Camme toolbars.

Then click on the X-Camme and choose *New-Flat Plate Cam*

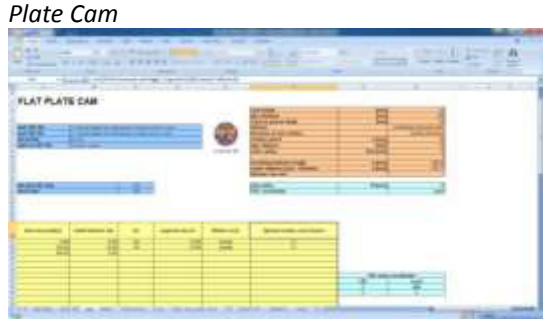

Figure 6. This page shows the basic data for geometric features on cam, in brown color and the law of movement in yellow color

In our example we have that: r_0=30 mm and the rotation is in counter-clockwise. Click in X-Camme→Data

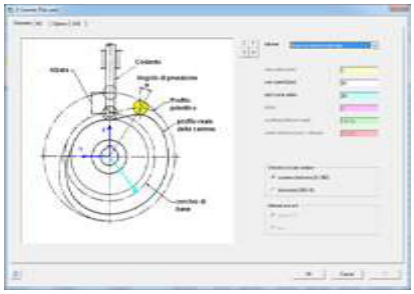

Figure 7. Determine the geometrical characteristics from X-Camme

And after we determine the geometrical characteristics define the law of movement

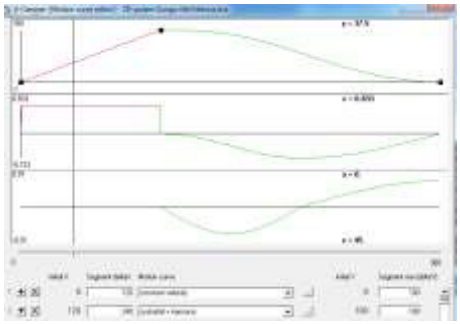

Figure 8. Define the law of movement

And we'll change the following information:
The lift is 100mm during which the cam rotates 120°.
The follower returns to its initial position with *cycloid + harmonic* motion.
And then click OK, and then click Calculate.
X-Camme get tabular data in order to: The angle of cam rotation from 0 to 360°, displacement, velocity, acceleration, radius of curvature, hall of pressure, cam profile coordinates , ect.

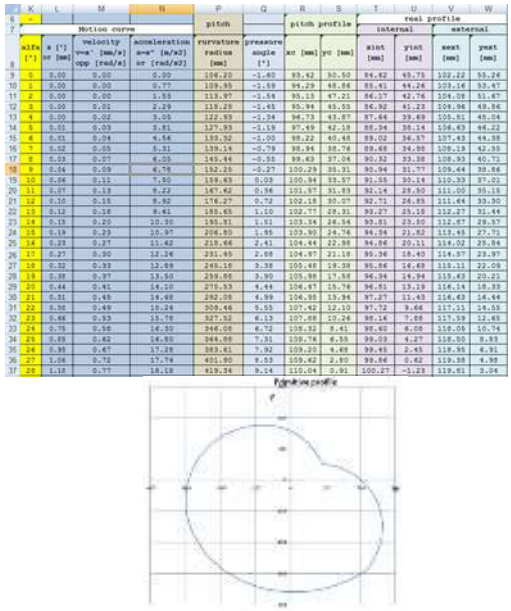

Figure 9. Tabular data, graphical presentation of the cam profile

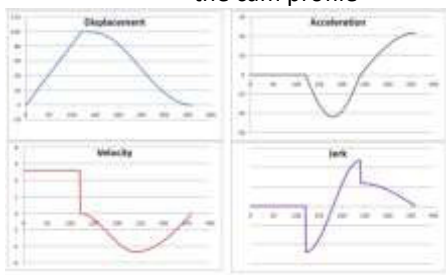

Figure10. Graphical data for displacement, velocity, acceleration and jerk

V-SIMULATION WORKING MODEL 2D

Open software Working Model 2D and will appear first page.

Figure 11. Working Model 2D first view

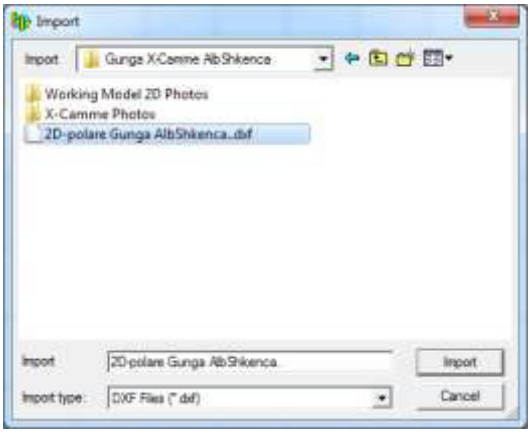

We will import X-Camme software files in the Dxf format. And will have

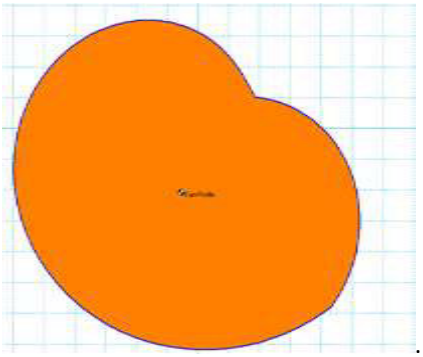

Figure 12. Imported Cam profile in Working Model 2D

Working Model 2D gives us data in graphical and tabular parameters: position, speed, acceleration, the position of the center of mass, the speed of the center of mass, acceleration of the center of mass, momentum, angular momentum, total force, gravity, electrostatic forces, etc. [6]

Figure 13. Tabular parameters of position, velocity, acceleration and force between roller and cam.

Simulation of Working Model 2D software

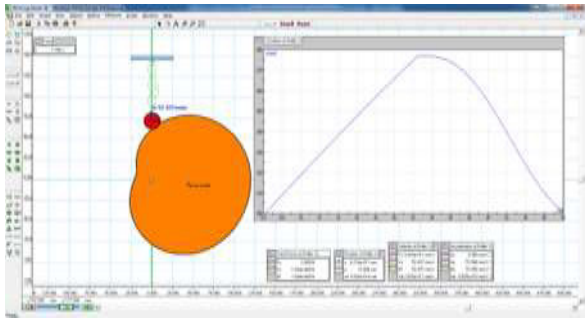

Figure 14. Simulation with Working Model 2D. (Video mode)

VI-CONCLUSIONS

In this paper among others, are treated the synthesis graphical way for the construction of the cam profile under a specific law using the X-Camme and Working Model software.

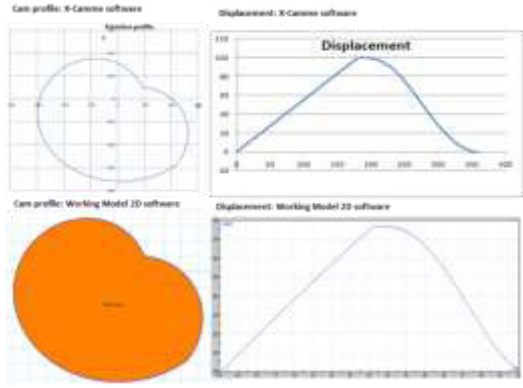

The conclusions of determining cam profile and defining the law of motion of X-Camme and Working Model 2D software are ***equivalent***.

VII- REFERENCES

1. Harold A. Rothbart, ''CAM Design Handbook'', McGraw-Hill, 2003

2. Erdman, A.G. Sandor, G.N. *Mechanism design*. Analysis and synthesis. Prentice-Hall, 1997.

3. Rivola A., Dispense del corso Meccanica Applicata alle macchine II: ''Meccanismi con came'' 2000-2001.

4. K.D.Bouzakis, S.Mitsi, I.Tsiafis: *Computer aided optimum design and NC milling of planar cam mechanisms*, International Journal of Machine Tools and Manufacture,Vol.37, No.8,pp. 1131-1142,1997.

5. CAVAGNA C., MAGNANI P., Metodo generale per lo studio e il tracciamento automatico di profili di camme, Progettare n° 14, 1981, ed. Jackson, Milano

6. Mateo S., *Working Model User's Manual*, Knowledge Revolution, CA, 1995.

AKTET **ISSN 2073-2244**
Journal of Institute Alb-Shkenca **www.alb-shkenca.org**
Revistë Shkencore e Institutit Alb-Shkenca **Copyright © Institute Alb-Shkenca**

THE ENTRANCE INTO MINI ROUNDABOUTS ON URBAN AREAS; A POTENTIAL RISK
HYRJA NË MINI-RRETHRROTULLIMET E ZONAVE URBANE; NJE RREZIK POTENCIAL

ALMA AFEZOLLI [1], ELFRIDA SHEHU[2]
Universiteti Politeknik i Tiranës, Fakulteti i Inxhinierisë së Ndërtimit, Tirane, Shqiperi
krasniqi1@yahoo.com[1], elfridaal@yahoo.com[2]

PËRMBLEDHJE
Ndër elementët e përgjithshëm të përshtatur në zgjidhjen e sistemimit të kryqëzimeve me rrethrrotullim, në këtë material synohet të jepen. Modernizimi i trafikut përmes fuqizimit të gjithë drejtuesave të mjeteve, që janë të detyruar të lirojnë rrugën, për të ndjekur një rrugë që çon në zvogëlimin e shpejtësisë; Përmirësimi i sigurisë falë eliminimit të pikave të konfliktit, përfshirë kryqëzimet aktuale të automjeteve, si ato të uljes së shpejtësisë me të cilën kalohet; Zvogëlimi i kohës së frenimit në krahasim me rregulluesin me semafor, kur rrotullimi përdoret në mënyrë të vazhdueshme; Përkufizimi i një metodologjie për llogaritjen e kapacitetit të hyrjes së rrethrrotullimeve dhe përgatitja e një procedure vlerësimi për ngopjen e secilës degë të hyrjes në kryqëzim. Formulimi i një procedure për llogaritjen e kapacitetit të degëve hyrëse, bazuar në matjet eksperimentale të kryera në mini-rrethrrotullimet e zonave urbane.
Fjalët çelës: rrethrrotullim, rrezik, siguri, degë, kapacitet, semafor

SUMMARY
Among the general elements, generally used in the systemization choice of a roundabout, this paper aims to give: Modernization of traffic through strengthening all the vehicle drivers, who are required to vacate the road, to follow a path that leads to the reduction of velocity; Improving of safety due to the elimination of conflict points, including intersections current vehicles, as they of velocity decreasing, with which passed; Reducing the time of deceleration in comparison to the semaphore regulator, when the rotation is used constantly; The definition of a methodology for calculating the capacity of roundabouts entry and preparation of an evaluation procedure for saturation of each branch of entry at the junction; The formulation of a procedure for calculating the capacity of incoming branches, based on experimental measurements performed on mini-urban roundabouts;
Key words: roundabout, risk, safety, branch, capacity, semaphore

INTRODUCTION

The regulatory system of road junctions in urban areas, through the adoption of the roundabout scheme, has now spread worldwide. Obviously, there are some significant limits on roundabouts' adaption within the urban environment. Particularly, the realization of a roundabout with priority the ring is not recommended in one of the following five cases:

- Configuration of the existing space such that does not allow the construction of a ring that ensures the possibility of maneuver to heavy vehicles and / or a vision sufficiently free;
- Rugged topography that does not allow the accommodation of a ring carriageway with the counter slopes acceptable;
- Direct adjustment of the traffic; The signage contemporary light is the main instrument of direct regulation of traffic: it consists in assigning a priority to certain traffic flows and carrying out the others; [1]
- Coordinated sequence of intersections regulated by semaphores (green wave). The inclusion of a roundabout in a sequence of intersections

controlled by semaphores, in general, has adverse effects on strategy of the sequence

- Precedence for lanes to public transport.

Roundabouts can be classified basing upon different function parameters: the size of the external diameter of the barrier, urban planning, typologies of roads and the quantities of circulating traffic.

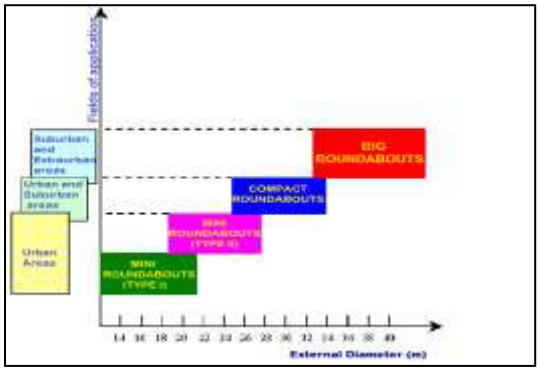

Figure 1- Classification of roundabouts basing on outside diameter and application area

With regard specifically to the urban context, we can refer to 4 possible roundabout schemes:

- Large roundabout with central insurmountable island of external diameter and 32-64 m;
- Compact roundabout (outer diameter 22 to 35 m); [2]
- Mini Roundabout of I type, with surmountable island (external diameter from 14 to 20 m);
- Mini Roundabout of II type, with surmountable or insurmountable island (external diameter from 18 to 24 m);

In this paper, we intend to propose a methodology for evaluating the functionality level of the mini-roundabouts.

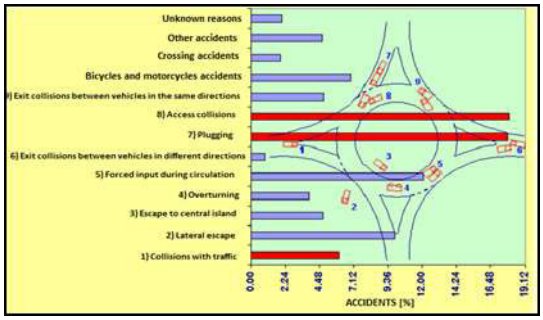

Figure - 2 Distribution of accidents on roundabouts

METHODS AND MATERIALS

EXPERIMENTAL DATA

We have analyzed two roundabouts in urban areas of Tirana, one in a highly urbanized area, Wilson Square and the other in a moderately urbanized area, in the entry part of the commercial center TEG. [2]

a)The first Mini roundabout is of type II, with four branches forming 90° angles between them. Geometrically, roundabout has a non circular central island: it is irregular ellipse diameters of 18.3 m 22.0 m. Carriageways have a width of 10:50 m in the branch D and 10:40 m in the branch B.

For this mini-roundabout type, there are no real trading zones; but can be identified maneuver trunks with modest length. Particularly it has: maneuver trunk A-B: Width = 6.20 m / Length = 13.40 m, maneuver trunk B-C: Width = 7.10 m / Length = 13.20 m, maneuver trunk C-D: Width = 8.20 m / Length = 13.30 m, maneuver trunk D-A: Width = 7.00m / Length = 14.20 m. [3]

Figure - 3 Mini roundabout 1

The second mini roundabout is of II type, with 5 branches in a moderately urbanized area. The widths of the incoming lanes are as follows: branch A = 6.40 m, branch B = 3.00 m, branch C = 5.90 m, D = 3.20 m branch, branch E = 4.00 m. Identification of the maneuver trunk is not clear between branches A and B, C and D of D and E; turning right comes directly and there are no real maneuver trunks. For the branch B and C the maneuver trunk is much visible that has a length of 20.10 m and a width of 6.20 m, as well as that between branches E and A with length 10.40 m and width 5.60 m. [1]

Figure - 4 Mini roundabout 2

The traffic data were obtained by direct registrations with the camera of the intersections and subsequent counting of vehicles. To analyze the efficiency of inputs, measurement campaigns For the first roundabout there were chosen two periods to count vehicles in the morning from 8:00 to 9:00 and in the afternoon from 17:00 to 18:00. For the second roundabout, periods of analysis were included from 8:00 to 9:00 in the morning and the second from 13:00 to 14:00 in the afternoon. There aren't taken into consideration holidays and days after the holidays, as well as Mondays, which are characterized by abnormal conditions, in terms of traffic

It was finally adopted the division into the three components of traffic: cars, trucks, motorcycles.

PROPOSAL OF A CALCULATING PROCEDURE FOR THE ENTRANCE CAPACITY IN THE ROUNDABOUTS

There is prepared an evaluation procedure for saturation of each branch of entry to the intersection. The saturation flux will be defined as the maximum number of vehicles that can enter to the ring branch, when there is no vehicle that prevents the maneuver. In the case of roundabouts, entry vehicles are obliged to give priority to those that are circulating in the ring, while those coming from the left. For this reason the circulating flow represents an obstacle for the free movement of the entry vehicles. When the entrance will be considered always free from such an obstacle, the entry vehicles (if they form a group), can reach a maximal number after one hour. [4]

The flow of saturation indicates the maximum volume of traffic that can be provided in a particular branch, but depends only on geometric conditions and not by traffic ones;

The procedure for determining the flow of saturation begins by studying the registrations taken at the two mini roundabouts. Firstly it is measured the interval between the two vehicles that successively introduced in the roundabout. There was taken care of the vehicles not affected by the others, for this reason are selected double isolated vehicles and double vehicles, that were part of ranks fourth and fifth. [5]

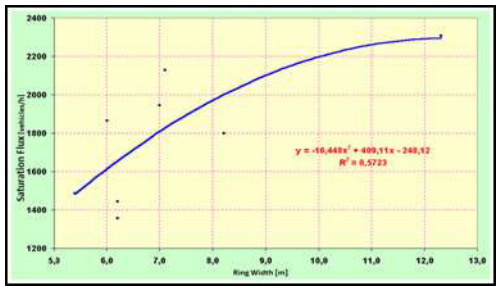

This criterion is adopted in accordance with the HCM procedure, which suggests, for on situ measurements of saturation flow of semaphores intersections, the use of introducing time for the vehicles at intersections, starting from the fourth vehicle on queue to avoid the influence of the latest vehicles of the other maneuvers and exclusion of departure of stopped vehicles. The saturation flow can be calculated by the following formula:

S=3600/tm (The average time of intervals, measured between two consequtive vehicles at the entrance).

	Branch	Saturation Flow	Entrance Width	Ring Width	Manouver Trunc Length
MINIROUNABOUT 1	A	1358 veh/h	4.1 m	6.2 m	14.2 m
	B	2130 veh/h	5.1m	7.1 m	13.4 m
	C	1800 veh/h	3,5 m	8.2 m	13.2 m
	D	1946veh/h	5.0 m	7.0 m	13.3 m
MINIROUNABOUT 2	A	2308 veh/h	4.7 m	12.3 m	25.0 m
	B	1446 veh/h	3.0 m	6.2 m	7.5 m
	C	1865 veh/h	5.9 m	6.0 m	21.0 m
	D	1488 veh/h	3.2 m	5.4 m	3.0 m

Table 1 Relation between saturation flow and geometrical elements of the mini-roundabouts

RESULTS AND DISCUSSIONS

From the performed measurements there are generated the following graphs and the relevant discussions, as well.

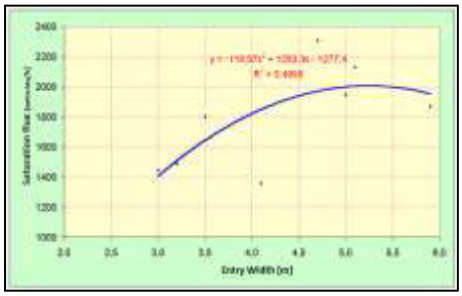

Figure 5 Relation between saturation flow (S) and the width of mini-roundabout ring (L_a)

Figure 6 Relation between saturation flow (S) and length of manoeuvre trunk (Z)

Figure 7 Relation of entrance flow (Q_{ec}) with circulating ring flow (Q_c)

The diagram, where are shown data measured on situ for entrances of two mini-roundabouts, allows the identification of three indicative groups for similar models of users' behavior, especially:

1. For incoming flow (Q_{ec}) less than se 650 veh/h, by increasing circulating (Q_c), increases dhe (Q_{ec});

2. In case when the incoming flow has a further increase (comparing with 650 veh/h dhe 1100 veh/h), the road users in the ring offer a less numbers of incoming vehicles; this is better shown by the declining performance of the regression curve. [2]

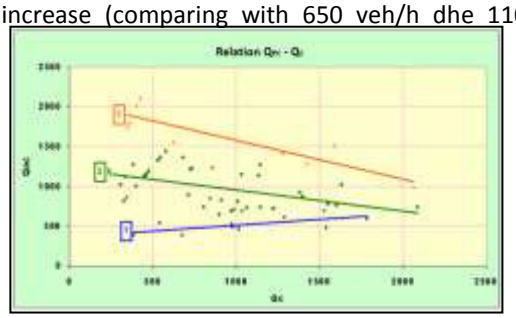

3. If the incoming flow is still high (compared with 1100 veh/h), it is noted a third functional level characterized by a forced reduction of the incoming flow by the increase of the circulating flow in the ring; in this case the regression curve results to have a sharpen slope that the above case

Recognition of geometric characteristics of roundabouts (Le, La, Z), the saturation flow (S), circular flow values before entries, allow to calculate the flow Q_{ec} in conditions of continued queue.

At the end it is possible to estimate the capacity in each entry. The ratio between the effective value of the incoming flow and the value of capacity, gives an indicative parameter of efficiency degree of the continuous flows, as well as the level of functionality of mini-roundabouts.

The ratio values Q_e/Q_{ec} about, or greater than one, shows the data of traffic congestion. It can be emphasized that the conditions of traffic congestion, often lead to abnormal behavior of drivers, or otherwise, recognizing the high level of risk, can degenerate by the entrance on the left side (as confirm accidents data reported at the beginning of the study) [5]

CONCLUSIONS

Through this methodology it is possible to follow a procedure for verifying the operation of

existing mini-roundabouts, and the assessment of the needs for carrying out any intervention modernization.

In the present paper, starting from experimental measurements performed in two mini-roundabouts on urban areas, it can be achieved in formulating a procedure for calculating the capacity of incoming branches.

It should be said that there are in the literature a series of relations which allow calculation of capacity at the entrance. These are empirical relations linking the incoming capacity with analogous parameters to those described in this report, but they have an application field regarding roundabouts with larger diameters compared with those of mini-roundabouts, as well. [4]

It can also be reemphasized how flow conditions of vehicles near the congestion, may increase the risk accepted by users. Definitely it requires detailed investigations by experts in the field for a better characterization of situations in terms of vehicles' traffic, adding also different geometric elements that constitute the schemes of roundabout intersections.

BIBLIOGRAPHY

[1] AA. VV. Highway Capacity Manual. Special Report 209 (Ed. Trasportation Research Board, 1994).

[2] R. Mauro, T. Esposito. Sintesi delle comunicazioni per il seminario di formazione tecnica "Rotatorie" – Urbania 24 febbraio 1999 – Pubblicazione edita da "Padova fiere".

[3] R. Mauro, M. Chinni. Il comportamento degli utenti in intersezioni a raso del tipo a rotatoria – Convegno di Pisa, 29-30 ottobre 1997.

[4] E. A. A. Shawaly, C. W. W. Li, R. Ashworth. Effects of entry signals on the capacity of roundabouts entries. A case-study of Moore Street roundabouts in Sheffield – Traffic Engineering + Control – n. 32/6 – Giugno 1991.

[5] W. C. K. O. Yee, M. G. Bell. The impact of accidents and driver behaviour of concentric lane-markings in small roundabouts – Traffic Engineering + Control – n. 27/5 – Maggio 1986.

AKTET **ISSN 2073-2244**
Journal of Institute Alb-Shkenca **www.alb-shkenca.org**
Revistë Shkencore e Institutit Alb-Shkenca **Copyright © Institute Alb-Shkenca**

PËRFORCIMI ME FRP I KOLONAVE BETONARME
STRENGTHENING OF REINFORCED CONCRETE COLUMNS USING FRP

IGLI KONDI[a], JULIAN KASHARAJ[a], ERVISA ORMENI[b]

[a]Departamenti i Konstruksioneve të Ndertimit dhe Intrastrukturës së Transportit, Fakulteti i Inxhinierisë së Ndërtimit, Universiteti Politeknik i Tiranës, Shqipëri,
i.kondi13@gmail.com
[b]Kompania "TEHA KONSTRUKSION", Tiranë, Shqipëri

PËRMBLEDHJE
Për arsye arkitektonike, strukturore apo të dëmtimit ose degradimit të materialeve përbërës, kolonave ekzistuese betonarme kërkohet tu rritet aftësia mbajtëse. Përdorimi i fibrave polimere FRP (Fiber Reinforced Polymer) përfaqëson një nga mënyrat më moderne të përforcimit. Evidentimi i domosdoshmërisë dhe i problemeve strukturore që lidhen me përforcimin e kolonave betonarme, duke u përqendruar në përdorimin e FRP, mënyrat e llogaritjes, ndikimi i tyre në rritjen e aftësisë mbajtëse të kolonave, përparësitë dhe të metat, përbëjnë qëllimin e studimit. Si rast studimor analizohen kolona betonarme ekzistuese në dy raste. Së pari analizohen kolonat ashtu siç janë dhe së dyti të përforcuara me FRP. Ndërtohen diagramat e ndërveprimit M - N dhe nxirren konkluzione përkatëse. Mbi bazën e një analize të përgjithshme, si edhe mbi bazën e rezultateve të rastit studimor konkret arrihet në përfundimin se përse duhet kryer përforcimi i kolonave, duke u ndalur në rolin e FRP për këtë qëllim.

SUMMARY
Because of architectural or structural reasons, damage or degradation of the materials composing, existing reinforced concrete columns, it is required to increase their capacity, or for them to be reinforced. The use of FRP (Fiber Reinforced Polymer) represents one of the most modern ways of strengthening. Identification of the problems associated with the strengthening of reinforced concrete columns, focusing on the use of FRP, the calculation methods, their impact on increasing the columns capacity, advantages and disadvantages, constitute the purpose of the study. Existing reinforced concrete columns are analyzed. Firstly the columns are analyzed as they are and secondly reinforced with FRP. Interaction diagrams M - N are constructed and relevant conclusions are drawn. On the basis of an overall analysis, as well as on concrete case study results we concluded on why the strengthening of the columns should be executed, focusing on the role of FRP for this purpose.
Keywords: strengthening, FRP (Fiber Reinforced Polymer), Eurocode, interaction diagrams.

Introduction

The key role of the FRP strengthening of existing reinforced concrete columns is qualitatively similar to the role of steel stirrups and consists on "rounding" the cross section of the element. FRP wrapping, creates a passive interaction system (without initial pressure of the FRP on the column), which is activated by transverse deformations (radial), that the column suffers from as a result of compressive forces. These deformations are supported by FRP. The effects of the wrapping depend on radial deformations that are impeded by FRP. FRP wrapping is realized by placing FRP sheets or stripes around the perimeter of the column, creating like so a continuous wrap with stripes. If the strengthening of the columns is realized with FRP stripes, then the best is for them to be perpendicular to the longitudinal axis of the element. Wrapping through FRP sheet avoids the phenomenon of the loss of stability of the longitudinal bars of the column, increases the

compression resistance of concrete, and increases the concrete ultimate deformation, εcu. Consequently, the ductility is increased; the compression capacity due to axial forces is increased as well as the flexural capacity. Figure 2 shows the deformation-strain curve for wrapped and unwrapped concrete. Increasing of the compression resistance and of the corresponding deformation of the FRP wrapped concrete, depends on the pressure of the wrap. Strengthening with FRP (elastic type until the point of rupture), compared with steel reinforcement strips (elastic - plastic type), creates a side pressure that increases with increasing of the radial deformation (transverse) of the column. Destruction of reinforced column comes due to the destruction of FRP. Conventionally saying, the destruction occurs when the deformation of FRP is 0.4%

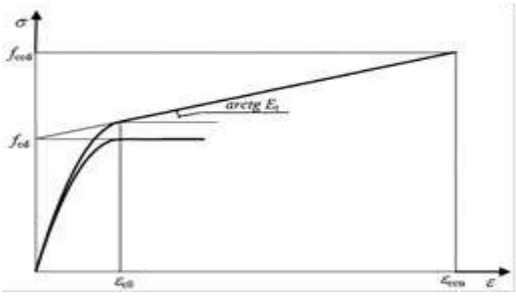

Figure 1. Deformation-Strain curve for wrapped and unwrapped concrete [2]

Figure 2. Applications of FRP reinforcement in columns [10]

Materials and methods

1. *Calculation of the columns in axial compression*

Calculations are based on Italian norms [2]. The condition that must be satisfied is:

$$N_{ed} \le N_{Rcc,d} \quad (1)$$

N_{Ed} – design, acting, compressive axial force

$N_{Rcc,\,d}$ – ultimate, bearing, compressive axial force

$$N_{Rcc,d} = \frac{1}{\gamma_{Rd}} \cdot A_c \cdot f_{ccd} + A_s \cdot f_{yd} \quad (2)$$

γ_{Rd} - partial safety coefficient, see Table 1.

A_c - cross sectional area of the element

f_{ccd} – design compression resistance of wrapped concrete

A_S – steel reinforcement area

f_{yd} - design resistance of steel

The following expression allows us to determine f_{ccd}:

$$\frac{f_{ccd}}{f_{cd}} = 1 + 2.6 \cdot \left(\frac{f_{l,eff}}{f_{cd}} \right)^{2/3} \quad (3)$$

f_{cd} - design compressive resistance of unwrapped concrete

$f_{l,\,eff}$ - effective pressure of the wrap

Wrapping is considered efficient if the following condition is realized:

$$\frac{f_{l,eff}}{f_{cd}} > 0.05 \quad (4)$$

From the pressure of the wrap (f_l) exerted by FRP, in the presence of radial deformation of the column, only a fraction of it helps in the capacity of the reinforced element. This fraction of f_l is indicated as $f_{l,\,eff}$ and is called "effective pressure of the wrap" and it depends on the cross sectional shape of the element as well as the on the way of strengthening.

$$f_{l,\,eff} = k_{eff} \cdot f_l \quad (5)$$

$k_{eff} \le 1$ - coefficient of performance

$$k_{eff} = V_{c,\,eff} / V_c \quad (6)$$

$V_{c,\,eff}$ - the volume of wrapped concrete

Vc - the total volume of reinforced concrete element

The wrap pressure can be expressed as it follows:

$$f_l = 0.5 \cdot \rho_f \cdot E_f \cdot \varepsilon_{fd,\,red} \quad (7)$$

ρ_f - geometric percentage of FRP. Depends on the shape of the section and on way of placing FRP (continuous or not).

In columns with round cross section, the expression (8) allows us to define ρ_f:

$$\rho_f = (4 \cdot t_f \cdot b_f) / (D \cdot p_f) \quad (8)$$

t_f - the thickness of the FRP

b_f - the height of the FRP stripe

p_f – the step between FRP strips

D – the diameter of the cross section

To better understand the above symbols see Figure 4. In the case of continuous wrap with FRP, $b_f / p_f = 1$ and:

$$\rho_f = 4 \cdot tf / D \quad (9)$$

E_f - module of elasticity of FRP in direction of fiber

$\varepsilon_{fd,\,red}$ - reduced ultimate deformation of FRP

In square cross section elements, the expression (10) allows us to define ρ_f:

$$\rho_f = [2 \cdot t_f \cdot (b + h) \cdot b_f] / [b \cdot h \cdot p_f] \quad (10)$$

t_f - the thickness of the FRP

b_f - the height of the FRP stripe

b and h - cross section dimensions

In the case of continuous wrap with FRP, $b_f / p_f = 1$ and:

$$\rho_f = [2 \cdot t_f \cdot (b + h)] / [b \cdot h] \quad (11)$$

$$k_{eff} = k_h \cdot k_v \cdot k_\alpha \quad (12)$$

k_H - horizontal efficiency coefficient

k_V - vertical efficiency coefficient

k_α - FRP slope coefficient

k_H - depends on the shape of the cross section of the element. For round section $k_H = 1.0$.

For rectangular section:

$$k_H = 1 - \frac{b'^2 + h'^2}{3 \cdot A_g} \quad (13)$$

Figure 3 helps to better understand the symbols that are part of the expression (13).

Ag - total area of the cross section of the element, $Ag = b \cdot h$.

k_V depends on the progress of FRP wrap, along the longitudinal axis of the element. k_v does not depend on the shape of the reinforced concrete element cross section. In cases of continued FRP wrap, $k_v = 1$. In cases of non-continuous wrap (striped) as shown in Figure 4, k_v is determined by the expression:

$$k_v = \left(1 - \frac{p'_f}{2 \cdot d_{min}}\right)^2 \quad (14)$$

d_{min} - the minimum size of the cross section. In round sections d_{min} is the diameter.

Recommend $p'_f \le d_{min} / 2$. Regardless of the form of cross section:

$$k_\alpha = \frac{1}{1 + (tg\alpha_f)^2} \quad (15)$$

α_f - the inclination angle of the fibers towards the perpendicular plan to the longitudinal axis of the element. So for a column that is reinforced with FRP, if these are placed perpendicular to the longitudinal axis then $\alpha_f = 0$ °.

Reduced calculating deformation of FRP is determined by the expression:

$$\varepsilon_{fd,\,red} = \min [\eta_a \cdot \varepsilon_{fk} / \gamma_f; 0004] \quad (16)$$

η_a - environmental coefficient

γ_f - partial safety coefficient of FRP

ε_{fk} - a conventional FRP deformation border. It is usually accepted 0.004.

Based on Figure 3, it can be seen that the actual surface of the wrap is only a part of the total area. This is due to the phenomenon of "arc" that is created inside the element. This phenomenon depends on the radius r_c that rounds the corners of the section.

For square sections, with width or height >90cm, FRP reinforcement has no effect. The same applies when b/h>2.

	γ_{rd}
Flexion/Compression with flexion	1.00
Shear/Torsion	1.20
Wrapping	1.10

Table 1. Partial safety coefficients of FRP [2]

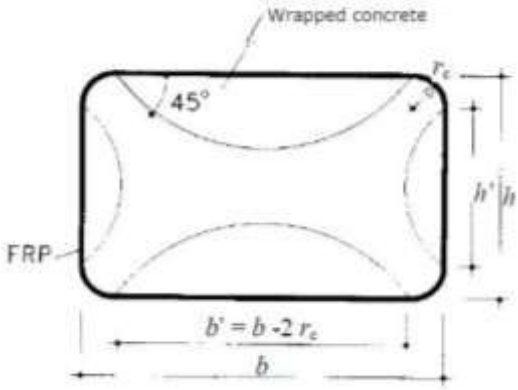

Figure 3. The column cross section reinforced with FRP [2]

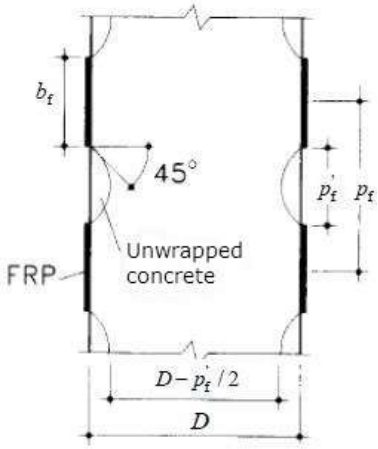

Figure 4. Placing of FRP along the column [2]

1. Calculation of the columns in compression with bending

In this case comes to our help the interaction diagram M - N. To better explain this, let us take a concrete example. We analyzed a reinforced concrete column with rectangular cross section, b = 30cm, h = 50cm, d '= 4 cm, d = 46cm, r_c = 1.5cm, A_S = 8.04cm2 (4ϕ16), A's = 6.16cm^2 (3ϕ16); S 500C steel, f_{yk} = 5000daN/cm^2, f_{yd} = 4348daN/cm^2, γ_s = 1:15, E_s = 2000000daN/cm^2, $\varepsilon_{yd} = f_{yd} / E_s$ = 4348/2000000 = 0.217%; Concrete C25/30, f_{ck} = 250daN/cm^2, γ_c = 1.5, f_{cd} = 141.7daN/cm2; FRP, E_f = 2700000daN/cm^2, p_f = 10cm, bf = 5cm, p'_f = 5cm, t_f = 0.167cm, f_{tk} = 27000daN/cm^2, $\varepsilon_{fk} = f_{tk} / E_f$ = 1%;

Interaction diagram will be built twice. The first time for unwrapped concrete resistance f_{cd}=141.7daN/cm^2. The second time for wrapped concrete resistance f_{ccd}. Figure 5 shows the interaction diagram for the unwrapped concrete, f_{cd}=141.7daN/cm^2.

We must now determine the value of f_{ccd} from expression (3).

$f_{l,\,eff} = k_{eff} \cdot f_l$ = 48.096 = 0.292 · 14.04daN/cm^2

$k_{eff} = k_h \cdot k_\alpha = k_v \cdot 0.347 \cdot 0.840 \cdot 1 = 0.292$

$$\frac{f_{ccd}}{f_{cd}} = 1 + 2.6 \cdot \left(\frac{f_{l,eff}}{f_{cd}} \right)^{2/3} \quad (3)$$

$$k_H = 1 - \frac{b'^2 + h'^2}{3 \cdot A_g} = 1 - \frac{27^2 + 47^2}{3 \cdot 1500} = 0.347$$

$Ag = b \cdot h = 30 \cdot 50 = 1500cm^2$

b '= b - 2 · 30-2 · RC · 1.5 = 27cm

h '= h - 2 · 50-2 · RC · 1.5 = 47cm

$$k_v = \left(1 - \frac{p'_f}{2 \cdot d_{min}}\right)^2 = \left(1 - \frac{5}{2 \cdot 30}\right)^2 = 0.840$$

Recommend $p'_f \le d_{min} / 2$. Indeed p'_f = 30/2 = 15cm ≤ 5cm.

$$k_\alpha = \frac{1}{1 + (tg\alpha_f)^2} = \frac{1}{1 + (tg0)^2} = 1$$

$f_l = 0.5 \cdot \rho_f \cdot E_f \cdot \varepsilon_{fd,red}$ = 0.5 · 0.00890 · 2700000 · 0.004 = 48.096daN/cm^2

$\rho_f = [2 \cdot t_f \cdot (b + h) \cdot b_f] / [b \cdot h \cdot p_f] = [2 \cdot 0.167 \cdot (30+50) \cdot 5] / [30 \cdot 50 \cdot 10] = 0.00890$

$\varepsilon_{fd,red} = \min[\eta_a \cdot \varepsilon_{fk} / \gamma_f;\ 0.004] = \min[1 \cdot 0.01/1.1;\ 0.004] = 0.004$

$$f_{ccd} = 141.7 \cdot \left[1 + 2.6 \cdot \left(\frac{14.04}{141.7} \right)^{2/3} \right] =$$

220.6daN/cm^2

Results and discussions

In Figure 5 are shown superimposed the two diagrams. In blue is shown the unwrapped concrete diagram. With red color is shown the wrapped concrete diagram.

Looking at Figure 5, we can say that the role of FRP is to increase compressive strength of concrete which is like increasing the class of concrete. This is why the compressed area (the area on the horizontal axis of the diagram) has a "bulge" of the M – N diagram, which means increasing the compression capacity. While in the tension area (area under the horizontal axis of the diagram) both diagrams are identical, as you know, in tension, the concrete contribution is negligible.

Figure 6 shows the interaction diagrams for three different instances of the module of elasticity of FRP. Of course with increased elasticity module increases the contribution of the FRP reinforcement in increasing the compressive resistance of concrete. Consequently, the ability of the respective capacity of reinforced concrete elements increases.

Increasing the contribution of the FRP reinforcement can be accomplished by increasing their elasticity module (E_f), increasing the thickness of the layer of FRP (t_f), increasing the width of the FRP strip (b_f), reducing the distance between the FRP strips (p_f). All these lead to increased resistance of wrapped concrete (f_{ccd}) and further lead to increase of the productivity of the element. From the qualitative point of view, building the interaction diagrams for the above factors, would derive some graphics very similar to that of Figure 6.

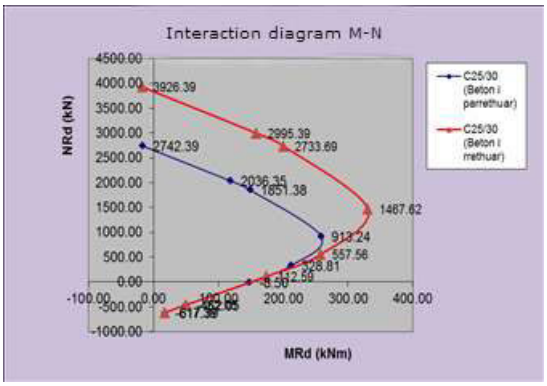

Figure 5. Interaction diagrams M-N of FRP reinforced and not reinforced element

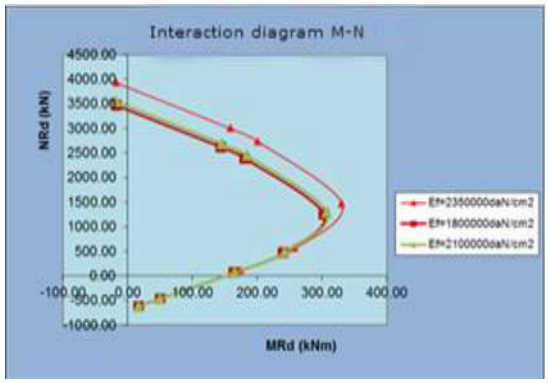

Figure 6. Interaction diagrams M-N of FRP reinforced elements for different elasticity modulus of FRP

Conclusions

The role of FRP is qualitatively the same as the role of steel stirrup. The role of FRP can be expressed as wrapping of the cross section of the element.

•FRP wrapping avoids the phenomenon of stability loss of the longitudinal bars of the column, it increases the compression resistance of concrete and it increases the concrete ultimate deformation ε_{cu}. Consequently, the ductility increases as well as the capacity towards axial compression forces and flexural moments.

Compared with other materials, the use of FRP in strengthening the structural elements has these advantages:

- High durability
- Low weight
- High resistance
- Easy usage
- Easy transport
- Very high resistance to fatigue
- Excellent architectural impact
- Resistant to corrosion
- Suitable even for elements with uneven surface
- Excellent opportunity to orientate the fibers in the right direction, according to the way the element works, depending on it's under stress condition
- Easy and short maintenance
- Can be used to reinforce the historical, architectural and aesthetic structures, in which

the use of other enforcement methods would lead to the violation of these values.

As negative side we can mention:

• High costs

• New materials and their technical problems are still not well known from those who use them

• Problems arise in the connection between FRP and reinforced concrete elements to which they are put.

References

1. Eurocode 2, January 2005.

2. CNR (COMMISSIONE NAZIONALE DELLE Ricerche) - Istruzioni for progettazione left, l'il ed esecuzione know interventi control that knows consolidamento mediante l'utilizzo statico know COMPOSITI fibrorinforzati, Marzo 2012.

3. TC Triantafillou - Guidelines for the dimensioning of REINFORCED Concrete Elements strengthened with CFRP (carbon fiber polymers REINFORCED), 1999.

4. RUBINO C., drink D., P. IANELLI - Rinforzo armato know STRUTTURE in Concrete, 2005.

5. AICAP - Guide all'uso dell'Eurocodice 2, 2006.

6. S. BARBATO - sismico Adeguamento know edifici in some impiego mediante l'know COMPOSITI fibrorinforzati material (FRP), 2003.

7. N. Pojani - Seismic Engineering, 2003.

8. A. BIONDI - Cemento armato, 2006.

9. A. CAROLIN - Carbon fiber REINFORCED polymers for Strengthening of structural elements, in 2003.

10. ALVARO V - COMPOSITI a matrix material for the rinforzi cementizia strutturali, 2006.Abstrakt.

AKTET **ISSN 2073-2244**
Journal of Institute Alb-Shkenca **www.alb-shkenca.org**
Revistë Shkencore e Institutit Alb-Shkenca **Copyright © Institute Alb-Shkenca**

PËRSHTATJA SIZMIKE E STRUKTURAVE BETONARME EKZISTUESE ME NDIHMËN E FRP (Fiber Reinforced Polymer)

SEISMIC RETROFITTING OF REINFORCED CONCRETE STRUCTURES USING FRP (Fiber Reinforced Polymer)

JULIAN KASHARAJ[a], IGLI KONDI[a], ERVISA ORMENI[b]

[a]Departamenti i Konstruksioneve të Ndertimit dhe Intrastrukturës së Transportit, Fakulteti i Inxhinierisë së Ndërtimit, Universiteti Politeknik i Tiranës, Shqipëri,
j.kasharaj69@yahoo.ca
[b]Kompania "TEHA KONSTRUKSION", Tiranë, Shqipëri

PËRMBLEDHJE
Një strukturë betonarme, e projektuar ndërtuar mbi bazën e normave antisizmike të Republikës së Shqipërisë, mund të mos i përmbushë rregullat antisizmike që përmbahen tek Eurokodet. Si pasojë del si detyrë përshtatja sizmike e saj. Evidentimi i domosdoshmërisë dhe i problemeve strukturore, që lidhen me përshtatjen sizmike, duke u përqëndruar në përdorimin e FRP, përparësitë dhe të metat, përbëjnë qëllimin e studimit. Si rast studimor është analizuar një strukturë e projektuar sipas normave antisizmike kombëtare. Kryhet analiza push - over e strukturës në dy raste. Së pari analizohet struktura ashtu siç është dhe së dyti e përforcuar me FRP. Në rastin e dytë fillimisht përforcohen trarët, pastaj kolonat dhe në fund të dyja. Ndërtohen kurbat e kapacitetit dhe nxirren konkluzionet përkatëse. Mbi bazën e rezultateve të analizës së strukturës ekzistuese arrihet në përfundimin se përse duhet kryer përshtatja sizmike, duke u ndalur në rolin e FRP për këtë qëllim.

SUMMARY
A reinforced concrete structure, designed and built on the basis of anti-seismic norms of the Republic of Albania, may not fulfill the new anti-seismic norms, contained in Eurocodes. Consequently seismic retrofitting emerges as a task. The identification of the structural problems related to the seismic retrofitting, focusing on the use of FRP, advantages and disadvantages, are the purpose of this study. We analyzed a structure that is designed according to the national anti-seismic norms. The push-over analyzes has been run two times. Firstly we analyze the structure as it is and secondly reinforced with FRP. In the second case initially we reinforced beams, then columns, then both of them. The capacity diagrams were built and relevant conclusions were drawn. On the basis of the results of the analysis of the existing structure we conclude why seismic retrofitting should be carried out, focusing on the role of FRP for this purpose.
Key words: seismic retrofitting, FRP, Eurocodes, pushover analysis

Introduction

Knowledge in the field of structural engineering is in continuous progress. Technical norms in general and especially anti-seismic norms are in constant development. As a result, a structure conceived, designed and built in a certain period of time, may not fulfill the rules of new anti-seismic norms. In this case interventions must be provided to the structure. There are many ways and materials for retrofitting existing structures. A more modern way is related to the use of Fiber Reinforced Polymer, FRP.

What does it mean, from a technical point of view, seismic retrofitting with the help of FRP? In seismic zones, intervention with FRP on

reinforced concrete elements is mainly related to achieving the following objectives:

•Increased the bending moment capacity, through the application of FRP in the direction of the axis of the element.

•Increased the shear force capacity, through the application of FRP, with fibers placed perpendicular to the axis of the element, or with a 45 ° angle.

•Increased compression capacity of elements through the FRP wrapping along the perimeter (FRP fencing).

•Increased ultimate deformation of concrete, ε_{cu}.

•Increase section ductility on beams or columns, by wrapping the FRP along the perimeter.

•Improve efficiency of joints, through adhesions with FRP along the perimeter.

•Avoidance, by wrapping the FRP along the perimeter, of the loss of stability of longitudinal steel bars for compressed elements.

•Increased tensile strength, joints beam - column, through the application of FRP strips with fiber located on the direction of strains.

Anti-seismic norms in the Republic of Albania

The structure that we will analyze has been projected on 1986. For this reason there it has been used the anti-seismic code of the 1978.

Regarding these norms, the seismic action is estimated on the basis of the MSK-64 scale. The Albanian territory is divided in three different zones with expected seismic intensity of 6, 7, 8. The horizontal seismic force it is given by the following expression:

$$S_k = Q_k \cdot K_c \cdot \beta \cdot m_k \quad (1)$$

Q_k - weigh

K_c – seismic coefficient, K_c = 1/40 (seismic intensity of 7), K_c = 1/20 (seismic intensity of 8), K_c = 1/10 (seismic intensity of 9)

β – dynamic coefficient, β = 0.9/T

T – period of vibration

m_k – distribution coefficient

$$m_k = \frac{X_{(xk)} \sum_{1}^{m} Q_j \cdot X_{(xj)}}{\sum_{1}^{n} Q_j \cdot X_{(xj)}^2} \quad (2)$$

$X_{(xk)}$ – the structure displacements during the vibrations in K point

$X_{(xj)}$ - the structure displacements during the vibrations in J point

Materials and methods

Nonlinear static analysis is performed by the application in the building of gravity loads and a system of horizontal forces, keeping unchanged own force reports, all scaled in such a way that the horizontal displacement of a "control point" of the structure, is gradually raised until the ultimate conditions are achieved. We will try to explain below in simple terms, what is in essence, the push - over analysis. This analysis shows in a precise way what happens to the structure when the earthquake hits. It shows how this structure behaves when the earth shakes. If we speak figuratively, push - over analysis imitates a giant set near the building that begins to push it always harder, until destruction. At first the building cracks, then it tilts terrifically, until finally destroyed, as if it was cardboard. At first you can notice visible cracks at the ends of a beam, then another, then at the ends of a column, then another, until the entire building is destroyed. The push-over analysis virtually leads the building to its destruction, to understand what happens. This is more or less, in simple terms the basic idea of the analysis. Let's move on with the reasoning. Assume that the entire structure is made of crystal. From the very first push of our giant (earthquake) buildings would become crumb. It is true that the crystal is strong, but it is breakable. For this reason it is not suitable to build a house. While reinforced concrete is a material, able to absorb and transmit the kinetic energy of the earthquake. At firs the reinforced concrete cracks, then the steel bars spread, pass on fluency and as a result the structure is deformed and a lot of earthquake energy is absorbed and transformed, while the destruction has not occurred. We must be very careful, because the whole structure should be ductile. It is sufficient for a single column not to be ductile (i.e. be of "crystal"), and due to earthquake it will be destroyed first. After the destruction of the first column, it will start a chain reaction that would

lead to the ultimate destruction of the entire building.

Practically, seismic retrofitting of a structure with the help of FRP, as explained above, is a set of reinforcement of its constituent elements, such as columns, beams, shear walls, floors, etc. In order to strengthen structural elements, for which the conditions are not satisfied by ultimate controls, FRP are used, which represent a valuable alternative compared to traditional techniques of placing steel plates, etc.

Flexural strengthening of beams for positive and negative moment is accomplished by applying layers of FRP, located in the direction of the beam axis. Reinforcement at the bottom of the beam is applied at the entire length of the beam in order for the anchorage to happen in the compression area and also guaranteed by the presence of the shear reinforcement. However, the beam-column joints, where flexural moments attire the upper fibers of the beam, wanting to ensure that the FRP reinforcement would be effective in this area, stainless steel angular profiles are used. At the other end of FRP, steel piasters are used to fix FRP in the body of the beam.

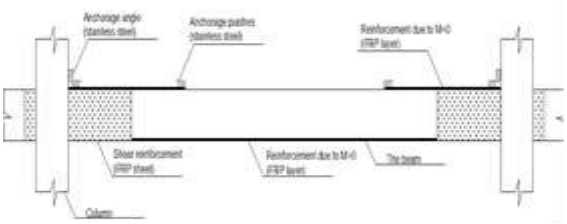

Figure 1. FRP strengthening of flexural beams

Analysis, modeling, calculation, seismic retrofitting of an existing reinforced concrete structure

An existing reinforced concrete structure designed according to anti-seismic norms of the Republic of Albania "Technical Design, KTP-1-1978", is analyzed. The structure belongs to a four-story building, which is located in Tirana and was designed in 1986 by the Institute of Research and Design of Military Works, Tirana. The structure of the building is reinforced concrete, prefabricated. The foundations are separated, connected with beams. Slabs are pre-prepared. The steel used is Ç - 3 with tensile strength R = 2100daN/cm^2. Foundations are realized with concrete, grade 250. All other elements are realized with concrete, grade 300.

To run the push – over analysis, the structure should be modeled as it is executed. To fulfill this, the building is modeled in CDS (Italian software) by putting one by one all the steel reinforcements of the structural elements (columns and beams).

Then we analyze the structure through the Push-Over and the following results are obtained.

Results and discussion

1.Force – Displacement diagram for the existing structure not reinforced with FRP.

We can see that none of the curves passes the push-over analysis.

The control is not satisfied for neither of Operational Level, Life Safety Level and Collapse Prevention Level.

2.Force - Displacement diagram for the existing structure when only the beams are reinforced with FRP.

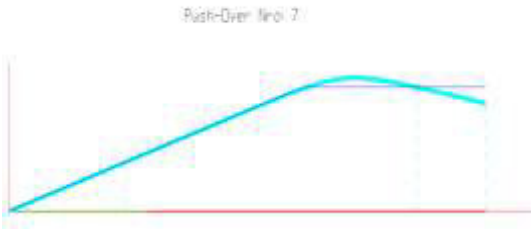

We can see a slight improvement, but most of the curves still don't pass the push-over analyze.

The control for Operational Level and Life Safety Level is satisfied in most of the curves, but the Collapse Prevention Level only on a few of them.

3.Force – Displacement diagram for the existing structure when only the columns are reinforced with FRP

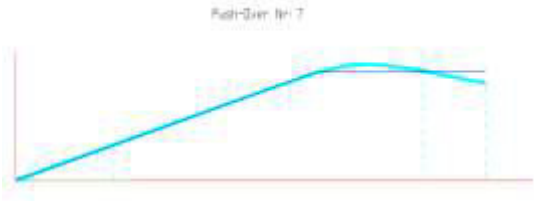

We can see an even bigger improvement of the curves, but some of them (exactly three of them) still don't pass the push-over analyze.
Most of them satisfy the three levels of control, but three of them do not satisfy the Collapse prevention level.
4.Force – Displacement diagram for the existing structure when both the beams and the columns are reinforced with FRP.

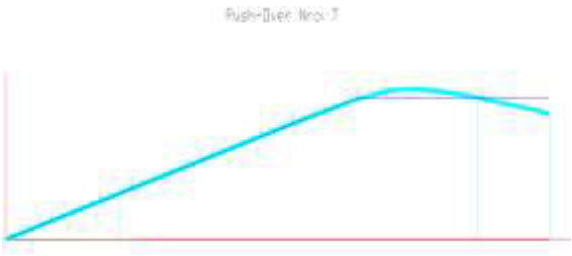

We can see that after the total reinforcment of the structure with FRP all the curves are improved evidently and the push – over analysis is realized 100%
All of the diagrams satisfy the three control levels.

Conclusions

1. Strengthening with FRP increases the bending moment capacity of the structure.
.
2. Strengthening with FRP brings increases shear capacity of the structure.
3. Strengthening with FRP increases compression capacity of the structure.
4. Strengthening with FRP increases the ductility of the structure.
6. Strengthening with FRP increases the torsion capacity of the structure.
7. Strengthening just the columns with FRP affects more than strengthening just the beams, regarding the maximum displacement of the structure due to horizontal force.
8. Strengthening with FRP satisfies the nonlinear static calculation otherwise known as Push-Over.
9. All of the above have a great impact on improving the technical performance of the structure regarding the seismic forces.

References

1.Eurocode 2, November 2005.
2.CNR (COMMISSIONE NAZIONALE DELLE RICERCHE) – Istruzioni per la progettazione, l'esecuzione ed il controllo di interventi di consolidamento statico mediante l'utilizzo di compositi fibrorinforzati, Marzo 2012.
3.TRIANTAFILLOU T.C – Guidelines for the dimensioning of reinforced concrete elements strengthened with CFRP (carbon fiber reinforced polymers), 1999.
4.RUBINO C., PINI D., IANELLI P. – Rinforzo di strutture in cemento armato, 2005.
5.AICAP – Guida all'uso dell'Eurocodice 2, 2006.
6.BARBATO S. – Adeguamento sismico di edifici in c.a. mediante l'impiego di materiali compositi fibrorinforzati (FRP), 2003.
7.POJANI N. – Inxhinieria Sizmike, 2003.
8.BIONDI A. – Cemento armato, 2006.
9. CAROLIN A. – Carbon fibre reinforced polymers for strengthening of structural elements, 2003.
10.ALVARO V. – Materiali compositi a matrice cementizia per i rinforzi strutturali, 2006
.

AKTET **ISSN 2073-2244**
Journal of Institute Alb-Shkenca **www.alb-shkenca.org**
Revistë Shkencore e Institutit Alb-Shkenca **Copyright © Institute Alb-Shkenca**

REPAIR WELDING OF STEEL PIPES
SALDIMI RIPARUES I TUBAVE TË ÇELIKUT

RRAHIM MAKSUTI[a] , HAMIT MEHMETI[a], MALUSH MJAKU[b] , MURSEL RAMA[a]
[a]Faculty of Geosciences, University of Mitrovica "Isa Boletini", rr. Minatori p.n., 40 000 Mitrovica, KOSOVA
[b]Faculty of Computer Sciences, University of Prizren "Ukshin Hoti", rr. "Rruga e Shkronjave" nr.1, 20 000 Prizren, KOSOVA
e-mail: rrahimmaksuti@yahoo.com

PËRMBLEDHJE
Saldimi riparues i tubave të çelikut në linjën e prodhimit është pjesë përbërëse e prodhimit të tubave të çelikut dhe realizohet me qëllim të largimit të defekteve që ndodhin gjatë prodhimit. Saldimi riparues, jo vetëm që i bën tubat e riparuar të përshtatshëm për përdorim, por shpeshherë e zgjatë afatshërbimin e tyre, falë përmirësimit të vetive mekaniko-teknologjike, nëse realizohet në mënyrë profesionale, me ndërgjegje të lartë, me pajisje të përshtatshme dhe në mënyrë sistematike. Qëllimi i punimit është saldimi riparues me hark elektrik me dorë i defekteve të tegelit të tubave me diametër Φ812x12mm, prej çeliku me mikropërlidhje API Grade X65, që ndodhin gjatë prodhimit. Prova dhe kontrolli pa shkatërrim realizohen për verifikimin e cilësisë së saldimit riparues. Rezultatet e provave dhe kontrollit, dëshmojnë se saldimi riparues i rikthen tubat e defektuar në gjendje të përshtatshme për përdorim, duke siguruar efikasitet dhe efektivitet të lartë të procesit të prodhimit.
Fjalët çelës: saldimi riparues, tuba, çelik, prova, kontroll.

SUMMARY
Repair welding of steel pipes in production line (in line) is an integral part of the production of steel tubes and implemented in order to remove the defects that occur during production. Repair welding, it does not only makes tubes suitable for use, but often is extending their service life, because of its improvement of mechanical and technological properties, if it is implemented professionally, conscientiously, with appropriate equipment and systematically. The aim of this paper is manual metal arc repair welding of defects in seam pipes with diameter Φ812x12mm, from micro-alloyed steel API Grade X65, which occur during the manufacturing process. Destructive and nondestructive testing were conducted to verify the quality of repair welding. Results of realized tests and inspction show that repair welding restores the defective pipes and makes them suitable for use, ensuring efficiency and effectiveness of the production process.
Key words: repair welding, pipes, steel, testing, inspection.

1. INTRODUCTION

Welded steel pipes are most widely utilized pipes for fluids transportation through pipelines in long distance. Submerged arc welding (SAW) is one of the most extensively method for production of high quality spiral welded carbon steel pipes suitable for transporting large volumes of oil and gas in long distance, but as with others production technologies, defects can occur. In this process, hot rolled coil is gradually formed into round shape through roll-forming stands, figure 1 and its edges are joined by submerged arc welding (SAW). Submerged arc welding (SAW) is traditionally considered as an efficient and highly productive joining technology where the welding arc and the weld pool are always covered with a layer of granular flux that protects the welding arc and welding pool from

atmospheric contamination [1]. Because during SAW of steel pipes is very difficult to avoid weld defects, weld repair becomes an inevitable part of the production process of welded steel pipes and this leads to the rework and the reduction in overall productivity [2]. Repair of pipes is a particular activity in the production line of steel pipes. Repair welding of defective pipes can be carried out as a logical procedure that ensures pipes usable and safe.

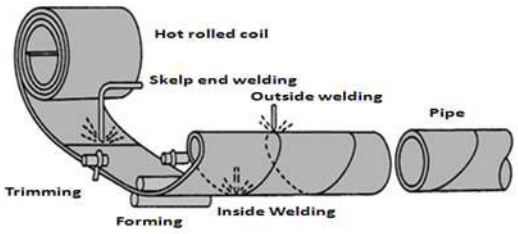

Fig.1. Schematic illustration of SAW of pipes

The commonest defects [3] that can occur during SAW (fabrication defects) of steel pipes include: porosity, slag inclusion, lack of fusion, incomplete penetration, cracks, craters, etc. All defects that considered detrimental to the structural integrity of steel pipes must be avoided by repair welding in production line.

For successful implementation of repair welding of steel pipes defects must be used suitable welding method, suitable welding consumables and skill welders [4].

The aim of this paper is manual metal arc repair welding of defects in seam pipes with diameter Φ812x12mm, from micro-alloyed steel API Grade X65, which occur during the manufacturing process.

2. MATERIALS AND METHODS

Spiral line pipes Ø813x12mm were fabricated using high strength steel coils X65 according to API 5L (American Petroleum Institute) standard [5], which chemical composition and mechanical properties are given in Table 1 and 2, according to the Certificate of Quality. Spiral line pipes Ø 813x12mm were welded in two-stage process by double sided Submerged Arc Welding (SAW) through an "X" groove configuration, according to the BLOHM+VOSS.

Tab.1. Chemical composition of steel coils X65

Steel coils	Chemical composition wt-%					
	C	Mn	Si	P	S	V
X65	0.10	1.38	0.36	0.029	0.009	0.055

Tab.2. Mechanical properties of steel coils X65

Steel coils	Mechanical properties						
	Re	Rm	A	Kv_1	Kv_2	Kv_3	Kv
				ISO-V-10 (0°C)			
X65	MPa		%	J			
	500	613	34.0	76.2	75.4	76.4	76.0

Automatic SAW of steel pipes were carried out under the protection of welding flux LWF 780, with chemical composition according to table 3 and the electrode S_2Mo, with chemical composition and mechanical properties according to table 4 and 5.

Tab.3. Chemical composition of welding flux LWF780

Welding flux	Chemical composition wt-%							
	SiO_2	MnO	CaO	MgO	Al_2O_3	TiO_2	CaF_2	Others
LWF780	18.0	14.0	2.0	5.0	41.0	9.0	4.0	7.0

Tab.4. Chemical composition of welding electrode S_2Mo

Welding electrode	Chemical composition wt-%			
	C	Mn	Si	Mo
S_2Mo	0.10	1.38	0.36	0.029

Tab.5. Mechanical properties of welding electrode S_2Mo

Welding electrode	Mechanical properties		
	Re	Rm	A
S_2Mo	MPa		%
	500	613	34.0

Pipes with defects in the spiral and in the transversal weld seam, identified by visual inspection, figure 2, were subjected to repair (repair welding) by manual arc welding (MAW) method, by skilled and certified welders, using basic electrodes EVB 60, which mechanical properties (according to the manufacturer attesting) are given in table 3 [6].

Tab.6. Mechanical properties of basic electrodes EVB 60

Welding electrode	Mechanical properties			
	Re	Rm	A	ISO-V-10 (0°C)
EVB60	MPa		%	J
	522	624	26.0	92.0

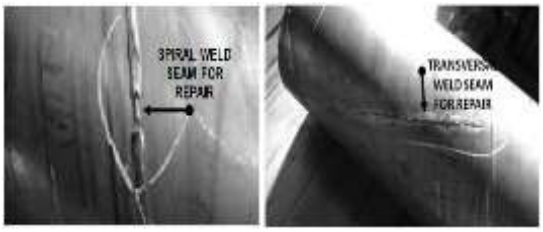

Fig.2. Pipes with defects in weld seam

Repair welding were performed after carefully preparing of the "V" groove, by grinding wheel, figure 3.

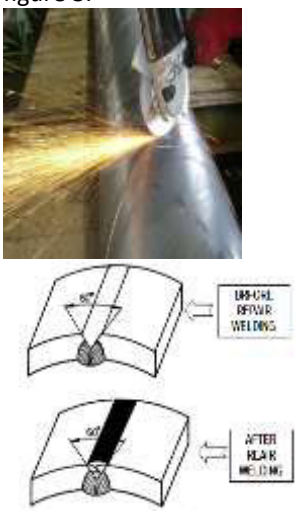

Fig.3. Preparation of the groove by grinding

After repair welding of the defective positions, in order to verify the quality of the repaired welding, were performed visual control and 100% X-ray nondestructive control, figure 4 and 5.

Fig.4. Visual control of the repaired weld seam

Fig.5. X-ray control of the repaired weld seam

After visual control and after positive evaluation of the quality of the repaired weld seam by 100% X-ray nondestructive control, were performed these testing:
-tensile testing,
-bend testing,
-hardness testing,
-metallographic analysis.

3. RESULTS AND DISCUSSIONS

Tensile testing results of the repaired spiral and transversal weld seam are presented in table 7. These values represents average of three specimens testing, separately in base metal (BM), repaired spiral weld seam (SW) and repaired transversal weld seam (TW). Table 3 shows increasing tendency of tensile strength (Rm) in the repaired weld seam as a results of the consumables materials and welding parameters. Average tensile strength for base metal (Rm=597MPa), for repaired spiral weld seam (Rm= 665MPa) and for repaired transversal weld

seam (Rm=618MPa) meets the standard requirements according to API for steel X65 (Rm_{min}=551MPa).

Tab.7. Tensile testing results

Specimens	Mechanical properties		
	Re	Rm	A
	MPa		%
Base metal (BM)	524	597	25.6
Repaired spiral weld seam (SW)		665	
Repaired transversal weld seam (TW)		618	

Bend testing were performed with the specimens bended in the outside of repaired spiral weld seam (SW) and in the outside of repaired transversal weld seam, figure 6.

Fig.6. Specimens after bend testing

During bend testing, repaired weld specimens from the spiral weld seam (SW) and from the transversal weld seam (TW), according to the API standard, were bended up to maximum bend angle (180°), without cracks or any others damages.

Hardness measurements (HV1 / 10), figure 7, were performed across the welded joint in the specimens after standard metallographic preparation and etching with 2% nital solution to develop the macrostructure and for hardess measurement.

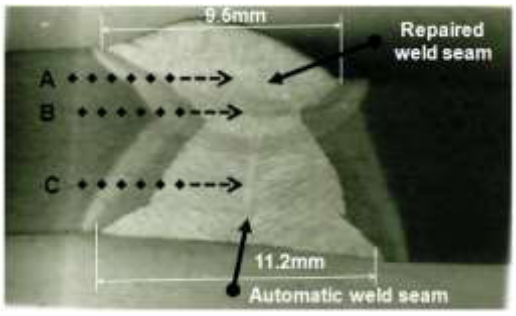

Fig.7. Macrography of repaired weld joint and hardness measurements positions

Results of hardness measurements (HV1/10) of the weld join after repair welding are presented in figure 8.

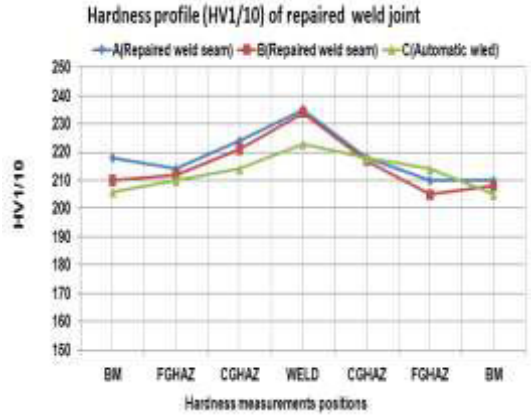

Fig.8. Hardness profile (HV1/10) of repaired weld joint

A macrograph of welded joint, figure 7 shows the overall macrostructure of the repaired weld seam, the automatic weld seam and the heat affected zone. Evidently that is achieved good penetration between repair weld seam and base metal and between repair weld and automatic weld. Results of hardness measurements also shows that hardness of repaired weld seam are nearly equal to the hardness of automatic weld seam. In general, the hardness began to increase in coarse grained heat affected zone (CGHAZ) toward the weld metal (W), becoming a maximum at the weld centerline (HVmax= 235HV1/10). The maximum hardness difference (ΔHVmax = 15HV1/10) between the repaired weld seam and automatic weld seam means that is realized homogeneous welded joint in aspect of mechanical properties.

4. CONCLUSIONS

Based on the review of the literature data experimental results, the following conclusion may be drawn:

-Welded joint of pipes Φ812x12mm after repair welding by manual arc welding (MAW) shows a

high plasticity, because all specimens are bended to the maximum bending angle without cracks or other damages.

-Welded joint of steel pipes Φ812x12mm after repair welding by manual arc welding (MAW) shows a high strength because all tensile testing results are higher than ultimate tensile strength requirements according to the API standard.

-Hardness profiles across repaired weld joint by manual arc welding (MAW) shows that the hardness values varies in the narrow range, so that welded joint is quite homogeneous in terms of hardness.

-Macrography of repaired weld joint shows a good penetration, a good relationship between manual arc welding (MAW) and base metal (BM) and between manual arc weldig (MAW) and automatic submerged arc welding (SAW).

-Repair welding of steel pipes plays a very important role because restores defective pipes in satisfactory condition for use, so successful implementation of repair welding provides high efficiency and effectiveness of the production process.

BIBLIOGRAPHY

[1] Degala VK, Suck JN (2014), Experimmental studies on Submerged Arc Welding Process, Journal of Welding and Joining, Vol.32, No.3, 1-10.

[2] Dan G (2009), Minimizing defects in Submerged Arc Welding, Welding Journal, September, 78-79.

[3] Leigh B, Grant V (2009), Welding defects, causes and correction, Australian Bulk Handling Review, July/August, 26-28.

[4] Bruce WA, Amend WE (2009), Guidelines for pipeline repair by direct deposition of weld metal, Welded pipeline Symposium, Welding Technology Institute of Australia, Sydney, 1-18.

[5] API (2004), American Petroleum Institute, Specification for line pipe, Washington, D.C.

[6] Maksuti Rr, Rama M, Aliti Rr (2012), Repair welding of the high frequency electric resistance welded joint, IXth Scientific Research Symposium with International participation, Metallic and Nonmetallic materials, Zenica, Proceedings, 119-123.

AKTET **ISSN 2073-2244**
Journal of Institute Alb-Shkenca **www.alb-shkenca.org**
Revistë Shkencore e Institutit Alb-Shkenca **Copyright © Institute Alb-Shkenca**

CELLULAR AND NUCLEAR ALTERATIONS OF CARP FISH (*CYPRINUS CARPIO*) ERYTHROCYTES AS SENSITIVE BIOMARKERS OF CITOTOXICITY AND GENOTOXICITY OF SITNICA RIVER WATERS (KOSOVO)

NDRYSHIMET QELIZORE DHE TE BËRTHAMËS NË ERITROCITET E KRAPIT (*CYPRINUS CARPIO*) SI BIOSHENJA TË NDJESHME TË CITOTOKSICITETIT DHE GJENOTOKSICITETIT TË UJËRAVE TË LUMIT SITNICA (KOSOVË)

ALIKO VALBONA[1], MORINA VALON[2], SULA ELDORES[3]
[1, 3] Department of Biology, Faculty of Natural Sciences, Tirana University
[2] Faculty of Geosciences and Technology, Prishtina University, Mitrovica, Kosovo
valbona.aliko@fshn.edu.al

SUMMARY
Cellular and nuclear abnormalities of carp fish (*Cyprinus carpio*) erythrocytes were evaluated in forty two fish specimens caught by electro fishing method (*Hans Grassl GmbH)* in three sampling sites Ferizaj, Vragoli and Plementin, alongside Sitnica River, during March-May and August-September 2010-2012. Physico-chemical analysis has shown that Sitnica River surface water and sediment are polluted by heavy metals [Pb (II), Cd (II), Cu (II), Cr (III, VI), Ni (II), Zn (II) and Mn (II) and phenols. 2000 RBC/specimen, stained according to Giemmsa-Romanowsky technique, were counted to evaluate erythrocyte abnormalities. Our results showed significant increase ($P<0.05$) in total erythrocyte abnormalities in fishes from polluted sites Vragoli and Plementin (respectively, 25.15±0.6* and 28.57±0.6*), compared to the less contaminated site, Ferizaj (1.9±0.6), which is located nearby river source. We can conclude that cellular and nuclear erythrocyte abnormalities are sensitive biomarkers of clastogenic effects of water pollution on fish erythrocytes and can be used for monitoring impact of heavy metals in water biota.
***Key words**: Erythrocyte abnormalities, biomarkers, Cyprinus carpio, Sitnica River, Kosovo.*

PËRMBLEDHJE
Çregullimet qelizore dhe bërthamore në eritrocitet e krapit (*Cyprinus carpio*) u vlerësuan në 42 individë peshqish të kapur me teknikën e elktrofishing (*Hans Grassl GmbH)* në tri vend-mostrime: Ferizaj, Vragoli dhe Plementin, përgjatë Lumit Sitnica, Kosovë, gjatë periudhave Mars-Maj dhe Gusht-Shtator 2010-2012. Analizat fiziko-kimike kanë treguar se ujërat sipërfaqësorë dhe sedimentet e lumit Sitnica, janë të ndotur me metale të rëndë [Pb (II), Cd (II), Cu (II), Cr (III, VI), Ni (II), Zn (II) dhe Mn (II)] dhe fenole. Për vlerësimin e çregullimeve eritrocitare u numëruan, 2000 RBC/individ, të ngjyrosur më parë, sipas teknikës Giemmsa-Romanowski. Rezultatet treguan rritje me kuptim ($P<0.05$) të çregullimeve eritrocitare te peshqit e vendeve të ndotura, Vragoli dhe Plementin (përkatësisht, 25.15±0.6* and 28.57±0.6*), krahasuar me atë më pak të ndotur, Ferizaj (1.9±0.6), që gjendet pranë burimit të rrjedhjes së lumit. Në përfundim, mund të themi se, çregullimet eritrocitare qelizore dhe bërthamore janë bioshenja të ndjeshme, të ndikimit klastogjenik të ndotjes së ujit, në eritrocitet e peshqve dhe si të tillë ato mund të përdoren për të monitoruar ndikimin e metaleve të rëndë në biotën ujore.
***Fjalët çelës:** Çregullime eritrocitare, bioshenja, Cyprinus carpio,Lumi Sitnica, Kosovë*

INTRODUCTION

Water pollution with heavy metals, affects various physiological processes in fish, including blood cells. In fish, toxic substances taken up from the water enter the blood and therefore, blood cells are among the first targets of toxicity, immediately after the gill epithelium. Therefore the effects of waterborne heavy metals are

related to their uptake from gills, resulting in interfere with blood circulating system and also blood cells (Vosyliene, 1999; Martinez et al. 2004). Fish erythrocyte morphology is more sensitive to various environment agents than basic red blood parameters (Vosyliene, 1999; Witeska, 2004), and cellular anomalies are sometimes observed without distinct decrease in their values (Gill et al. 1985; Witeska, 2010). According to Sharma et al. (2007) fish erythrocytes were more sensitive to water pollution compared to other biological endpoints and thus should be included in the routine fish bioassay.

Erythrocyte anomalies may result from various physiological disturbances (Witeska et al. 2010). Evelyn and Traxler (1978) reported cytoplasmic inclusions and erythrocyte degeneration: irregular outlines, nuclear displacement, condensation and leakage of nuclear material and cytoplasmic vacuolation due to necrosis viral infection of erythrocytes. Buckley (1976) observed Heinz bodies, poikilocytosis, clumped chromatin, ragged cell membranes, altered staining properties, and hemolysis in erythrocytes of Oncohinchys kisutch from water contaminated with chlorinated sewage. Frequencies of nuclear anomalies such as irregular nucleus shape, vacuolation, binuclei and micronuclei that indicate genotoxic effects often increases in fish exposed to water pollution (Ergene et al. 2007), but many also fluctuate seasonally (Boge and Roche, 1996) observed cytotoxicity of various phenolic compounds in the erythrocytes of *Dicentrarchus labrax*. Erythrocyte anomalies were also reported in fish subjected to intoxication with heavy metals. Gill and Pant (1987) observed erythrocyte swelling, poikilocytosis, vacuolation, amitosis, deformation and deterioration of cell membranes in *Barbus conchonius* exposed to chromium, and nuclear aberrations such as chromatin condensation, nuclear puffs and chromatin leakage in the same species subjected to cadmium intoxication (Gill and Paint, 1986). Witeska (2010) observed various erythrocyte anomalies in common carp fish, *Cyprinus carpio*, intoxicated subletally with heavy metals. Toxicity of metals to carp erythrocytes ranged (according to the frequency of erythrocyte anomalies): Pb>Zn>Cd>Cu, and the changes induced by various metals, was similar: nuclear malformation, chromatin condensation, cell swelling, and malformation. Karuppasamy et al. (2005) reported increased fragility, rupture of erythrocyte membrane and hemolysis in *Channa punctatus* subletally exposed to cadmium.

Heavy metals are the most noxious pollutants owing to their diverse effects. Some metals are soluble in water and readily absorbed into the living organisms. Metal ions of high toxicity are known to cause deleterious impact on organs and blood level in fish (Voysyliene, 1999). They form metal complexes with the structural proteins, enzymes and nucleic acids and interrupt their functions. For example, cadmium is a non essential, non-biodegradable element reported to be a major contaminant that causes adverse effects on the aquatic system (Gill and Paint, 1986). Lead pollutant induces lipid peroxidation in tissues and causes an irreversible damage to the respiratory organs of fish (Witeska, 2010). Nickel induces a morphological transformation and chromosomal aberration in cells. Nickel in combination with cobalt induces convulsions, DNA strand breakage and organ damage (Evelyn and Traxler, 1978). Hexavalent chromium is relatively mobile in the environment and is acutely toxic, mutagenic, teratogenic and carcinogenic to aquatic organisms (Buckley, 1976).

Sitnica River is one of the most important rivers in Kosovo. It is surrounded by agricultural land and settlements with unresolved wastewater discharge positioned downstream from the significant industrial plants (Arbneshi *et al*., 2008). Small rivers like Granacka, Drenica, Llapi and Prishtevka are subjoined. These rivers are also recipients of waste waters of different urban and industrial centers (Korca *et al*., 2002). A considerable amount of raw waters from agricultural wrought surfaces is flown down to Sitnica River. Physic-chemical analysis has shown that Sitnica River surface water and sediment quality is endangered by heavy metals [Pb (II), Cd (II), Cu (II), Cr (III, VI), Ni (II), Zn (II) and Mn (II) and

phenols. Anomalous values of Fe, Mg, Cr, Ni and Zn, far exceeded the allowed values of the fourth category of the quality of surface waters, posing possibly toxic threats to river biota.

Until now, studies on the adverse effects of heavy metals (Pb, Cd, Cu, and Zn) and phenols on fish specimens from Sitnica River in Kosovo are scarce (Morina et al, 2012; Morina et al. 2013). The aim of this present study was to evaluate *in-situ* the cellular and nuclear alterations in carp fish (*Cyprinus carpio*) erythrocytes induced by Sitnica River water contaminants, in order to use them as sensitive and reliable biomarkers of cytotoxic and genotoxic effects of water pollution on freshwater biota.

MATERIALS AND METHODS

Study areas and collection of specimens

Three sites (S1-Ferizaj; S2-Vragoli and S3-Plementin) were chosen for fish collection and investigation of water pollution effect of Sitnica River on fish erythrocyte morphology along with one reference site on the upper section of the river (Fig.1).

Figure 1 Localization of sampling sites in Sitnica River.

Animals

In total, 21 cyprinid fish individuals (*Cyprinus carpio*) were collected with electro fishing method from three sites along Sitnica River: [Ferizaj (n=8), Vragoli (n=5) and Plemetin (n=8)] during the period March-May and August-September of 2010-2012. Ferizaj was used as reference site, because it is less contaminated, as it's close to river source. The fish collected were maintained in boxes, in water from the sampling site, constantly aerated, and transported alive to the laboratory and there identified in accordance with Rakaj (1995).

Slide procedure

Blood smears were prepared with fresh blood obtained by caudal vein puncture using a syringe without anticoagulant. A drop of blood were immediately smeared on two clear glass slides for each fish specimens, air dried, and then fixed in absolute methanol for 10 minutes. Each slide was stained using 10% Giemsa-Romanowsky solution (*Sigma-Aldrich*) for 30 minutes. All slides were prepared and stained by the same individual. Slides were examined using a Zeiss oil-immersion light microscope with 1000X magnification. 2000 erythrocytes per smear were evaluated in order to determine the erythrocyte morphology and nuclear abnormalities. Erythrocyte abnormalities were classified according to Claxton *et al*. (1998).

Statistical analysis

Data of cell and nuclear abnormalities showed a non-normal distribution. The results are presented as median values ± SD. One sample T-test and Paired samples T-test were used to evaluate differences of eyrthrocyte abnormalities between sampling sites. In both cases, p value <0.05 was considered for statistical significance.

RESULTS & DISSCUSSIONS

Ten types of abnormalities (5 nuclear and 5 cellular) observed in all fish individuals are shown in Figure 2 and Figure 3.

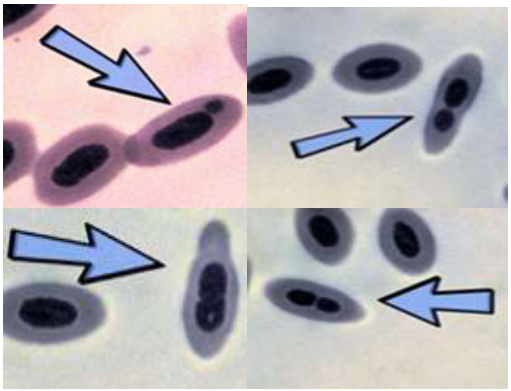

Figure 2 Nuclear abnormalities in carp fish (A) micro-nucleated; (B) bi-nucleated with cytoplasmic bridge; (C) bilobed and vacuolizated; (D) binucleated.

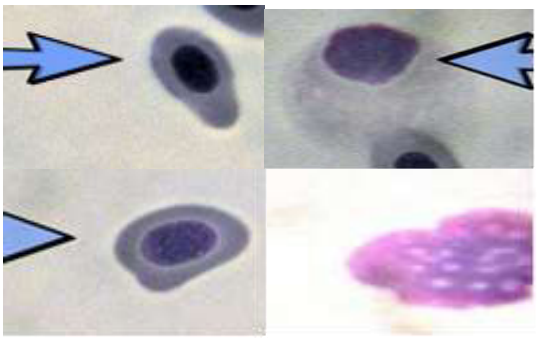

Figure 3 Cellular abnormalities in carp fish (A) deformed and echinocytic; (B) apoptotic with nuclear extrusion; (C) deformed and swollen; (D) apoptotic.

Normal fish erythrocyte of *C. carpio* is elliptical in shape with centrally placed nucleus in the clear and homogenous cytoplasm. Such normal erythrocytes were observed in control fish group. 5 types of nuclear abnormalities included blebbed (B), binucleated (BN), micronucleated (MN), lobed (L) and notched nuclei (N), were observed. Whereas, among cellular abnormalities, enucleated (EN), vacuolated (VC), deformed (DC), echinocytic (EC), and apoptotic or karryorhetic cells (AP), were the most frequent founded.

Our results showed significant increase ($P<0.05$) in total erythrocyte abnormalities (Fig. 3) in fishes from polluted sites Vragoli and Plementin (respectively, 25.15±0.6* and 28.57±0.6*), compared to the less contaminated site, Ferizaj (1.9±0.6). The most frequent erythrocyte abnormalities were cell deformity, nuclear deformity, micro nucleated cells and karryorhetic or apoptotic cells.

In the present study a higher frequency of total cellular and nuclear abnormalities in erythrocytes of *C. carpio*, was found in specimens from Vragoli and Plementin Sitnica River, Kosovo, sampling sites, demonstrate for the presence of genotoxic chronic stress as a consequence of long-term pollution there (Fig. 4). Our findings are in accordance with high levels of heavy metals found in the River from other previous studies (Arbneshi et al., 2008).

Erythrocyte nuclear deformities can be explained by the fact that as far that the cell detect an affected region began a process of repair and elimination of the chromatin (Shimizu et al., 1998; Ergene et al., 2007). The affected part is then moved to the periphery of the nucleus and is eliminated by exocytose. Thus, prior the complete elimination, the nuclear membrane may present imperfections, characterizing the nuclear abnormalities.

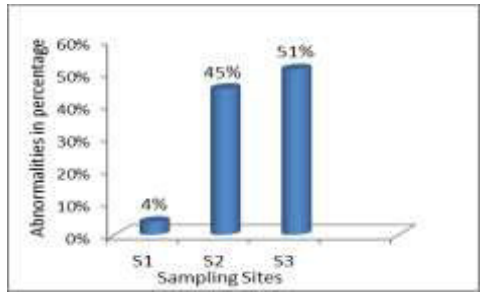

Figure 4 Frequency of total erythrocyte abnormalities in carp fish from Ferizaj (S1), Vragoli (S2), and, Plementin (S3), Sitnica River, Kosovo.

The finding of a higher number of nuclear abnormalities together with micronucleated erythrocytes indicates that the mechanism of exocytose can be interrupted; not being very efficient, because frequently it cannot eliminate completely the fragment inside the nucleus,

remaining in the periphery of nuclear membrane (Shimitzu et al., 1998).

Another explanation could be the evidence of oxidative stress induced by the presence of heavy metals in the river sediments and surface waters. Thus, in oxidative stress, one of the first targets is the cell membrane that, by having its permeability and selectivity altered by lipid peroxidation, becoming the nucleus more susceptible and, therefore, might form nuclear abnormalities and micronuclei, respectively.

On the other side, erythrocyte cells under heavy metal effects, but not only, change their form in order to compensate for low water oxygen content. So they tend to become round or tear-drop in shape. Cellular abnormalities results later into cell death. In the fish from Vragoli and Plementin sampling sites, we found more degenerating erythrocytes with nuclear extrusion signs or in karyorhectic state. The presence of deformed erythrocytes and cytoplasmic vacuolization suggested that toxicants present in the Sitnica River can cause hypoxic conditions which result in depression of ATP that lead to abnormal shape of erythrocytes. Further, toxicants interrupted the lipid solubility of membranes of erythrocytes resulting in vacuolated and ultimately leading to apoptosis. Similar findings are reported also from other researchers (Witenska, 2004; Akahori, 1999).

CONCLUSIONS

The results obtained from this study clearly demonstrated that the carp population of Sitnica River is suffering toxic effects of heavy metal pollution. The increase in the formation of erythrocyte abnormalities (nuclear and cellular) in fish individuals from the polluted sites, is a sensitive biomarker of clastogenic effects of water pollution on the peripheral red blood cells of fish and it can be used for monitoring of heavy metal impact in fresh water biota.

AKNOWLEDGEMENTS

We want to thank Dr. Leart Berdica for helping in photographing erythrocytes, and MSc. Eliana Ibrahimi, for the statistical evaluations.

REFERENCES

Akahori AZ, T Jozwiak, Gabryelak, R Gondko (1999), Effect of zinc on carp (*Cyprinus carpio L*.) erythrocytes. Comp.Biochem.Physiol. 123, 209-215.

1.Arbneshi T, Rugova M, Berisha L (2008), The concentration levels of lead, cadmium, copper, zinc and phenols, in the water of Sitnica River. J. Int. Environmental Application & Science, Vol 3 (2), 66-73.

2.Boge G, Roche H (1996), Cytotoxicity of phenolic compounds on *Dicentrarchus labrax* erythrocytes. Bull. Environ.Contamin.Toxicol. 57, 171.

3.Buckley JA (1976), Heinz body hemolytic anemia in Coho salmon (*Oncorhynchus kisutch*) exposed to chlorinated waste water. J.Fish.Res.Bd.Can. 34, 224.

4.Ergene S, Cavas T, Celik A, Koleli N, Kaya F (2007), Monitoring of nuclear abnormalities in peripheral erythrocytes of three fish species from Goksu delta (Turkey): genotoxic damage in relation to water pollution. Ecotoxicology 16, 385-391.

5.Evelyn TPT, Traxler GS (1978), viral erythrocyte necrosis natural occurrence in Pacific salmon and experimental transmission. J.Fish.Res.Bd.Can. 35, 903-908.

6.Gill TS, Paint JC (1985), Erythrotycic and leukocytic response to Cd poisoning in a freshwater fish, *Puntius conchonius*. Environmental Research. 36, 327-332.

7.Gill TS, Paint JC (1986), Chromatin condensation in the erythrocytes of fish following exposure to *Cd. Bull. Environ.Contam.Toxicol.* 36, 199-204.

8.Gill TS, Paint JC (1987), Hematological and pathological effects of chromium toxicosis in the freshwater fish, *Barbus conchonius Ham*. Water, Air & Soil Pollution. 35, 241-246.

9.Karuppasamy R, Subathras S, Puvaneswari S (2005), Hematological responses to exposure to sublethal concentration of Cd in air breathing fish, *Chara punctatus*. J. Environ.Biol. 26, 123-128.

10.Korça B, Jusufi S, Shehdula M, Bacaj M (2002), Surface Water Pollution in Kosovo, Scientific Conference: Technical-Technological Sustainable Development and Environment, Proceeding Book, pp. 43-49, Published by Macedonian Ecological Society. Skopje.

11.Morina V, Aliko V, Gavazaj, F, Kastrati Dh (2012), Use of blood parameters as biomarkers of contaminant exposure in fish specimens from Sitnica River, Kosovo. JIEAS, 7/5, 971-977.

12.Morina V, Aliko V, Sula E, Gavazaj F, Ferrizi Rr, Kastrati Dh (2013), Physiological response of fish to water pollution in Sitnica River, Kosovo. Indian Streams Research Journal, 3/1, 1-5.

13.Rakaj N (1995), Iktiofauna e Shqipërisë, Shtëpia Botuese e Librit Universitar, Tiranë. 700 p.

14.Sharma KP, Sharma S, Singh PK, Kumar S, Grover R (2007), A comparative study on characterization of textile waste waters (untreated and treated) toxicity by chemical and biological tests. Chemosphere 69, 48-53.

15.Shimitzu N, Itoh H, Utiyama H, Wahl GM (1998), Selective entrapment of extra-chromosomally amplified DNA by nuclear budding and micronucleation during S-phase. Journal of Cell Biology, 140/6, 1307-1320.

16.Voysyliene MZ (1999), The effect of heavy metals on hematological indices of fish (survey). Acta Zool. Lituanica. 9, 76-81.

17.Witeska M (2004), The effect of toxic chemicals on blood cell morphology in fish. Fresenius Environmental Bulletin. 12a, 1-5.

18.Witeska M, Kondera E, Szymanska M, Ostrysz M (2010), Hematological changes in common carp (*Cyprinus carpio* L.) after short term lead (Pb) exposure. Polish Journal of Environmental Studies. 19, 825-830..

AKTET **ISSN 2073-2244**
Journal of Institute Alb-Shkenca **www.alb-shkenca.org**
Revistë Shkencore e Institutit Alb-Shkenca **Copyright © Institute Alb-Shkenca**

THE INFLUENCE OF WOOD SPECIES ON STATIC BENDING STRENGTH OF FINGER JOINT CONNECTION
NDIKIMI I LLOJIT TË DRURIT MBI REZISTENCËN NË PËRKULJE STATIKE TË BASHKIMIT FINGER-JOINT

BESNIK HABIBI[a], DRITAN AJDINAJ[a]
[a]Department of Wood Industry; Agricultural University of Tirana
Kodër-Kamëz, 1029, Tiranë, ALBANIA
e-mail: besnikhabipi@hotmail.com

PËRMBLEDHJE
Një studim u krye për vlerësimin e ndikimit të llojit të drurit mbi cilësinë e lidhjeve finger-joint. U studiuan 5 llojet drusore më të përdorur në Shqipëri, ahu (*Fagus sylvatica* L), lisi (*Quercus petraea* Sp), plepi (*Populus alba* L.), pisha (*Pinus pinea* L.) dhe bredhi (*Abies alba* Mill.). Kampionet u pregatitën duke përdorur ngjitës polivinil acetati D1. Dhëmbët u prodhuan me lartësi 10 mm, hap 6 mm dhe trashësi në majë 2 mm. Nga secili lloj drusor u prodhuan 24 kampione me dimensione 20×20×320 mm, të cilat u kondicionuan dhe u testuan në përkulje statike duke aplikuar metodën e specifikuar në standardin ISO 3133. Rezistencën më të lartë e paraqiti lidhja nga druri i ahut me 61.49 N/mm^2, pasuar nga ajo e drurit të pishës me 53.43 N/mm^2, ai i lisit me 53.34 N/mm^2, i plepit me 46.35 N/mm^2 dhe në fund u renditën lidhjet nga druri i bredhit me 43.04 N/mm^2. Rezultatet e përftuara u diskutuan nën fokusin e një analize për vlerësimin e performancës së lidhjeve finger-joint nga drurë të ndryshëm, duke synuar në përdorimin optimal të kësaj lidhje zdrukthtare.
Fjalët çelës: finger-joint, rezistenca në përkulje statike.

SUMMARY
A research was carried out to evaluate the influence of wood species on the strength of finger joint connections. There were studied 5 common Albanian wood species, beech (*Fagus sylvatica* L), oak (*Quercus petraea* Sp), poplar (*Populus alba* L.), pine (*Pinus pinea* L.) and fir (*Abies alba* Mill.). Samples were prepared applying polyvinyl adhesive D1. Teeth were 10 mm in length, with 6 mm pitch and 2 mm width of fingertips. 24 samples from each wood species, with dimensions 20x20x320 mm, were conditioned and tested in static bending applying the method according to norm ISO 3133. Wood beech showed the highest strength value 61.49 N/mm^2, followed by pine with 53.43 N/mm^2, oak with 53.34 N/mm^2, poplar with 46.35 N/mm^2 and in the end was lined fir wood with 43.04 N/mm^2. The research results obtained were discussed in order to analyze and evaluate the performance of finger jointing from different wood species, aiming to an optimal utilization of this type of connection.
Key-words: finger joint, static bending strength.

INTRODUCTION

Engineered wood based materials have been developed over the years with the aim to avoid some of the disadvantages of solid wood. Materials like glued-laminated timber, I joists and trusses, as well as some solid wood panels used for furniture manufacturing, justify their performance due to finger joint connections, which are decisive elements of their strength.

Finger joint is a type of end joint developed from scarf joint and has been used since from the beginning of twentieth century [1]. Such joints can not only joint the short pieces of lumber to long ones, but also effectively enhance the

utilization of low-grade materials, especially for N-S structural applications.

The properties of finger-jointed lumber are affected by many different factors such as the wood species, adhesive type and curing time, finger geometry, processing parameters, wood moisture content as well as pre-treatment of wood.

Selection of wood material is the first basic step in manufacturing of finger-joints connections. Even under the most favorable conditions, strength of a finger joint will be lower than strength of clear wood [2]. Many studies have showed that wood species with density higher than 700 kg/m^3 give uncertain performance, while those with lower density appear to be more predictable in their performance [3].

It is known that the same wood species, originated by different geographical localities, presents different strength of finger joint connection. Comparison between wood beech originated by Albania and Greece showed different values of MOR and MOE values [4]. Also, Vassiliou examined the bending strength (modulus of rupture and modulus of elasticity) of finger–jointed from turkey oak (*Quercus cerris* L.), hungarian oak (*Quercus conferta* Kit.) and holm oak (*Quercus ilex* L.). From tests resulted that hungarian oak presented the highest value of MOR, followed by turkey and holms oak. MOE ranged in the same level for all three species [5]. Other studies have showed a strong correlation of wood species on strength of structural finger joint.

Vrazel and Sellers studied the strength of three wood species, keruing (*Dipterocarpus* spp.), southern pine (*Pinus* spp.), and Douglas-fir (*Pseudotsuga menziesii* D.). Joints were subjected to three test procedures: a tension test, a bending test, and a bending test following a cyclic delamination procedure. Given adequate adhesive performance, strength and stiffness of the joints studied were dependent on density of the wood species, with keruing having the greatest density [6].

Comparison between wood species commonly used for making glulam products, Douglas fir (*Pseudotsuga menziesii*, D), southern yellow pine (*Pinus* spp., S), western hemlock (*Tsuga heterophylla*, Hem), and SPF (spruce-pine-fir) and Japanese cedar (*Cryptomeria japonica*, J), showed a correlation between tensile strength of finger-jointed lumber and wood species [7]. A study on African hardwoods, Obeche (*Triplochiton scleroxylon*), Makore (*Tieghemella heckelii*) and Moabi (*Baillonella toxisperma*) showed that finger-joints from low density Obeche exhibited the highest joint eficency, followed by that from the medium-density Makore and the high density Mohabi [8,9].

In this research, the effect of five common Albanian wood species on bending strength of finger joint connection, bonded with polyvinyl adhesive, is studied. It aims to give information about opportunities for production and application of a better quality and performance of wooden products and wider possibilities for industrial uses.

MATERIALS AND METHOD

There were studied 5 common Albanian wood species, beech (*Fagus sylvatica* L), oak (*Quercus petraea* Sp), poplar (*Populus alba* L.), pine (*Pinus pinea* L.) and fir (*Abies alba* Mill.).

Wood material for production of samples was selected from pieces of kiln dried boards. From selected pieces were sawn blocks without deformations or structure defects with dimensions of cross-section 5×6 cm, and various lengths. Fingers profiles were produced on one head of each block by means of a spindle moulder with sliding table. The geometric profile of cutter heads (knifes), which means the geometric profile of fingers is shown in Figure 1.

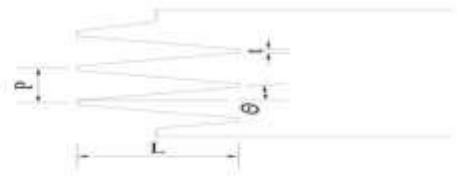

Figure 1- Geometric profile of fingers

Pitch P = 6 mm, length L = 10 mm, width of fingertips t = 2 mm and slope angle Θ = 10°.
There were produced five series of fingers perpendicular with blocks edges (straight fingers, figure 2).

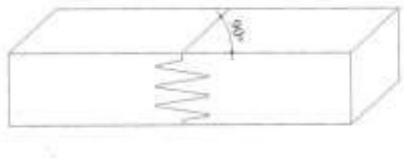

Figure 2 Finger-joint with straight fingers

Following fingers production and combination of blocks two by two, a PVA D1 glue (Neon, ALBANIA) was applied on one profiled head by roller brush. The quantity of glue was referred to industrial application 170÷240 [gr/m^2], resulting in 2.5÷2.7 [gr.] per piece. It was verified by weighing the pieces before and after application of glue. Then, the blocks couples were pressured manually by means of hand grip vices for a period of 24 hours. With regard to adhesive and pressure application, devices and techniques used in the study were typically for handicraft and small scale production, which has given the biggest share of finger-joint production in Albania. After, the jointed blocks were cut and planed to final dimensions 20×20×320 mm, to produce bending strength samples according to the standard ISO 3133 [10].
The samples were conditioned to reach equilibrium moisture content around to 12%, and were tested by means of mechanical testing machine (Controlab, FRANCE). Modulus of rupture (MOR) was calculated in N/mm^2 according to standards ISO 3133 as follows:

$$MOR = \frac{3P_{max} \times l}{2bh^2}$$

where P_{max} was the breaking load in newtons (N), l was the distance between the centres of supports in millimetres (mm), b was the breadth of the test piece in (mm), h was the height of the test piece in (mm).

In total were tested 120 samples, 24 for each series of samples. After testing, the density of wood was measured according to the standard ISO 3131, using pieces provided by destroyed samples [11].

RESULTS AND DISCUSSIONS

Mean values of modulus of rupture (MOR), together with respective standard deviations measured in static bending tests, as well as mean values of respective wood densities are shown in Table 1.

Table 1 Results of modulus of rupture (MOR)

Wood species	Density [g/cm^3]	Stand. Dev.	MOR [N/mm^2]	Stand. Dev.
Beech	0.647	0.053	61.49	6.27
Oak	0.761	0.064	53.34	4.96
Poplar	0.443	0.052	46.35	4.92
Pine	0.461	0.037	53.43	5.44
Fir	0.525	0.041	43.04	5.02

The bending strength (MOR) of tested samples ranged from 43.04 N/mm^2 to 61.49 N/mm^2. On the first sight MOR values of harder woods appeared to be higher comparing to those of other woods. Pine presents an exception, because even it has a lower density than oak wood, shows almost the same value of MOR.
Analyse of MOR values shows that between oak and beech exist a negative correlation. Oak as wood with 18% higher density than beech presents 13% lower MOR value and this is in the same line with results of other studies [8,9]. The same situation appeared to be and between fir and pine wood. Fir wood with 14% higher density than pine, presents almost 20% lower MOR values.
The contrary is for poplar wood which presents the lowest MOR value of finger-joint connection among broadleaves species.
In figures 3 and 4 are shown variations of density and MOR values referring to wood species in study.

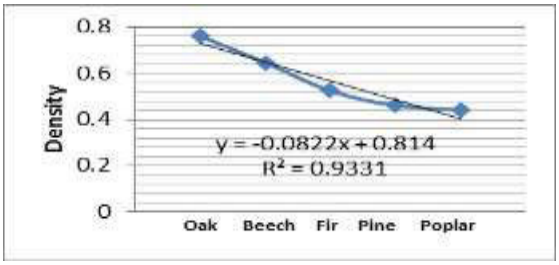

Figure 3 Density variation

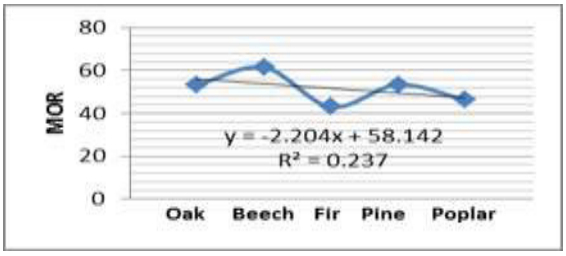

Figure 4 MOR variation

CONCLUSIONS

Based on research results obtained during this study we can say that wood species affect strongly the strength of finger-joint connections. In general, broadleaves produce finger-joint connections stronger than coniferous, referring to length teeth up to 10 mm, for N-S structural uses.

By the other hand, within both groups of wood species, with reduction of density, the MOR value is increased in notable percentage. Poplar wood is an exception from this phenomenon.

The results of the study and the state of art of technology by means of finger-joint is produced, offer to wood processing industry good opportunities for a better selection and utilization of wood species for production of finger-joint connections.

REFERENCES

1.Jokerst, RW (1981), Finger-jointed wood products. Res. Pap. FPL 382. USDA Forest Serv., Forest Prod. Lab., Madison, Wis. USA.

2.USDA Forest Service, Forest Products Laboratory (199, Wood Handbook: Wood as an Engineering Material. Gen. Tech. Rept. FPL-GTR-113. Forest Prod. Soc., Madison, WI.

3.Lamb-Shine D, Wands RW (1982), Structural finger-joints. In: C.F.L. PRINS (Ed.). Proceedings of Seminar on Production, Marketing and Use of Finger-Jointed Sawn Timber Committee of the United Nations Economic Commission for Europe. Martinus Nijhof/Dr. W.Junk Publishers, Hague, Boston, London.

4.Vassiliou V, Barboutis I, Ajdinaj D, Thoma H (2009), PVAc bonding of finger-jointed beech wood originated from Albania and Greece. Proceedings of ICWSE 2009, Brasov, ROMANIA.

5.Vassiliou V, Karastergiou S, Barboutis I (2005), Bending strength properties of finger jointed Oakwood's (*Quercus cerris* L.). Holz als Roh-und Werkstoff, Springer-Verlag.

6.Vrazel, M. and Sellers, T.J. (2003) The effects of species, adhesive type and cure temperature on the strength of a structural finger-joint. Forest Products Journal, 54(3), 66-75.

7.Yeh MC, Lin YL, Huang YC (2011), Evaluation of the tensile strength of structural finger-jointed lumber. Taiwan Journal Forestry Sciences, 26(1), 59-70.

8.Ayarkwa J, Hirashima Y, Sasaki Y, Yamasaki M (2000), Influence of finger-joint geometry and end pressure on tensile properties of three finger-jointed Tropical African Hardwoods. Southern African Forestry Journal 188, 37-49.

9.Ayarkwa J, Hirashima Y, Sasaki Y (2000), Effect of finger-joint geometry and end pressure on the flexural properties of finger-jointed Tropical African Hardwoods. Forest Products Journal 50(11/12), 53-63.

10.ISO 3133 (1975) Wood – Determination of ultimate strength in static bending. International Organization for Standardization, CH-1211, Genève, SWITZERLAND.

11.ISO 3131 (1975) Wood – Determination of density for physical and mechanical tests. International Organization for Standardization, CH-1211, Genève, SWITZERLAND.

AKTET
Journal of Institute Alb-Shkenca
Revistë Shkencore e Institutit Alb-Shkenca

ISSN 2073-2244
www.alb-shkenca.org
Copyright © Institute Alb-Shkenca

SOME MONITORING DATA ON BACTERIAL LOAD OF ERZENI RIVER, ALBANIA
TË DHËNA MONITORUESE PËR NGARKESËN BAKTERIALE NË LUMIN ERZEN, SHQIPËRI

ETLEVA HAMZARAJ[a], GJENA DURA[a]
[a]Department of Biology, Faculty of Natural Sciences, University of Tirana, Blvd. "Zog I", No. 1, Tirana, Albania
etleva.hamzaraj@fshn.edu.al

PËRMBLEDHJE
Bakteret janë treguesit idealë të ndotjes mikrobike të ujërave sipërfaqësorë sepse i përgjigjen shumë shpejt ndryshimit të kushteve të mjedisit. Koliformët fekalë, *E. coli*, dhe enterokokët fekalë janë indikatorët më të mirë për vlerësimin e ndotjes fekale. Qëllimi i këtij studimi ishte të monitoronim cilësinë e ujit të Lumit Erzen, si një nga lumenjtë e rëndësishëm në Shqipëri, duke u bazuar në indikatorët mikrobiologjikë. Mostrat u mblodhën çdo muaj nga Tetori 2013 deri në Korrik 2014 në tre stacione përgjatë lumit. Indeksi MPN u përdor për të përcaktuar koliformët fekalë në ujë, ndërsa numri i bakterve heterotrofe u përcaktua duke numëruar kolonitë në pjata me PCA, të kultivuara me 0.1ml mostër pas hollimeve të njëpasnjëshme. Sikurse pritej në mostrat e mara nga stacionet afër zonave urbane vërehet një ngarkesë e lartë me koliformë fekalë. Ndikimi i njeriut në cilësinë e ujit të lumit Erzen është më se evident.
Fjalë çeles: cilësia e ujit, baktere koliforme, heterotrofë, indeks MPN

ABSTRACT
Bacteria are ideal sensors for the indication of microbial pollution of surface water bodies because of their fast response to changing environmental conditions. Faecal coliforms, E. coli and intestinal enterococci are good indicators for the assessment of faecal pollution. The aim of this study was to monitor water quality of Erzeni River, as one of important rivers in Albania, based on microbiological indicators. Samples are collected every month from October 2013 till July 2014 in three stations along the river. MPN index is used for evaluation of total coliform bacteria in water, while the number of heterotrophic bacteria is determined by counting colonies on plates with PCA, cultivated with 0.1 ml sample after a series dilutions. As it was expected, there is a high load of feacal coliform bacteria and heterotrophs in sample stations near urban areas. The human impact in the quality of water of Erzeni river is more than evident.
Key words: water quality, coliform bacteria, heterotrophs, MPN index

INTRODUCTION

Assessing the quality of aquatic environments traditionally relied on measurements of the concentrations of inorganic and organic materials. Recently has become important biological monitoring, which can assess the degree of contamination of an ecosystem and ecological conditions of an area using living organisms that live in it (3).

Indicator organisms are a fundamental tool monitoring used to assess changes in water quality, and the possible presence of pathogenic organisms that are difficult to detect. An indicator organism provides evidence for the presence or absence of pathogens that survive in similar physical and chemical conditions, as well as similar nutrient requirements (9). Types of indicator organisms are total coliforms, fecal coliforms, *Escherichia coli*, the bacteria producing H_2S. It is important to note that an indicator is not necessarily a pathogen, although some types of *E. coli* are pathogenic. *E. coli* and *Enterobacter* are used as biological indicators because they have been shown to be good indicators of fecal

contamination. In addition, their behavior (durability, long life, movement) in the environment is assumed to be similar to current pathogens of interest. Faecal pollution of water can lead to health problems because of the presence of infectious microorganisms. These may be derived from human sewage or animal sources (14, 3).

Erzeni stems from the highlands of Shëngjergji, east of Tirana. The length of this river with great flow is 108 km. The river is considered clean in his mountain course, but in the second half of the course is contaminated in every village or locality where it passes. The river traverses areas as Bërzhitë, Mullet, Petrelë, Vaqarr, Shijak and Sukth. Flows into the Adriatic Sea near Sukth in Durres north 41º26 '12 "N 19º 27' 35 '.

Figure 1. Map of Erzeni rivër

Materials and methods

For determining the microbial load in the waters of the Erzeni river samples were taken at three sampling points: Mullet, Damian, Shijak during a 10 month period from October 2013 to July 2014. Microbiological tests were carried out in the Laboratory of Microbiology at the Faculty of Natural Sciences, University of Tirana. Sampling and testing were conducted in accordance with International Standard methods (8, 12).

MPN index was used for evaluation of total coliform bacteria in water. Diluted samples were cultivated in series of five tubes with Lactose Broth, that were incubated at 35°C, for the preliminary test, and at 44°C for the confirmation test, for 24 to 48 h. The MPN index was calculated by using the MPN statistical tables and is expressed as the number of organisms per 100 ml (CFU/100 ml) (1, 10, 13).

The number of heterotrophic bacteria was determined by counting colonies on plates with Plate Count Agar, cultivated with 0.1 ml sample after three series dilutions (11, 6).

Table 1. Faecal coliform standards for rivers, ISO 7899-1

Quality	**Very good**	**Good**	**Bad**	**Very bad**
Faecal coliforms CFU/100 ml	250-500	500-1000	1000-2000	> 2000

Table 2. Heterotrphic bacteria standards for rivers

	I Class	**II Class**	**III Class**	**IV Class**	**V Class**
Quality	**Very good**	**Good**	**Poor**	**Bad**	**Very bad**
Heterotrophs CFU/ml	≤ 500	>500-10000	>10000-100000	>100000-750000	>750000

Results and Discussion

Total coliform bacteria are a collection of relatively harmless microorganisms that live in large numbers in soils, plants and in intestines of warm-blooded (humans) and cold-blooded animals. If many coliforms are present in a given water sample, there is a good likelyhood that pathogens might also be present. Total coliform counts are normally about 10 times higher than fecal coliform counts (7).

As mentioned above for determining the microbial load in Erzeni river samples were collected and analyzed from three sampling points during ten months from October 2013 to July 2014. So during the period of investigation we analyzed 30 water samples for total coliform bacteria and heterotrophic bacteria. Our data show that there is a very high load with total coliform bacteria of water of Erzeni river, which is much higher than in some other rivers of Albania (5). The results obtained for coliform bacteria are

presented in Figure 2 where it is evident that in Mullet the number of coliform bacteria is lower than in two other points throughout the sampling period (with a maximum of 24000 CFU/ml), while the count in two other sampling sites is much higher (with a maximum of 110000 CFU/100 ml) (Fig. 2). Mullet is also the area with less urban impact on water quality of the river, while the other two points are closer to residential areas, and here the impact of human activity on microbial quality of river water is clear enough. According to faecal coliform standards for rivers, ISO 7899-1, the water of Erzeni river is of bad (11% of samples) and very bad (89% of samples) quality (Table 3).

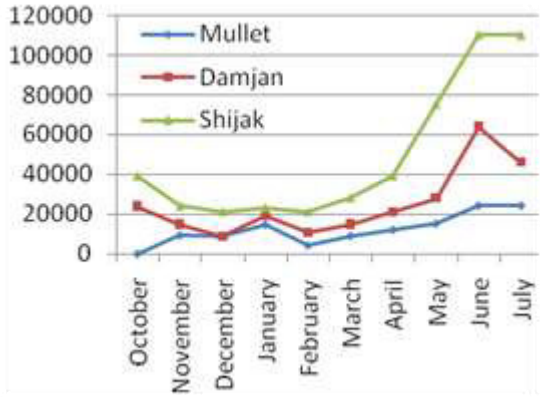

Figure 2. Faecal coliforms in three sampling sites along Erzeni rivër

Faecal coliforms	Quality	Sampling point			Total
		1. Mullet	2. Damjan	3. Shijak	
	Very Good	0.0%	0.0%	0.0%	0.0%
	Good	0.0%	0.0%	0.0%	0.0%
	Bad	22.22%	11.11%	0.0%	11.11%
	Very Bad	77.78%	88.89%	100%	88.89%
Total		100%	100%	100%	100%

Table 3. Water quality according to faecal coliforms

There are many environmental factors that influence the presence of bacteria in water, and one of them is temperature. As it was expected, the number of total coliform bacteria increased from winter (with a minimum of 4300 CFU.100 ml^{-1} in Fabruary, 2014, in Mullet) to summer (with a maximum of 110000 CFU.100 ml^{-1} in July, 2014, in Shijak), a pattern that is normally influenced by seasonal changes of temperature (Fig. 3). The highest value of total coliform bacteria in water is registered in July, which in our opinion could be due to higher temperatures during this season. On the other hand we observe an increase of bacterial load during January, despite the low temperatures. These aparently not normal values could be due to heavy rain conditions that can result in high fecal and total coliform counts downstream from sewage discharge points.

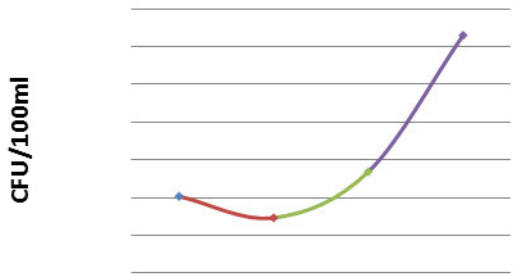

Figure 3. The mean number of faceal coliform bacteria in different seasons

We also determined the number of heterotrophic bacteria, as an indicator of water quality for surface waters. The heterotrophic plate count includes all of the microorganisms that are capable of growing in or on a nutrient-rich solid agar medium. The situation refering to sampling sites is almost similar to that of faecal coliform

bacteria, that means that the lowest number of heterotrophic bacteria is found in sampling site Mullet (Fig. 4).

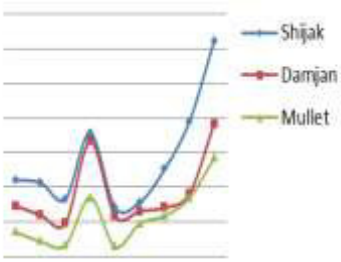

Figure 4. Heterotrphic bacteria in three sampling sites along Erzeni river

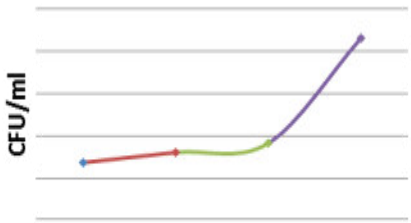

Figure 5. The mean number of heterotrophic bacteria in different seasons

As far as the dynamic of heterotrophic bacteria number during the year of investigation is concerned, what we observed is a slow increase from autumn to spring and a sharp increase in the number of these bacteria during summer, which could be due to higher temperatures during this season (Fig. 5).

Conclusion

The obtained results for the investigated groups of bacteria show, in general, the impact of human activities in water quality. The highest faecal coliform counts are observed near the urban areas.

Referring to faecal coliform standards for rivers the water of Erzeni river is of very bad quality and is a high potential risk to public health. On the other hand the heterotrophic bacteria count do not show a great variability during the period of investigation, except summer when environmental factors, like temperature, have a distinct impact.

REFERENCES

1. American Public Health Association (APHA-AWWA-WPCF) (1988), Standard methods for the examination of water and wastewater, Washington, DC, USA, ed. 20.
2. Barrel RAE, Hunter PR, Nichols G, (2000), Microbiological standards for water and their relationship to health risk, Commun Dis Pub Health, 3, 8-13.
3. Borrego JJ, Figueras MJ, (1997), Microbiological quality of natural waters, Microbiologia, 13 (4), 413-26.
4. Hamzaraj E, Lazo P, Koja O, Paparisto A, Laknori O, Duka S, (2012), Seasonal dynamics of bacterial indicators in the albanian part of Prespa Lake, Asian Journal of Chemistry, 25, 759-762.
5. Hamzaraj E, Lazo P, Paparisto A, Laknori O, Duka S, Dahriu O, (2012), Water quality from microbiological point of view of Vjosa river, Albania, Balwois 2012, Ohrid, Republic of Macedonia.
6. Lokoska L, Jordanoski M, Veljanoska-Sarafiloska E (2004), The water quality of the Lake Prespa and its tributaries, Proceedings of Ist Simposium of Ecologists of the Republic of Montenegro, Tivat, Montenegro.
7. Madigan M T, Martinko JM, Stahl D, Clark DP (2012), Brock Biology of Microorganisms, 13th Edition, Pearson Education.
8. Meybeck M, Chapman D, Helmer R (1989), Global Assessment of Fresh Waters Quality – A First Assessment, Basil Blackwell, Oxford, 307 p.
9. Reiss M, Chapman J (2000), Environmental Biology, Cambridge Advanced Sciences.
10. UNEP/WHO (1996), Water Quality Monitoring - A Practical Guide to the Design and Implementation of Freshwater, Quality Studies

and Monitoring Programmes, Jamie Bartram and Richard Balance eds.
11. UNESCO/WHO/UNEP (1996), Water Quality Assessment: A Guide to the use of Biota, Sediments and Water in Environmental Monitoring, Second Ed., Chapman D.
12. WHO (1984), Microbiological Methods for water quality monitoring, Second report, Copenhagen.
13. WHO (2006), Guidelines for Drinking Water Quality, First Addendum to the Third Edition, Volume 1, 491-493.
14. WHO (2012), Guidelines for safe recreational waters, Volume 1, Coastal and fresh waters.